


 Cite this: *RSC Adv.*, 2025, 15, 10902

# Exploring the role of strontium-based nanoparticles in modulating bone regeneration and antimicrobial resistance: a public health perspective

 Uchenna Uzoma Akobundu,<sup>a</sup> Ikhazuagbe H. Ifijen,<sup>id</sup>\*<sup>b</sup> Prince Duru,<sup>c</sup> Juliet C. Igboanugo,<sup>d</sup> Innocent Ekanem,<sup>e</sup> Moshood Fagbolade,<sup>f</sup> Abiola Samuel Ajayi,<sup>g</sup> Mayowa George,<sup>h</sup> Best Atoe<sup>i</sup> and John Tsado Matthews<sup>j</sup>

Strontium-based nanoparticles (SrNPs) have emerged as a versatile and promising class of nanomaterials with a wide range of potential applications in healthcare, particularly in the fields of bone regeneration and combating antimicrobial resistance (AMR). Recent research has highlighted the unique properties of SrNPs, including their ability to promote osteogenesis, enhance bone healing, and exhibit strong antimicrobial activity against multidrug-resistant pathogens. These attributes position SrNPs as innovative therapeutic agents with the potential to address challenges such as osteoporosis, bone infections, and the growing global AMR crisis. This comprehensive review critically examines the dual functional potential of SrNPs by analyzing their synthesis methods, physicochemical properties, biological interactions, and translational applications in orthopedic and antimicrobial therapies. Specifically, the review emphasizes SrNPs' ability to enhance bone density, accelerate fracture healing, and reduce the economic burden associated with prolonged treatment and rehabilitation for bone-related diseases. Furthermore, their novel application as antimicrobial agents is explored, highlighting their ability to target bacterial metabolic pathways and combat the rise of antibiotic resistance. The review focuses on the synthesis methods used for SrNPs, particularly co-precipitation, hydrothermal synthesis, and sol-gel techniques. Each method is explored for its ability to produce SrNPs with controlled size, shape, and functionality, while addressing their scalability, cost-effectiveness, and environmental impact. Additionally, the toxicological risks associated with SrNPs are also explored, emphasizing the need for comprehensive preclinical and clinical evaluations to ensure safety for humans and ecosystems. The regulatory and ethical landscape of SrNPs highlights the need for global safety protocols, equitable access, and international cooperation to ensure ethical nanotechnology use. Environmental fate studies address bioaccumulation risks and ecological concerns. This review identifies opportunities and challenges in advancing bone regenerative medicine and combating AMR while emphasizing sustainable and ethical SrNP development for researchers, policymakers, and stakeholders.

 Received 13th January 2025  
 Accepted 20th March 2025

DOI: 10.1039/d5ra00308c

[rsc.li/rsc-advances](http://rsc.li/rsc-advances)

## 1 Introduction

Bone-related disorders, including osteoporosis, fractures, and bone infections, impose a significant burden on global healthcare systems, affecting millions of individuals annually. These

conditions are not only debilitating but also costly to manage, with long-term implications for patient quality of life and economic stability.<sup>1,2</sup> Simultaneously, the rise of antimicrobial resistance (AMR) presents a severe public health crisis, threatening the efficacy of antibiotics that are critical for managing

<sup>a</sup>University of Tennessee, 1000 Volunteer Blvd, Knoxville, TN 37916, USA

<sup>b</sup>Department of Research Outreach, Rubber Research Institute of Nigeria, Iyanomo, Benin City, Nigeria. E-mail: larylans4u@yahoo.com

<sup>c</sup>Emergency Medicine Department, University of Tennessee Medical Center, 1924 Alcoa Hwy, Knoxville, TN 37920, USA

<sup>d</sup>Department of Health, Human Performance and Recreation, University of Arkansas, 155 Stadium Drive, Fayetteville, AR 72701, USA

<sup>e</sup>College of Engineering Technology and SHEQ Specialist-Rochester Gas and Electric (RG&E), Rochester Institute of Technology (RIT), Rochester, NY, USA

<sup>f</sup>Department of Biological Sciences, Mississippi State University, 295 Lee Boulevard, Mississippi State, MS 39762, USA

<sup>g</sup>Texas Southern University, 3100 Cleburne St, Houston, TX 77004, USA

<sup>h</sup>Biological and Agricultural Engineering, Kansas State University, 1016 Seaton Hall, Manhattan, KS 66506, USA

<sup>i</sup>Atoe Specialist Medical Centre Limited, 54, Atoe Street, Off Adolor College Road, Ugbowo, Benin City, Edo State, Nigeria

<sup>j</sup>Department of Chemistry, Ibrahim Badamasi Babangida University, Lapai, Niger State, Nigeria


infections, including those associated with bone-related injuries and implants. The convergence of these challenges highlights an urgent need for innovative approaches that address both bone regeneration and infection control.<sup>3–5</sup>

Strontium (Sr), a trace element with known osteoinductive properties, has emerged as a promising candidate in the search for such solutions.<sup>6</sup> Beyond its well-documented role in bone metabolism, Sr has demonstrated potential in modulating bacterial growth, making it a dual-purpose agent in regenerative medicine and antimicrobial therapy. Strontium-based nanoparticles (SrNPs) have further amplified the therapeutic potential of Sr by offering enhanced bioavailability, controlled release profiles, and customizable surface properties.<sup>7–9</sup> Unlike traditional strontium salts, SrNPs can be engineered to achieve targeted biological interactions, presenting a significant advancement in addressing bone-related health challenges and infections.<sup>10,11</sup>

However, managing bone diseases in an aging population alongside the escalating threat of antibiotic-resistant pathogens remains an increasingly complex issue. Current therapeutic strategies often fall short due to limitations in drug efficacy, side effects, and the risk of recurrent infections, especially in orthopedic applications. In this context, SrNPs present a unique opportunity to bridge these gaps by providing an integrated solution that combines both bone regeneration and antimicrobial defence mechanisms.<sup>12–15</sup>

This review aims to explore and synthesize existing knowledge on SrNPs, focusing specifically on their application in bone regeneration and AMR management. By examining the underlying mechanisms, recent advancements, and potential future developments of SrNPs, the study seeks to provide a comprehensive understanding of how these nanoparticles can address two of the most pressing challenges in modern healthcare. The dual functionality of SrNPs offers not only a promising pathway for improved patient outcomes but also represents a significant leap toward sustainable and multi-functional biomedical solutions.

## 2 Methodology for literature selection

To ensure a comprehensive and rigorous review of the role of strontium-based nanoparticles in modulating bone regeneration and antimicrobial resistance, a systematic approach was employed for selecting relevant research articles. The literature search was conducted using Scopus, Web of Science, PubMed, and Google Scholar.

The search strategy incorporated specific keywords, including “strontium-based nanoparticles,” “bone regeneration,” “osteogenesis,” “antimicrobial resistance,” and “public health implications”. Studies were selected based on their relevance to bone regeneration and antimicrobial resistance, with a focus on those exploring the role of strontium-based nanoparticles in promoting osteogenesis or combating microbial infections. Preference was given to experimental and clinical studies that provided mechanistic insights, *in vitro* or *in vivo*

findings, and potential therapeutic applications. Only high-impact and peer-reviewed sources were included to ensure scientific validity and reliability. Recent advancements and emerging trends were prioritized, particularly those highlighting novel applications, synergistic effects, or innovative formulations of strontium-based nanomaterials in biomedical contexts.

Articles that did not directly address the scope of the review, lacked sufficient experimental data, were not peer-reviewed, or focused on unrelated applications of strontium-based materials were excluded. Additionally, duplicate publications and studies with inconclusive or contradictory findings without substantial supporting evidence were critically assessed before inclusion.

## 3 Synthesis strategies and structural modifications of strontium-based nanoparticles

### 3.1 Synthesis techniques

The synthesis of strontium-based nanoparticles (SrNPs) is a critical factor in determining their physicochemical properties, which, in turn, influence their biological performance and functionality in biomedical applications. Different synthesis methods offer varying degrees of control over parameters such as size, morphology, crystallinity, and surface properties. Presented below is a detailed discussion of three widely utilized synthesis techniques: co-precipitation, hydrothermal methods, and sol-gel processes.<sup>16–18</sup> Table 1 presents a comparative analysis of the advantages and limitations of the co-precipitation, hydrothermal, and sol-gel synthesis techniques.<sup>19–23</sup>

**3.1.1 Co-precipitation.** Co-precipitation is among the most commonly employed techniques for synthesizing SrNPs, owing to its simplicity, cost-efficiency, and scalability, making it suitable for both laboratory and industrial applications. The method involves the chemical precipitation of strontium ions ( $\text{Sr}^{2+}$ ) from an aqueous solution by reacting with a suitable precipitating agent, such as ammonium hydroxide ( $\text{NH}_4\text{OH}$ ) or sodium hydroxide ( $\text{NaOH}$ ).<sup>24,25</sup> This reaction occurs under controlled pH and temperature conditions, which are critical for ensuring the uniformity and reproducibility of the resulting nanoparticles.<sup>26</sup>

The synthesis process begins with the mixing of precursor salts, commonly strontium nitrate ( $\text{Sr}(\text{NO}_3)_2$ ), with the precipitating agent in an aqueous medium. This interaction leads to the formation of insoluble strontium-based compounds, which subsequently nucleate and grow into nanoparticles. To enhance the quality of the nanoparticles, additives such as surfactants or stabilizers are often incorporated. These additives play a vital role in controlling particle size, preventing aggregation, and ensuring a stable dispersion of the nanoparticles.<sup>27,28</sup>

Co-precipitation is particularly advantageous for producing large quantities of SrNPs, making it highly suitable for applications in areas such as coatings for orthopedic implants and composite materials used in bone tissue engineering. The ability to scale up this method without compromising product



Table 1 The advantages and limitations of co-precipitation, hydrothermal, and sol-gel synthesis techniques

Technique	Advantages	Disadvantages
Co-precipitation	<ul style="list-style-type: none"> <li>- Simple and cost-effective method</li> <li>- Scalable for large production</li> <li>- Uniform and crystalline nanoparticles</li> <li>- Short reaction time</li> </ul>	<ul style="list-style-type: none"> <li>- Limited control over particle size and morphology</li> <li>- Potential for aggregation without stabilizers</li> <li>- pH and temperature control are crucial</li> </ul>
Hydrothermal	<ul style="list-style-type: none"> <li>- Precise control over nanoparticle size, shape, and crystallinity</li> <li>- Suitable for producing high-quality nanoparticles</li> <li>- Applicable for advanced biomedical uses (e.g., drug delivery)</li> </ul>	<ul style="list-style-type: none"> <li>- Requires high temperature and pressure, making it more complex and energy-intensive</li> <li>- Expensive equipment (autoclave)</li> </ul>
Sol-gel	<ul style="list-style-type: none"> <li>- High stability and tunable compositions</li> <li>- Good for preparing nanoparticles with customized surface properties</li> <li>- Suitable for applications requiring chemical and thermal stability</li> <li>- Ability to form nanostructured materials</li> </ul>	<ul style="list-style-type: none"> <li>- Complex process with multiple steps (e.g., hydrolysis, polymerization)</li> <li>- Requires calcination at high temperatures</li> <li>- Can be time-consuming</li> </ul>

quality further highlights its utility in practical applications.<sup>29,30</sup> A comparative analysis of the advantages and limitations of the co-precipitation technique, particularly in relation to hydrothermal and sol-gel processes, is presented in Table 1.

For example, in the study by Mohammadi *et al.* (2017), strontium hexaferrite (SrFe<sub>12</sub>O<sub>19</sub>) nanoparticles (SrNPs) were synthesized using the co-precipitation technique, which was chosen for its simplicity and effectiveness in producing nanoparticles with well-defined properties.<sup>31</sup> The synthesis process involved the precipitation of Sr<sup>2+</sup> ions in an aqueous solution, with various chelating agents and surfactants used to control the particle size and morphology. The researchers screened several parameters, including calcination temperature and the type of chelating agent, to determine the optimal conditions for synthesis. Amino acids such as proline, alanine, and aspartic acid, as well as surfactants like SDBS, PVP, and EDTA, were evaluated for their impact on the final nanoparticle properties.

Among these, alanine emerged as the most effective chelating agent, leading to the formation of nanoparticles with the desired properties. In contrast, the surfactants caused an increase in particle size, which was less desirable for the targeted applications. The synthesized SrFe<sub>12</sub>O<sub>19</sub> nanoparticles exhibited notable photocatalytic activity in the degradation of methyl orange under visible light irradiation ( $\lambda > 400$  nm), with a high degradation rate of 95% achieved within 220 minutes. This indicates the potential of these nanoparticles for environmental and industrial applications, particularly in wastewater treatment.

The structural and morphological characteristics of the SrNPs were analyzed using several techniques. Fig. 1 (as referenced in the study) provides scanning electron microscopy (SEM) images that reveal nearly spherical nanoparticles with an average size of 90 nm. The X-ray diffraction (XRD) patterns confirmed the crystalline structure of the nanoparticles, with Rietveld refinement providing precise structural data (Fig. 2). The crystallite size was found to be influenced by the fabrication method, with a smaller crystallite size observed in the co-

precipitation method compared to other methods. Furthermore, the magnetic properties of the SrNPs were investigated using a vibrating sample magnetometer (VSM), and a saturation magnetization ( $M_s$ ) value of 32 emu g<sup>-1</sup> was reported. The co-precipitation technique used in this study successfully yielded SrFe<sub>12</sub>O<sub>19</sub> nanoparticles with enhanced photocatalytic properties, suitable for visible light degradation applications. The particle size, morphology, and magnetic properties were influenced by the choice of chelating agents and other synthesis parameters, with alanine providing the most promising results for achieving nanoparticles with optimal properties.

In the study by Ali *et al.* (2019), pure and Sr-doped cerium oxide (CeO<sub>2</sub>) nanoparticles (with 3 mol% and 5 mol% Sr doping) were synthesized using a simple aqueous co-precipitation method.<sup>32</sup> The synthesis involved cerium nitrate hexahydrate and strontium chloride hexahydrate as precursors without the

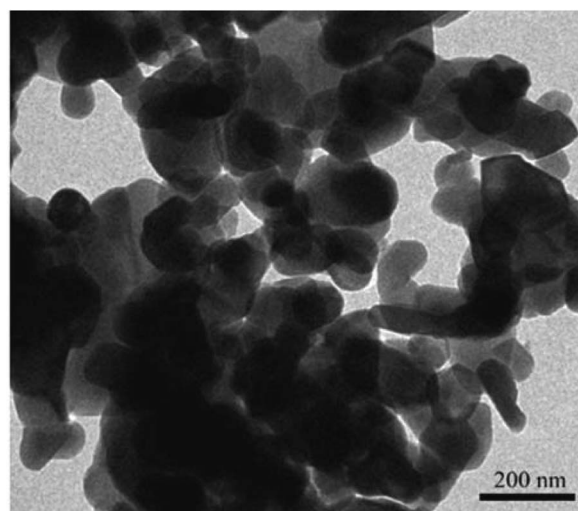


Fig. 1 Micrographs of strontium hexaferrite obtained by transmission electron microscopy (TEM) of the SGP sample.<sup>31</sup>



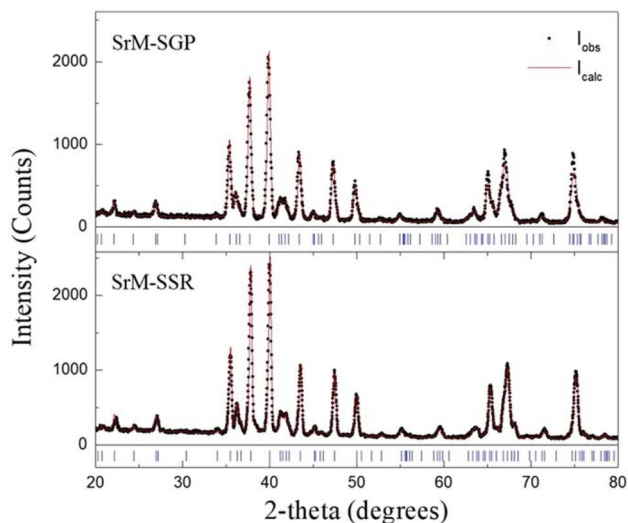


Fig. 2 X-ray patterns and Rietveld refinement adjusts for the strontium hexaferrite prepared by the sol-gel Pechini (SGP) method and the solid-state reaction (SSR) method.<sup>31</sup>

use of any capping agents. This approach resulted in the formation of nanoparticles with distinct structural and optical properties, which were thoroughly characterized using techniques such as X-ray diffraction (XRD), scanning electron microscopy (SEM), transmission electron microscopy (TEM), energy-dispersive X-ray (EDX), Raman spectroscopy, and UV-Vis spectroscopy.

The SEM images presented in Fig. 3a and b show that the 3 mol% and 5 mol% Sr-doped CeO<sub>2</sub> nanoparticles exhibited dot-like structures with noticeable agglomeration. The lack of a capping agent contributed to this agglomeration, as particles tend to cluster due to high surface energy. However, the agglomeration was more prominent in the 3 mol% Sr-doped CeO<sub>2</sub> nanoparticles. These results highlight the influence of doping concentration on particle morphology, where higher Sr-doping led to increased agglomeration. To further confirm the particle morphology and size, TEM images presented in Fig. 4a and b revealed that the average particle size of the

3 mol% Sr-doped CeO<sub>2</sub> nanoparticles was around  $8 \pm 1$  nm, and that of the 5 mol% Sr-doped CeO<sub>2</sub> nanoparticles was  $5 \pm 1$  nm. Interestingly, the particle size decreased with increasing Sr doping, likely due to the substitution of Ce(IV) ions by smaller Sr ions. This ion substitution causes lattice contraction, leading to a reduction in nanoparticle size. The XRD analysis confirmed that the synthesized nanoparticles exhibited a fluorite structure, which is typical for CeO<sub>2</sub>. The crystallite size, determined by Debye-Scherrer analysis, was found to be in the range of 6–10 nm, consistent with the results from the SEM and TEM images. The slight variation in crystallite size with different doping concentrations is attributed to the influence of Sr on the CeO<sub>2</sub> lattice.

The UV-Vis spectroscopy analysis revealed a significant change in the band gap of the Sr-doped CeO<sub>2</sub> nanoparticles. The band gap of pure CeO<sub>2</sub> was around 3.2 eV, while for the 3 mol% and 5 mol% Sr-doped CeO<sub>2</sub> nanoparticles, the band gap increased to 3.7 eV. This blue shift in the band gap indicates that Sr doping affects the electronic structure of CeO<sub>2</sub>, which may be related to the modification of the absorption characteristics and enhanced photocatalytic properties. The shift of the absorption edge to lower wavelengths also suggests that Sr doping enhances the material's ability to absorb in the visible light region. In a nutshell the co-precipitation method effectively synthesized Sr-doped CeO<sub>2</sub> nanoparticles with tunable particle size and optical properties. The results from SEM, TEM, and XRD analyses confirmed the spherical morphology and fluorite structure of the nanoparticles, while the optical properties demonstrated a shift in the band gap with increasing Sr doping. These findings suggest that the co-precipitation method is a promising route for synthesizing cerium oxide-based nanoparticles with enhanced photocatalytic properties.

In a study carried out by Huynh *et al.* (2021), the synthesis of strontium lanthanum vanadate (La<sub>1-x</sub>Sr<sub>x</sub>VO<sub>3</sub>, LSVO) nanoparticles (NPs) was achieved through a modified co-precipitation method followed by hydrogen reduction.<sup>33</sup> The aim was to produce well-dispersed LSVO NPs with a homogeneous size distribution, which is essential for their application in electrochemical devices, particularly in solid oxide fuel cells. Traditional synthesis methods had been unable to achieve such

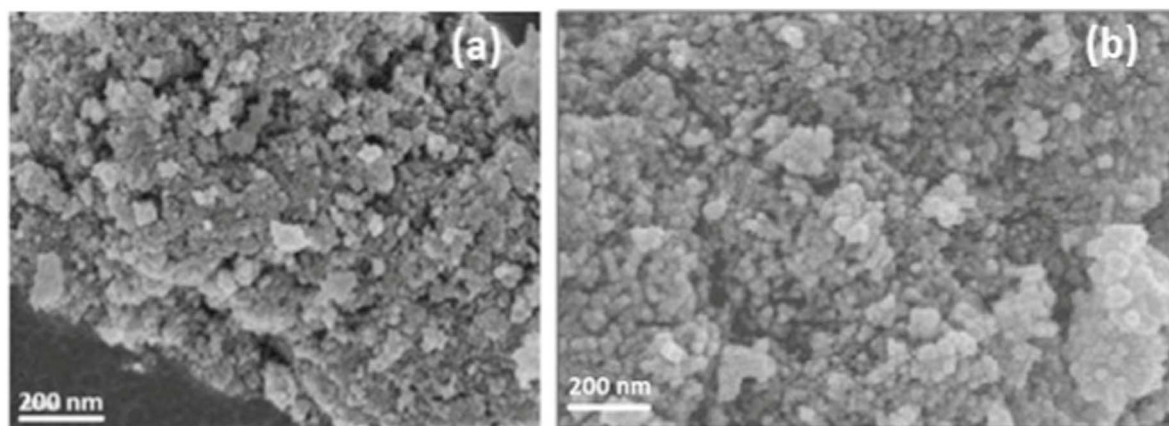


Fig. 3 SEM images of (a) 3 mol% Sr-doped CeO<sub>2</sub> NPs. (b) 5 mol% Sr-doped CeO<sub>2</sub> NPs.<sup>32</sup>

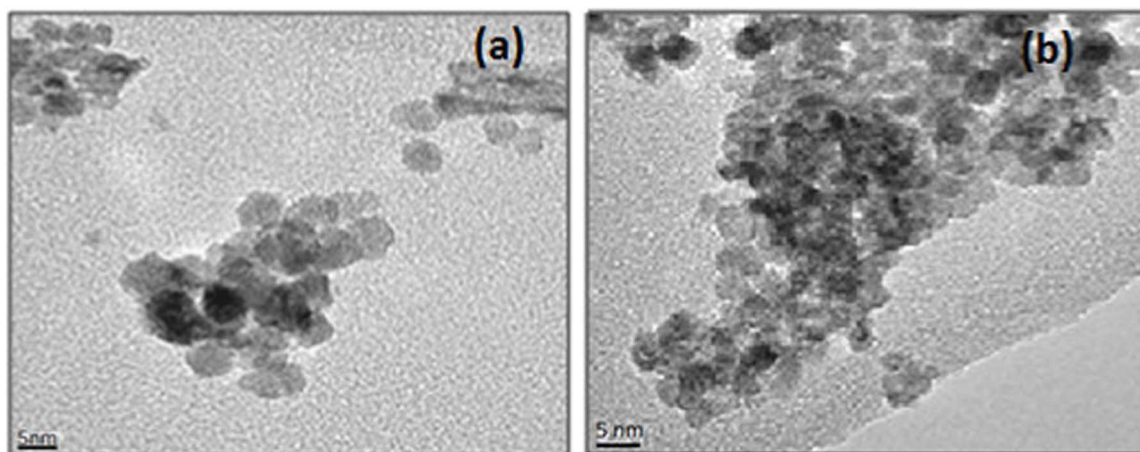


Fig. 4 TEM images of (a) 3 mol% Sr-doped  $\text{CeO}_2$  NPs. (b) 5 mol% Sr-doped  $\text{CeO}_2$  NPs.<sup>32</sup>

uniformity, often resulting in poor dispersion and size variation.

The co-precipitation technique played a crucial role in overcoming these challenges. By using this method, the researchers were able to achieve LSVO NPs with uniform sizes in the range of 50–100 nm, which is important for their electrochemical performance. The NPs were free of any secondary phases, as confirmed by X-ray diffraction (XRD) analysis. This indicates that the modified co-precipitation method not only produced nanoparticles with controlled size but also ensured high purity and crystallinity, which are essential for the material's functional properties in devices.

The hydrogen reduction step at a relatively low temperature of 700 °C further contributed to enhancing the material's properties. This low-temperature treatment helped to maintain the structural integrity of the NPs while facilitating the reduction of the vanadate precursor, which is critical for optimizing the electrical conductivity and work function of LSVO NPs.

The effect of Sr substitution was also studied, showing that the presence of Sr in the LSVO structure influenced the work function values of the NPs, which were measured in the range of 2.13 to 3.62 eV. This variation in work function is important for optimizing LSVO's performance in thermionic devices. The co-precipitation method used in this study successfully produced homogeneous, well-dispersed LSVO NPs with a controlled size and a high degree of purity. This method significantly enhanced the material's suitability for electrochemical applications by improving its electrical conductivity and work function, making it a promising candidate for solid oxide fuel cell anodes and thermionic devices.

Vallimeena and Helina (2023) investigated the synthesis of 3D cauliflower-shaped Sr-doped  $\text{SnO}_2$  nanoparticles using a simple co-precipitation method.<sup>34</sup> This study focuses on producing nanoparticles with a unique 3D morphology, which can significantly enhance light harvesting and electron transport—two crucial features for photocatalytic applications. The co-precipitation method allowed the researchers to synthesize Sr-doped  $\text{SnO}_2$  NPs at ambient temperature without the need

for high-temperature conditions, which is an advantage in terms of energy efficiency and controlling the nanoparticle size. The addition of 7 wt% Sr doping played a significant role in modifying the structure and improving the photocatalytic properties of the  $\text{SnO}_2$  nanoparticles. The resulting nanoparticles exhibited a 3D cauliflower-like morphology, which is not only visually striking but also beneficial for photocatalysis. The increase in surface area and the 3D structure enhanced the light absorption and charge transport across the grain boundaries, which are essential for photocatalytic efficiency.

X-ray diffraction (XRD) analysis revealed that both pure  $\text{SnO}_2$  and Sr-doped  $\text{SnO}_2$  exhibited a tetragonal structure, indicating that Sr doping did not significantly alter the crystalline phase but contributed to modifying the particle morphology. Photoluminescence (PL) spectra further supported the idea that the Sr-doped nanoparticles exhibited better charge splitting, which translates to improved photocatalytic activity. The electrochemical impedance spectroscopy (EIS) results showed that the charge transfer resistance of the 3D cauliflower-shaped Sr-doped  $\text{SnO}_2$  nanoparticles was low, validating the enhanced electron transport properties. This feature is crucial for photocatalytic processes, where efficient electron transfer is necessary to drive reactions such as dye degradation.

The study's significant finding was that the 3D cauliflower-shaped morphology of the Sr-doped  $\text{SnO}_2$  nanoparticles led to higher photocatalytic activity under visible light compared to pure  $\text{SnO}_2$ , as demonstrated by the degradation of methylene blue (MB) dye solution. In general, the co-precipitation method was successful in synthesizing 3D cauliflower-shaped Sr-doped  $\text{SnO}_2$  nanoparticles with excellent photocatalytic properties. The unique morphology and the role of Sr doping in improving light harvesting, electron transport, and charge splitting made these nanoparticles highly effective for photocatalytic applications under visible light.

**3.1.2 Hydrothermal methods.** Hydrothermal synthesis is a versatile and efficient method for the crystallization of SrNPs from an aqueous solution under elevated temperature and pressure conditions within a sealed autoclave. This technique is



particularly valued for its ability to produce nanoparticles with precise control over size, shape, and crystalline structure, which are critical attributes for biomedical applications.<sup>35,36</sup>

The process begins with the dissolution of precursors, such as strontium salts, along with a reducing or oxidizing agent in water. The prepared solution is then placed in an autoclave, where it is subjected to high temperatures (typically ranging from 120–300 °C) and elevated pressures. These conditions promote the nucleation and controlled growth of SrNPs under supersaturated states, ensuring uniformity and reproducibility. The reaction parameters, including temperature, pressure, and reaction duration, are meticulously adjusted to fine-tune the physicochemical properties of the nanoparticles.<sup>37,38</sup>

Hydrothermal methods are particularly well-suited for producing high-quality SrNPs designed for specific biomedical uses, such as drug delivery systems and implant coatings. The precise control over particle characteristics offered by this technique allows for the customization of nanoparticles to meet the stringent requirements of advanced medical applications. Table 1 illustrates a comparative analysis of the hydrothermal method in relation to the co-precipitation and sol-gel processes.<sup>39</sup>

For example, Zhang *et al.* (2015) successfully synthesized strontium titanate (SrTiO<sub>3</sub>) nanoparticles through a single-step hydrothermal process at 220 °C under strong alkaline conditions, using anatase titanium dioxide (TiO<sub>2</sub>) and strontium hydroxide octahydrate (Sr(OH)<sub>2</sub>·8H<sub>2</sub>O) as starting materials.<sup>40</sup> The X-ray diffraction (XRD) analysis confirmed that the product matched the standard SrTiO<sub>3</sub> data, indicating high purity and crystallinity. The crystalline structure was further refined with the help of Highscore Plus and Maud software, ensuring the product was free from secondary phases, a common issue in other synthesis methods.

The hydrothermal method controlled the morphology and particle size of the SrTiO<sub>3</sub> nanoparticles, resulting in uniform cubic-shaped particles with sizes ranging from 32 to 45 nm. Field emission scanning electron microscopy (FE-SEM) and energy dispersive spectroscopy (EDS) confirmed the regular

cubic morphology and perovskite phase of the nanoparticles. SEM images (Fig. 5) show cubic nanoparticles with uniform sizes, demonstrating the effectiveness of the hydrothermal process in producing well-dispersed particles. For instance, the SEM image of sample S2-40 further highlighted the uniform cubic crystals, reinforcing the consistency of the hydrothermal synthesis.

The study also examined the influence of varying the Sr/Ti molar ratio and reaction duration on the particle properties. Increasing the Sr/Ti ratio from 1 to 2 resulted in smaller particles, while extending the reaction time from 20 to 60 hours led to larger particles. SEM images (Fig. 6) illustrate these trends, with samples having a higher Sr/Ti ratio and longer reaction times showing larger particle sizes. This behavior was consistent with the particle size distribution, ranging from 32 to 45 nm. Transmission electron microscopy (TEM) micrographs (Fig. 7) confirmed the regular cubic morphology, with the selected area electron diffraction (SAED) pattern revealing the polycrystalline nature of the material. The high-resolution TEM (HRTEM) image showed clear lattice fringes corresponding to the (110) crystal plane, supporting the XRD results and highlighting the excellent crystallinity.

The hydrothermal process also resulted in nanoparticles with a high specific surface area (up to 32.98 m<sup>2</sup> g<sup>-1</sup>), enhancing their potential for photocatalytic applications. This was an improvement over SrTiO<sub>3</sub> nanoparticles synthesized by solid-state reactions, which typically have smaller surface areas. TEM images (Fig. 8) further confirmed the consistency of particle sizes and morphologies observed in the SEM and XRD analyses, reinforcing the role of the hydrothermal method in producing nanoparticles with high surface area and uniform shape. Overall, the hydrothermal synthesis of SrTiO<sub>3</sub> nanoparticles produced high-quality, uniform particles with excellent crystallinity and large surface area, making them suitable for various advanced material applications, especially in photocatalysis.

In the study by Ueno *et al.* (2015), silver (Ag) nanoparticle-loaded strontium titanate (SrTiO<sub>3</sub>) nanoparticles were

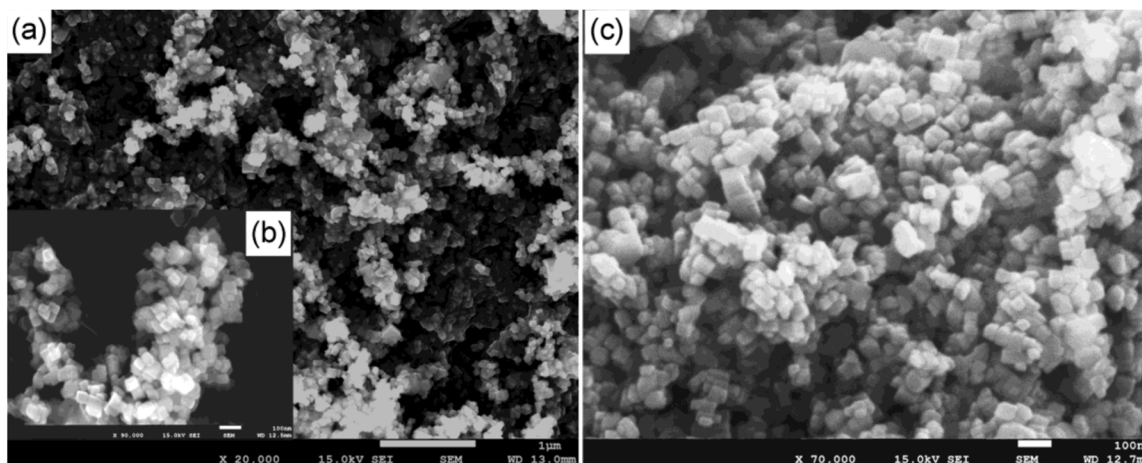


Fig. 5 SEM micrographs of the SrTiO<sub>3</sub> nanoparticles: (a and b) S1-40, (c) S2-40.<sup>40</sup>

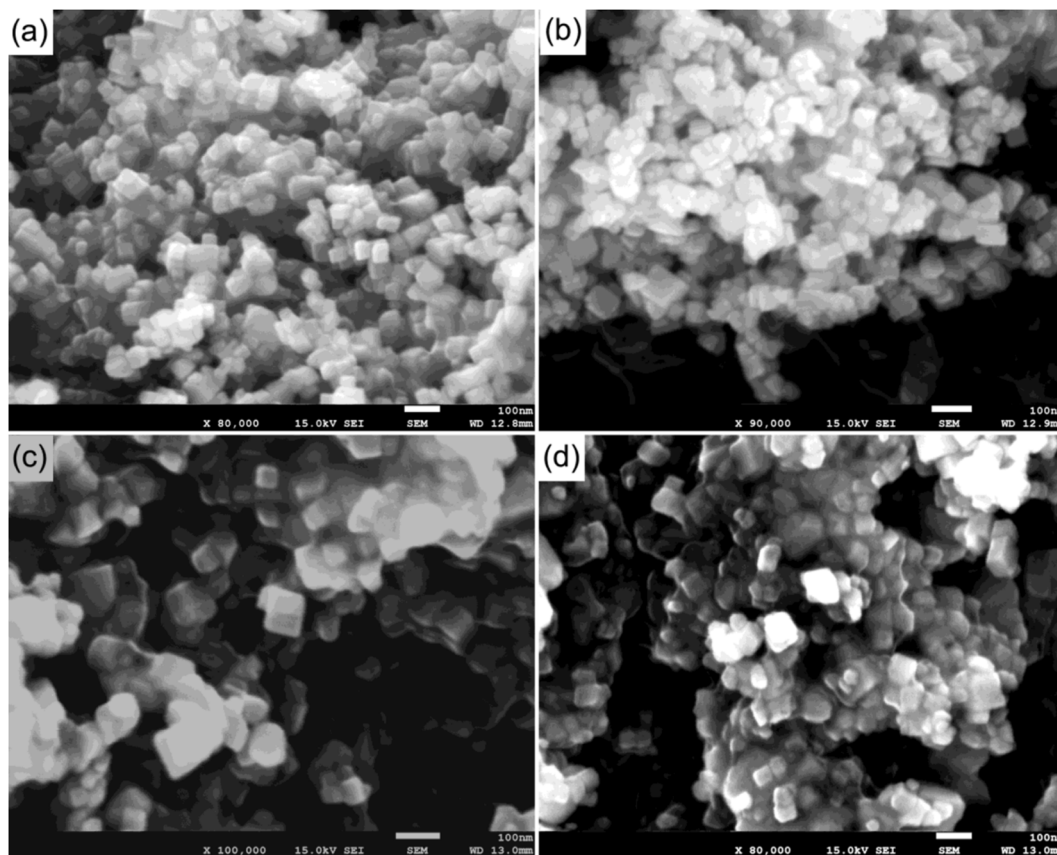


Fig. 6 SEM micrographs of SrTiO<sub>3</sub> nanoparticles: (a) S1-20, (b) S2-20, (c) S1-60, (d) S2-60.<sup>40</sup>

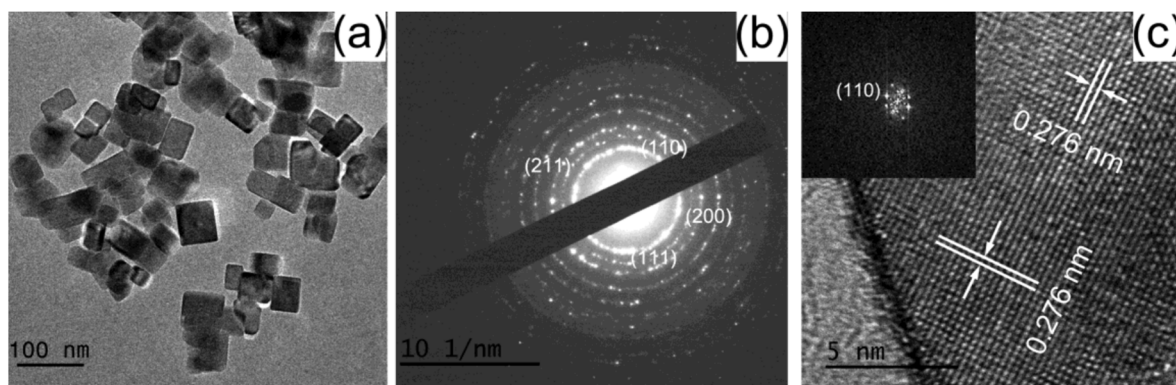


Fig. 7 TEM micrographs of S1-20: (a) 100 nm, (b) SAED, (c) HRTEM.<sup>40</sup>

synthesized using a sol-gel-hydrothermal method.<sup>21</sup> The process involved preparing titanium oxide precursor gels incorporating Ag<sup>+</sup> and Sr<sup>2+</sup> ions at various molar ratios, followed by hydrothermal treatment at 230 °C in Sr(OH)<sub>2</sub> aqueous solutions. The XRD patterns of the synthesized hybrid particles, demonstrated that precursor gels without Sr<sup>2+</sup> ions (Ag : Sr : Ti = 1 : 0 : 4) produced hybrid nanoparticles containing impurities such as anatase- and rutile-type TiO<sub>2</sub>. In contrast, gels with Sr<sup>2+</sup> ions yielded impurity-free Ag-SrTiO<sub>3</sub> hybrid particles. A notable shift in the XRD peaks originating from SrTiO<sub>3</sub> was observed,

indicating the incorporation of hydroxyl groups into the SrTiO<sub>3</sub> lattice, which was further corroborated by thermogravimetric analysis (TG-DTA).

The TG-DTA analysis, revealed a weight loss up to approximately 2.5%, suggesting the presence of hydroxyl groups in the hybrid particles. The incorporation of these groups contributed to a slight peak shift in the XRD patterns of SrTiO<sub>3</sub>. The weight loss attributed to hydroxyl ions increased with the Sr molar fraction in the precursor gels. This structural modification,



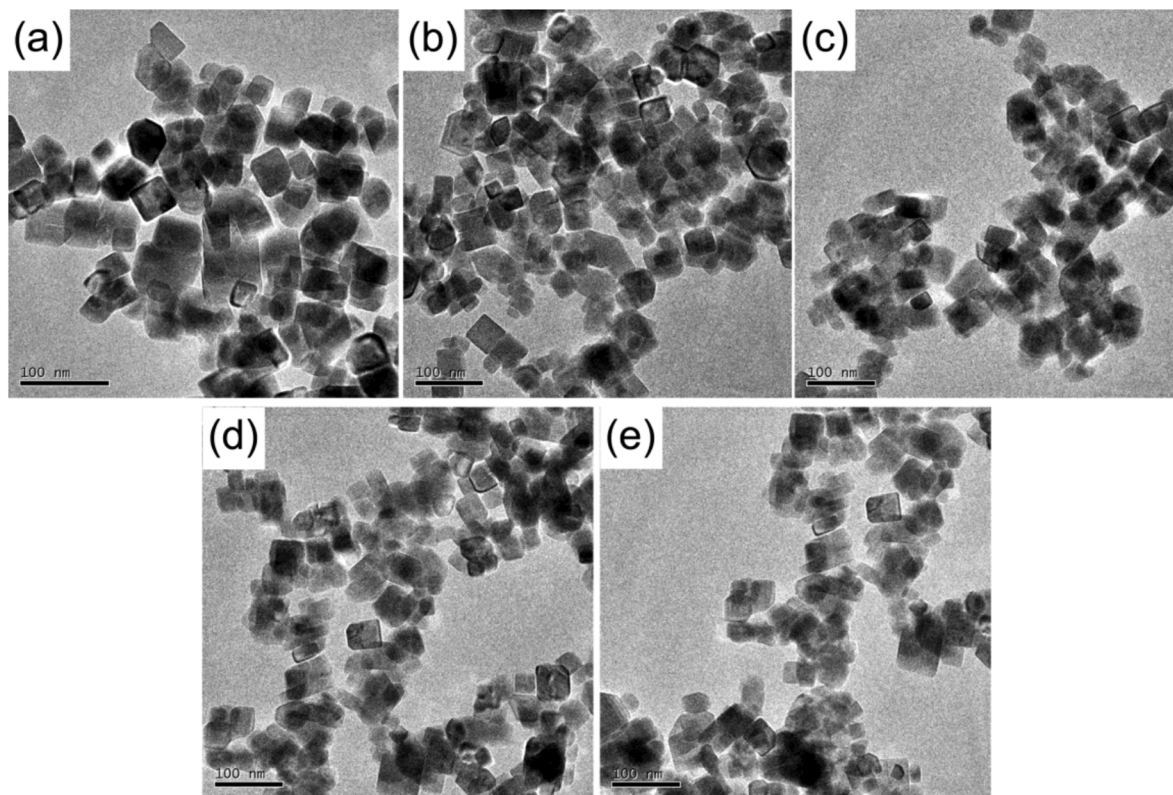


Fig. 8 TEM micrographs of SrTiO<sub>3</sub> nanoparticles: (a) S2-20, (b) S1-40, (c) S2-40, (d) S1-60, and (e) S2-60.<sup>40</sup>

induced by hydroxyl incorporation, highlighted the role of the Sr content in tailoring the hybrid particle properties.

Secondary electron images obtained *via* STEM, revealed the dendritic structure of the Ag–SrTiO<sub>3</sub> hybrid particles, with the particle size decreasing as the Sr molar fraction increased (Fig. 9). This dendritic growth mechanism was consistent with diffusion-limited aggregation phenomena, where rapid nucleation and anisotropic surface tension induced the characteristic branching. Ag nanoparticles formed concurrently with SrTiO<sub>3</sub> dendrites, as Ag<sup>+</sup> ions released from the dissolving precursor gels reacted with OH<sup>−</sup> ions under hydrothermal conditions, resulting in nanocrystalline Ag precipitates decorating the SrTiO<sub>3</sub> surfaces.

The XRD patterns confirmed the presence of Ag and SrTiO<sub>3</sub> phases without observable shifts in the SrTiO<sub>3</sub> peaks, indicating consistent structural integrity irrespective of the Ag content (Fig. 10). The findings underscored the versatility of the sol–gel–hydrothermal synthesis technique in producing hierarchical hybrid nanoparticles with tunable properties, making them promising candidates for multifunctional applications.

Zhou *et al.* (2020) utilized this technique to prepare Sr-doped hydroxyapatite (HA) nanoparticles, demonstrating that Sr incorporation influenced the lattice parameters and crystal size while maintaining the overall crystallinity regardless of increasing Sr concentrations.<sup>41</sup> Both experimental results and density functional theory simulations agreed on the structural adjustments caused by Sr doping, which preferentially occupied specific calcium sites in the HA lattice. This resulted in

improved structural stability, as evidenced by favourable formation energies.

In a similar vein, Boulkroune *et al.* (2019) synthesized Sr-doped ZnS nanoparticles *via* a surfactant-free hydrothermal route.<sup>42</sup> The Sr incorporation did not introduce new crystalline phases but influenced the crystallite size, ranging from 2.24 to 2.51 nm, and led to the aggregation of nanoparticles into spherical forms. Furthermore, Sr doping altered the optical properties, reducing the bandgap energy from 3.42 eV to 3.38 eV and enhancing the photocatalytic degradation of methyl orange, indicating improved photocatalytic activity with increased Sr content.

Phoon *et al.* (2018) explored hydrothermal synthesis for producing strontium titanate (SrTiO<sub>3</sub>) nanoparticles, varying reaction temperatures between 60 °C and 180 °C.<sup>43</sup> The nanoparticle size and morphology were strongly temperature-dependent, with the sample prepared at 150 °C exhibiting the most uniform size (approximately 47 nm), high surface area (17.00 m<sup>2</sup> g<sup>−1</sup>), and the best photoelectrochemical water-splitting performance. The hydrothermally synthesized nanoparticles were subsequently deposited on fluorine-doped tin oxide (FTO) glass, where optimized deposition parameters yielded films with high uniformity and enhanced photocurrent densities, further advancing their hydrogen generation capabilities.

Devi *et al.* (2020) examined the impact of hydrothermal growth duration on SrTiO<sub>3</sub> nanoparticle properties. By extending the growth period from 12 to 48 hours, the morphology



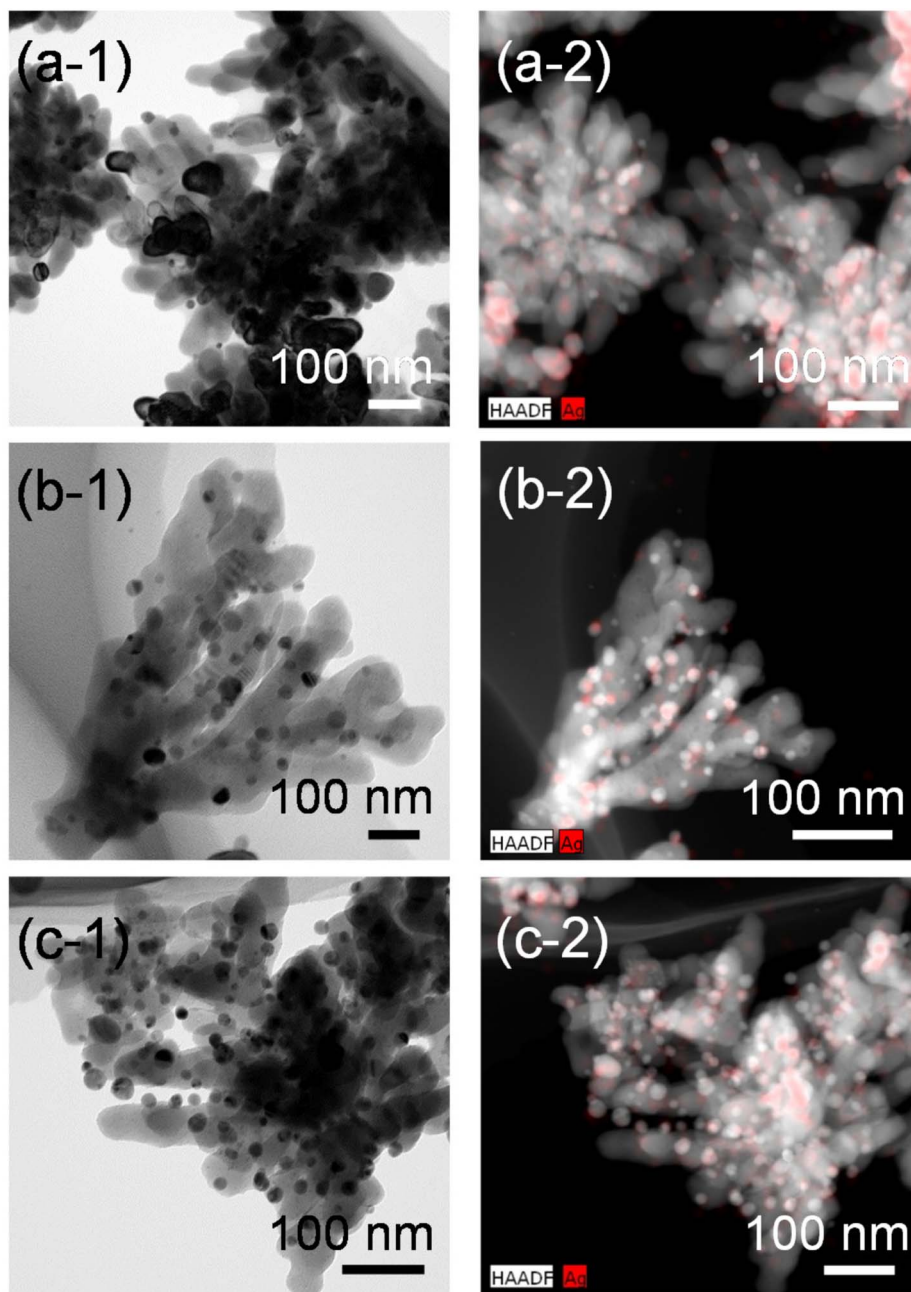


Fig. 9 FE-TEM images of the Ag–SrTiO<sub>3</sub> hybrid particles synthesized from the gels with molar ratios of (a-1) Ag : Sr : Ti = 1 : 4 : 4; (b-1) 2 : 4 : 4 and (c-1) 4 : 4 : 4 by the hydrothermal treatment at 230 °C for 6 h in Sr(OH)<sub>2</sub> aqueous solutions. (a-2–c-2) Corresponding high-angle annular dark field (HAADF)-STEM images with STEM-energy dispersive X-ray spectroscopy (EDX) mapping of the hybrid particles shown in (a-1–c-1), respectively. Red-colored regions correspond to the Ag nanoparticles.<sup>21</sup>

evolved from spherical to cubic, while crystallinity improved as evidenced by increased diffraction peak intensities.<sup>44</sup> Enhanced crystallinity and cubic morphology contributed to improved thermoelectric properties, with the sample grown for 24 hours achieving a significant power factor. Rahman *et al.* (2020) synthesized both bare and N-doped SrTiO<sub>3</sub> nanoparticles using a citric acid-assisted hydrothermal method.<sup>45</sup> Post-calcination, the nanoparticles exhibited monodispersity with an average size of 50 nm but also displayed surface roughness and oxygen vacancies due to annealing. Nitrogen doping effectively altered

the electronic band structure, extending light absorption into the visible spectrum and improving photocatalytic performance. These studies collectively illustrate the versatility and effectiveness of the hydrothermal synthesis technique in tailoring structural, morphological, and functional properties of Sr-based nanoparticles.

**3.1.3 Sol-gel processes.** The sol-gel method is a highly adaptable chemical process utilized for synthesizing SrNPs with exceptional stability and customizable compositions. This technique transitions a system from a liquid “sol” (a colloidal



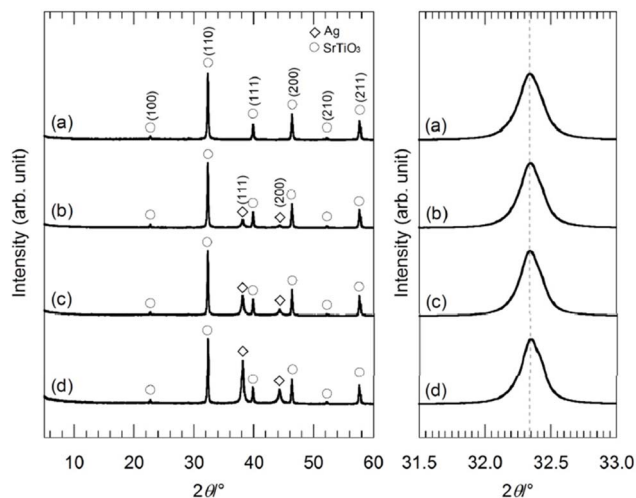


**Fig. 10** (Left) XRD patterns of the hybrid particles synthesized from the precursor gels with molar ratios of (a) Ag : Sr : Ti = 0 : 4 : 4; (b) 1 : 4 : 4; (c) 2 : 4 : 4; and (d) 4 : 4 : 4 by the hydrothermal treatment at 230 °C for 6 h in Sr(OH)<sub>2</sub> aqueous solutions; (Right) XRD peaks of the hybrid particles indexed as (110) of SrTiO<sub>3</sub> in the  $2\theta$  range of 31.5–33.0°.<sup>21</sup>

suspension of precursors) to a solid “gel” phase through controlled chemical reactions.<sup>46,47</sup>

In the sol–gel process, strontium precursors such as alkoxides or nitrates undergo hydrolysis and subsequent polymerization, forming a three-dimensional network. The resulting gel is carefully dried to remove solvents and then subjected to calcination at high temperatures. This step eliminates organic residues and converts the gel into crystalline SrNPs. By fine-tuning reaction parameters and incorporating additives like stabilizers or surfactants, the surface characteristics of the nanoparticles can be modified, and issues such as particle aggregation can be minimized.<sup>48,49</sup>

The sol–gel method is particularly advantageous for applications demanding superior chemical and thermal stability. It is well-suited for creating bone scaffolds that must withstand

physiological stresses or antimicrobial coatings that encounter challenging environmental conditions. The method’s ability to tailor composition and enhance durability makes it a preferred choice for these specialized applications.<sup>49,50</sup> Table 1 provides a comparative analysis of the sol–gel method, hydrothermal synthesis, and co-precipitation techniques.

For example, the study by Romańczuk-Ruszk *et al.* (2022) employed a sol–gel synthesis method to create binary xerogel systems of Al<sub>2</sub>O<sub>3</sub>/SrCO<sub>3</sub> with Sr/Al molar ratios of 0.1, 0.25, 0.5, and 1.0.<sup>51</sup> The metallic strontium precursor played a crucial role in influencing the final properties of the xerogels. This synthesis approach facilitated the formation of highly dispersed and stable strontium carbonate phases, which are critical for the high dispersion and catalytic activity of platinum nanoparticles deposited on these supports.

The annealing process significantly influenced the morphological and structural characteristics of the xerogels, as demonstrated by SEM and TEM analyses. SEM micrographs in Fig. 11 revealed that the xerogels with a Sr/Al ratio of 1.0 exhibited a non-homogeneous structure when annealed at 1000 °C (1273 K), with noticeable phase aggregation. However, annealing at higher temperatures, such as 1150 °C (1423 K) and 1300 °C (1573 K), resulted in a monolithic structure with uniform composition and no evidence of crystallized strontium phases. This transformation suggests the critical role of thermal treatment in achieving a homogeneous material with enhanced structural integrity.

TEM analysis further provided insights into the nanoscale properties of these xerogels. As shown in Fig. 12, samples annealed at 500 °C displayed varying morphologies depending on the Sr/Al molar ratio. At lower ratios (0.1), the structure remained relatively amorphous, while at higher ratios (1.0), strontium-rich phases became more prominent. These observations align with the XRD data, confirming the distribution and aggregation behavior of the strontium carbonate phases within the sol–gel systems.

When platinum nanoparticles were incorporated into the xerogels and the samples were annealed at 500 °C, distinct

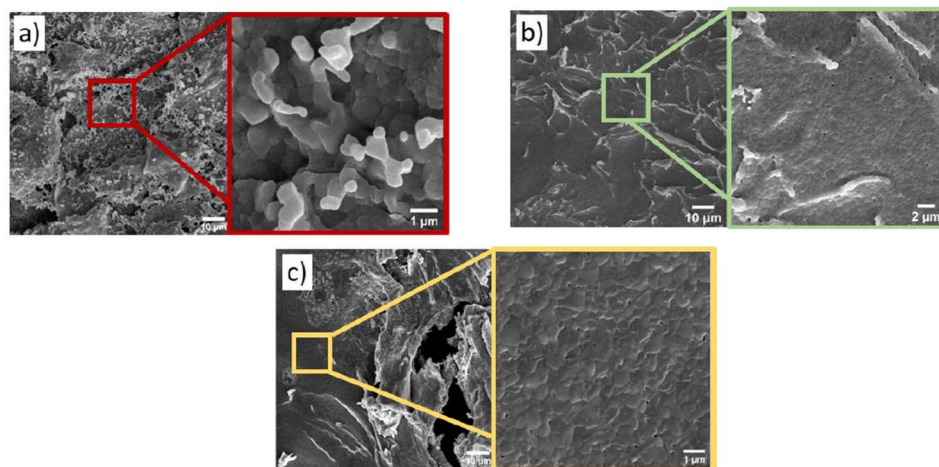


**Fig. 11** SEM micrographs of surface Al<sub>2</sub>O<sub>3</sub>/SrCO<sub>3</sub> xerogels with the 1.0 Sr molar ratio annealed at: (a) 1000 °C (1273 K), (b) 1150 °C (1423 K), and (c) 1300 °C (1573 K).<sup>51</sup>



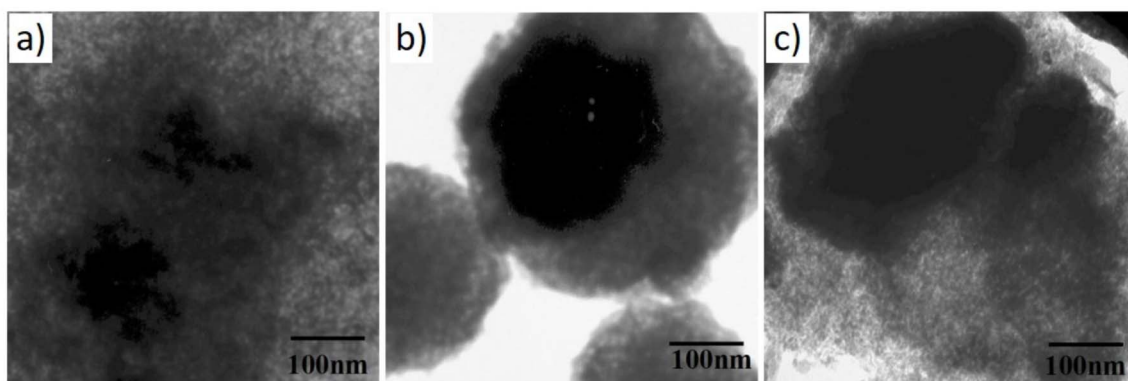


Fig. 12 TEM images of  $\text{Al}_2\text{O}_3/\text{SrCO}_3$  xerogels annealed at 500 °C, illustrating different Sr/Al molar ratios: (a) 0.1, (b) 0.5, and (c) 1.0.<sup>51</sup>

structural variations were observed depending on the Sr/Al molar ratio, as illustrated in Fig. 13. The sample with a 0.5 Sr/Al ratio exhibited unique rod-shaped crystals, which were absent in the other ratios. TEM images also highlighted the presence of amorphous alumina, aggregated strontium carbonate phases, and platinum nanoparticles. The red-marked regions in the images indicate the distribution of platinum, demonstrating effective incorporation and dispersion of the catalyst material. Notably, the high dispersion of platinum, ranging from 42% to 50%, underscores the potential of these materials for catalytic applications.

Overall, the sol-gel synthesis enabled precise control over the composition, morphology, and structural properties of  $\text{Al}_2\text{O}_3/\text{SrCO}_3$  xerogels, making them suitable as supports for platinum-based catalysts. These materials demonstrated a combination of stability, homogeneity, and high dispersion of active phases, which are desirable attributes for catalytic systems in industrial and environmental applications.

In the study by Rehman *et al.* (2022), the sol-gel method was employed to synthesize  $\text{Co}^{2+}$ -substituted strontium hexaferrite nanoparticles ( $\text{Sr}_{1-x}\text{Co}_x\text{Fe}_{12}\text{O}_{19}$ ) with varying cobalt concentrations ( $x = 0.0-0.50$ ).<sup>52</sup> The sol-gel process, a widely used technique for producing nanoparticles, involves the conversion of a solution into a gel phase followed by heat treatment to form

solid nanoparticles. This approach provides precise control over the particle size and composition, making it ideal for the synthesis of ferrites with well-defined structural and magnetic properties.

The X-ray diffraction (XRD) analysis of the synthesized nanoparticles, shown in Fig. 14, revealed the formation of a hexagonal structure characteristic of  $\text{SrFe}_{12}\text{O}_{19}$ . The diffraction peaks, corresponding to the (1 1 0), (1 1 2), and other planes, confirmed the formation of strontium hexaferrite without secondary phases in the undoped sample. However, as the cobalt concentration increased, an undesired hematite phase ( $\text{Fe}_2\text{O}_3$ ) appeared in the XRD spectra, which was likely due to the oxidation of magnetite during calcination. Despite this, the hexagonal structure of the strontium ferrite was maintained, with the peak positions shifting, suggesting the successful substitution of  $\text{Co}^{2+}$  for  $\text{Sr}^{2+}$  ions, which caused slight changes in the crystallographic sites due to the difference in ionic radii. This phase transition and the structural stability of the ferrite were crucial for the enhanced magnetic properties of the doped samples.

The scanning electron microscopy (SEM) images depicted in Fig. 15 revealed that the nanoparticles had a spherical morphology with a uniform distribution, and their size remained consistent around 20–25 nm, regardless of the cobalt concentration. This uniformity is essential for maintaining

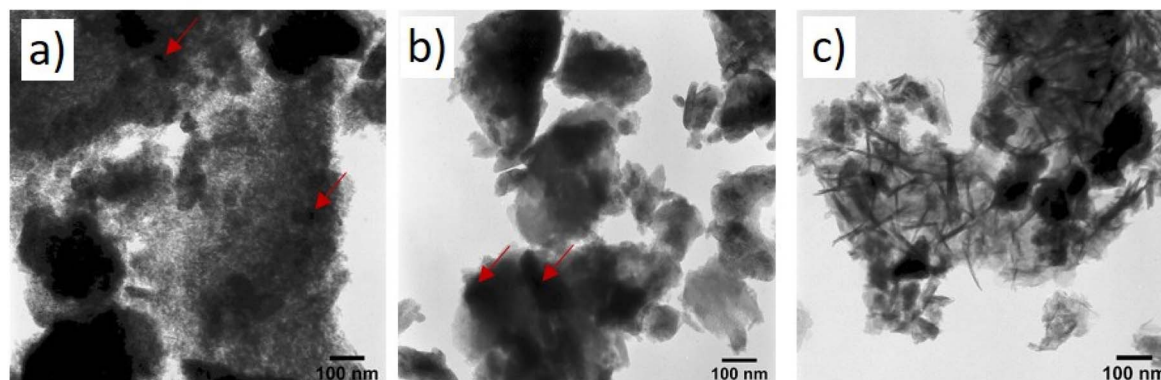


Fig. 13 TEM images of  $\text{Al}_2\text{O}_3/\text{SrCO}_3$  sol-gel incorporated with Pt after annealing at 500 °C, showing molar ratios of: (a) Sr : 0.1 Pt, (b) Sr : 0.25 Pt, and (c) Sr : 0.5 Pt.<sup>51</sup>



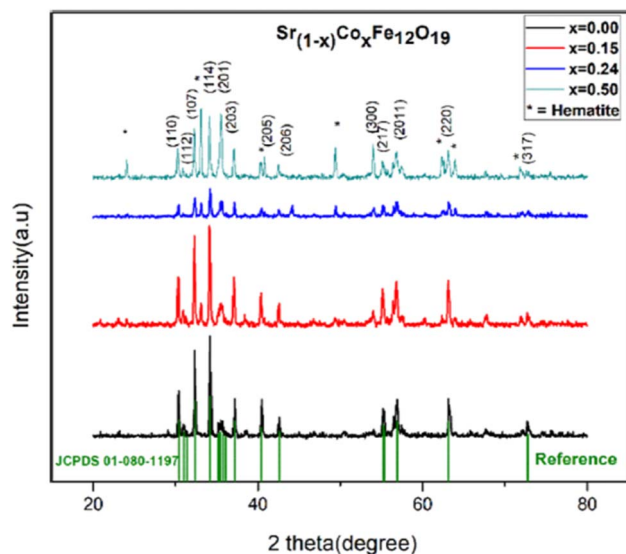


Fig. 14 XRD pattern of  $\text{Sr}_{1-x}\text{Co}_x\text{Fe}_{12}\text{O}_{19}$ .<sup>52</sup>

consistent magnetic and electrical properties across the samples. The SEM images also indicated minimal agglomeration, which is beneficial for optimizing the material's performance in various applications, including magnetic and electronic devices.

The sol-gel method enabled the preparation of nanoparticles with a well-maintained stoichiometry, as confirmed by the

energy-dispersive X-ray (EDX) analysis. The elemental composition was in agreement with the expected ratios of strontium, cobalt, iron, and oxygen, ensuring the desired composition for the magnetic material. Moreover, the Fourier-transform infrared (FTIR) spectra provided further insight into the structure of the nanoparticles, with characteristic absorption bands observed around  $600\text{ cm}^{-1}$  and  $400\text{ cm}^{-1}$ , corresponding to the stretching vibrations of the metal-oxygen bonds in the tetrahedral and octahedral sites of the hexagonal structure.

This synthesis route allowed for the effective incorporation of cobalt into the strontium hexaferrite structure, which not only preserved the hexagonal geometry but also influenced the magnetic and electrical properties, making these nanoparticles suitable for various high-frequency applications such as microwave absorption and electronics.

Sharma *et al.* (2022) explored the synthesis of yttrium-substituted strontium hexaferrite nanoparticles ( $\text{SrFe}_{12-x}\text{Y}_x\text{O}_{19}$ ) using the sol-gel method.<sup>53</sup> This synthesis technique was selected due to its ability to provide precise control over the composition and structure of the nanoparticles. X-ray diffraction (XRD) analysis confirmed the formation of a single-phase M-type hexagonal structure, with no secondary phases observed, indicating successful yttrium substitution into the strontium hexaferrite lattice. Fourier-transform infrared (FTIR) spectroscopy provided additional evidence of the hexagonal ferrite structure, with absorption bands at low wavenumbers that correspond to the stretching vibrations of metal-oxygen bonds in the tetrahedral and octahedral sites, confirming the

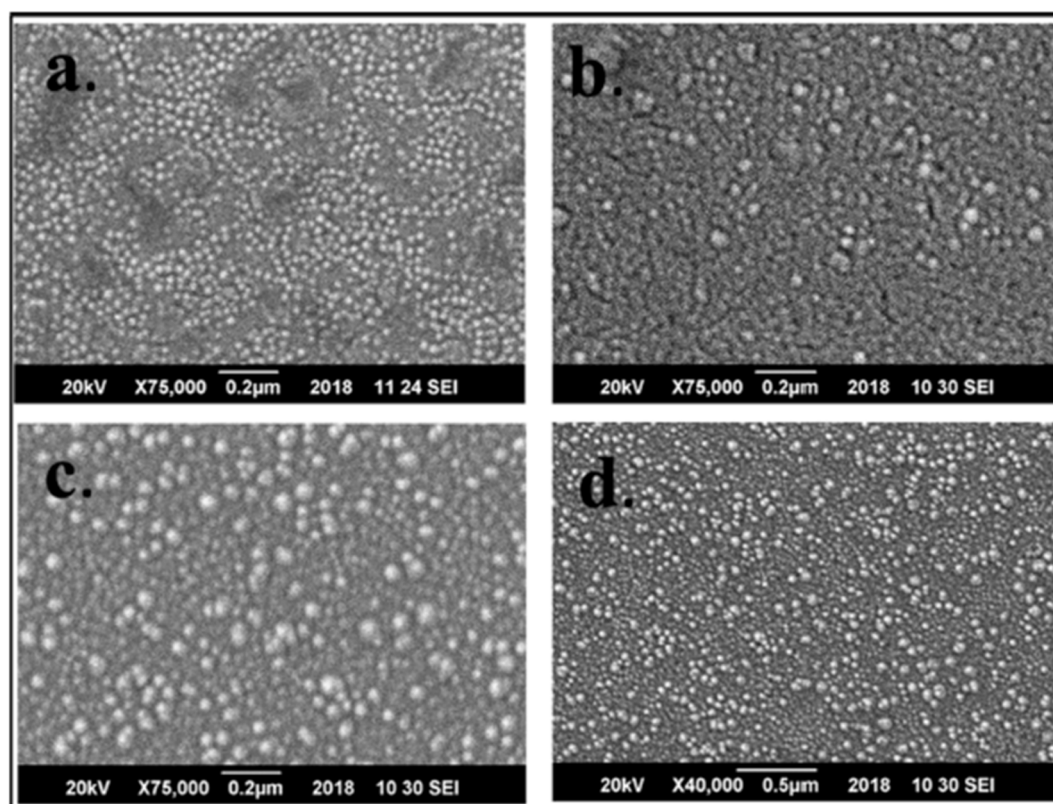


Fig. 15 Morphological analysis using SEM for  $\text{Sr}_{1-x}\text{Co}_x\text{Fe}_{12}\text{O}_{19}$  (a)  $x = 0$ , (b)  $x = 0.15$ , (c)  $x = 0.24$ , and (d)  $x = 0.5$ .<sup>52</sup>



characteristic features of ferrite materials. The magnetic properties of the synthesized nanoparticles were investigated using a vibrating sample magnetometer (VSM). The results revealed a decrease in both saturation magnetization ( $M_s$ ) and coercivity ( $H_c$ ) values upon yttrium substitution. This decrease was attributed to the non-magnetic nature of  $Y^{3+}$  ions, which replaced the magnetic  $Fe^{3+}$  ions in the crystal lattice, thus altering the magnetic interactions within the material. These findings are significant in understanding the role of yttrium in modifying the magnetic properties of strontium hexaferrite and its potential applications in magnetic devices.

Leite *et al.* (2018) focused on the synthesis and biological evaluation of bioactive glass nanoparticles (BGNPs), specifically strontium-doped BGNPs (BGNPs<sub>Sr</sub>), produced *via* the sol-gel method.<sup>54</sup> The sol-gel process allowed for the controlled incorporation of strontium, with BGNPs having a diameter of 55 nm and BGNPs<sub>Sr</sub> a slightly larger diameter of 75 nm. Despite the increase in size, the structural integrity of the nanoparticles was maintained, and no significant alterations were observed due to the inclusion of strontium. The cytocompatibility of both types of nanoparticles was assessed using human umbilical vein endothelial cells (HUVECs) and SaOS-2 cells, with the nanoparticles exhibiting excellent biocompatibility. Notably, the incorporation of strontium in the BGNPs enhanced the tubule networking behavior of HUVECs, suggesting that strontium plays a role in promoting endothelial cell functions relevant to vascularization. Moreover, the dissolution products of the BGNPs, particularly BGNPs<sub>Sr</sub>, supported osteogenic differentiation of human adipose stem cells (hASCs). The BGNPs<sub>Sr</sub> nanoparticles enhanced the expression of key osteogenic genes and proteins, demonstrating their potential to promote bone formation without the need for typical osteogenic inducers. This study highlights the potential of strontium-doped bioactive glass nanoparticles as a valuable tool in bone tissue engineering, particularly in applications that require both osteogenic differentiation and vascularization.

The study by Zhang *et al.* (2014) highlighted a water-based sol-gel synthesis method for fabricating single-crystal strontium hydroxyapatite (SrHAp) nanorods. The process utilized strontium nitrate and diammonium hydrogen phosphate as precursors.<sup>55</sup> This low-temperature sol-gel method was notable for its simplicity, achieving gelling without requiring catalysts or templating agents. The characterization of SrHAp nanorods synthesized through this method revealed their high crystallinity and structural purity.

The X-ray diffraction (XRD) analysis demonstrated that the synthesized materials exhibited a pure hexagonal SrHAp phase (JCPDS no. 33-1348) with no evidence of peak shifts or secondary phases. These results confirmed the successful formation of SrHAp with refined lattice parameters and  $d$ -spacing values aligning closely with the standard SrHAp database. Crystallite size estimation using Scherrer's formula further validated the nanoscale features of the materials, which were consistent with dimensions observed in electron microscopy studies.

Fourier-transform infrared (FTIR) spectroscopy confirmed the chemical composition of the synthesized SrHAp powders.

Prominent bands associated with phosphate groups were detected, alongside weak bands from carbonate impurities likely originating from environmental  $CO_2$  during synthesis. The presence of hydroxyl and water adsorption bands underscored the material's structural integrity, as expected for pure hydroxyapatite.

Scanning electron microscopy (SEM) analysis provided critical insights into the morphological evolution of SrHAp nanocrystals with aging time (Fig. 16). After 24 hours of aging at 60 °C, irregular agglomerated particles dominated the sample (Fig. 16A). Extending the aging time to 48 hours produced uniform, rod-like nanoparticles with diameters of approximately 30 nm and lengths ranging from 120–180 nm (Fig. 16B). This transformation highlights the role of aging time in controlling particle morphology, as extended aging facilitated anisotropic growth along the  $c$ -axis, leading to the formation of stable SrHAp nanorods.

Transmission electron microscopy (TEM) provided additional structural details for the 48-hour aged sample (Fig. 17). The TEM images confirmed the formation of uniform nanorods, consistent with the SEM findings. High-resolution TEM (HRTEM) imaging (Fig. 17) and the corresponding fast Fourier transformed (FFT) pattern established the single-crystal nature of the nanorods. The measured interplanar distances (0.36 nm along the growth direction and 0.28 nm perpendicular to it) were in good agreement with the  $d$ -spacing of the (002) and (300) planes reported in the literature for SrHAp.

The study concludes that aging time is a crucial parameter for optimizing the morphology and crystalline quality of SrHAp synthesized by the sol-gel method. The approach offers a straightforward and catalyst-free pathway for producing high-purity, monodisperse SrHAp nanorods. This synthesis technique holds potential for applications in areas requiring highly crystalline hydroxyapatite materials.

Schmidt *et al.* (2014) successfully synthesized strontium fluoride (SrF<sub>2</sub>) nanoparticles using the fluorolytic sol-gel method.<sup>56</sup> The characterization of these nanoparticles was performed using dynamic light scattering (DLS), X-ray diffraction (XRD), transmission electron microscopy (TEM), and nitrogen adsorption/desorption measurements (BET). The nanoparticles exhibited a hydrodynamic diameter of approximately 6 nm, with crystallite sizes below 10 nm and a high surface area of 180 m<sup>2</sup> g<sup>-1</sup>. The sols remained highly transparent and stable for several months but tended to undergo gelation over time. The aging process was studied using wide-angle X-ray scattering (WAXS), revealing that Ostwald ripening was not responsible for the gel formation. Fluorine-containing crystalline species were detected by XRD and solid-state <sup>19</sup>F magic-angle spinning (MAS) NMR spectroscopy, indicating the formation of an intermediate phase during the fluorosis reaction.

Youssef *et al.* (2018) synthesized strontium titanate (SrTiO<sub>3</sub>) nanopowders using both sol-gel and solid-state methods to investigate how the synthesis method influences the material's properties.<sup>57</sup> Characterization included X-ray diffraction (XRD), infrared (IR) spectroscopy, thermogravimetric analysis (TGA), differential thermal analysis (DTA), scanning electron



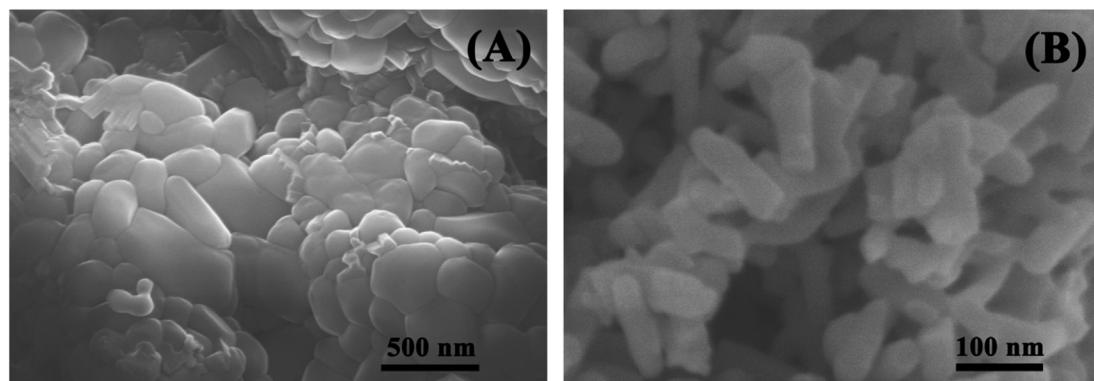


Fig. 16 SEM images of the synthetic crystals aged at 60 °C for 24 hours (A) and 48 hours (B).<sup>55</sup>

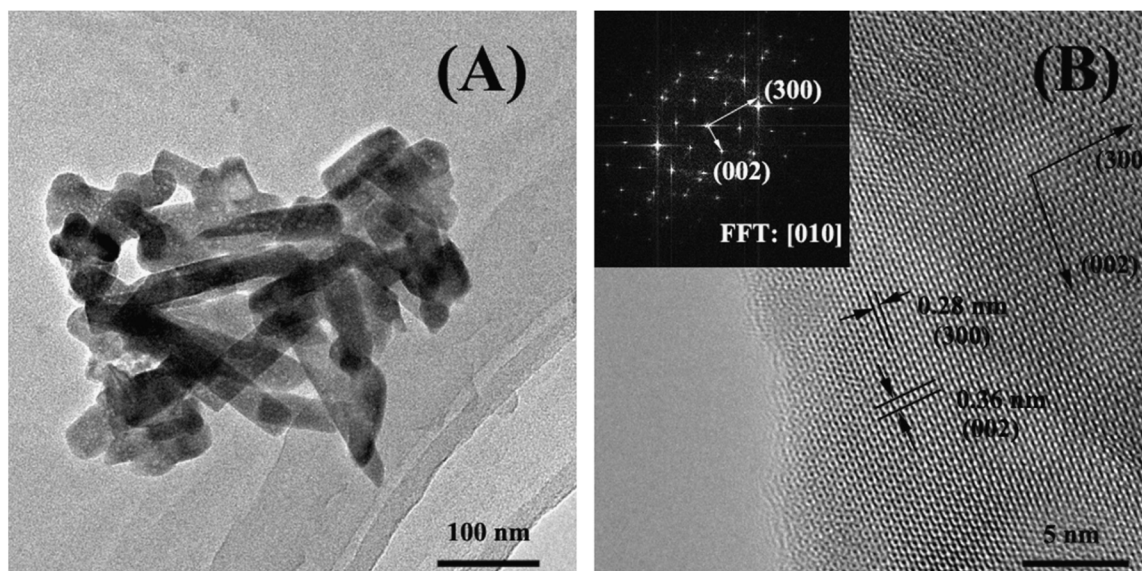


Fig. 17 TEM images of the SrHAp sample aged at 60 °C for 48 hours: (A) a low-magnification image, and (B) a high-magnification image along with the corresponding fast Fourier transformed (FFT) pattern.<sup>55</sup>

microscopy (SEM), and transmission electron microscopy (TEM). XRD analysis confirmed the formation of SrTiO<sub>3</sub> and anatase TiO<sub>2</sub>, depending on the method used. The solid-state route led to the formation of microcrystalline particles, while the sol-gel method produced a more homogeneous nanoparticle sample with sizes in the nanometer range. TEM images revealed nanoparticles with an average size of about 10 nm. The sol-gel synthesized sample exhibited higher magnetization and dielectric constants compared to the solid-state synthesized sample, highlighting the effect of synthesis method on the material's magnetic and dielectric properties.

Alimuddin & Rafeeq (2021) synthesized strontium oxide (SrO) nanoparticles using a simple and cost-effective sol-gel method with strontium nitrate and sodium hydroxide at room temperature.<sup>58</sup> Characterization techniques including X-ray diffraction (XRD), scanning electron microscopy (SEM), and Fourier-transform infrared (FTIR) spectroscopy were used. XRD patterns confirmed the crystalline nature of the nanoparticles,

with crystallite sizes of approximately 80 nm, calculated using the Debye-Scherrer formula. SEM revealed that the morphology of the nanoparticles varied with temperature; at room temperature, they were pseudo-spherical, at 400 °C they formed cubic shapes, and at 600 °C they became cylindrical due to agglomeration. The FTIR spectrum showed a peak at 854.64 cm<sup>-1</sup>, corresponding to the Sr-O bond.<sup>59</sup>

Kumar *et al.* (2023)<sup>59</sup> conducted a comprehensive study on the synthesis and characterization of rare-earth yttrium (Y<sup>3+</sup>)-substituted strontium hexaferrite (SrFe<sub>12-x</sub>Y<sub>x</sub>O<sub>19</sub>) nanoparticles using a chemical-based sol-gel technique, providing a broader perspective compared to Sharma *et al.* (2022).<sup>53</sup> Both studies confirmed the formation of a single-phase hexagonal structure through X-ray diffraction (XRD), with Sharma *et al.* highlighting the absence of secondary phases as evidence of successful yttrium substitution. Kumar *et al.* (2023)<sup>59</sup> further analyzed the crystallite sizes and strain using the Williamson-Hall method, revealing slight lattice constant variations with increasing Y<sup>3+</sup>



content, which were not explicitly discussed in Sharma *et al.*<sup>53</sup>'s study.

In terms of morphology, Kumar *et al.* (2023)<sup>59</sup> employed scanning electron microscopy (SEM) to illustrate hexagonal crystal symmetry with agglomeration, while also using transmission electron microscopy (TEM) and high-resolution TEM (HRTEM) to confirm lattice fringe distances and grain size variations. These imaging techniques provided a more detailed structural assessment compared to Sharma *et al.* who did not present SEM or TEM data. The magnetic properties of the synthesized nanoparticles were a key focus in both studies, with each reporting a decrease in saturation magnetization ( $M_s$ ) due to the replacement of magnetic  $\text{Fe}^{3+}$  ions by non-magnetic  $\text{Y}^{3+}$  ions. However, while Sharma *et al.*<sup>53</sup> observed a concurrent decrease in coercivity ( $H_c$ ), Kumar *et al.*<sup>59</sup> found that  $H_c$  increased from 5983 to 6595 Oe with higher  $\text{Y}^{3+}$  content, suggesting an enhancement in magnetocrystalline anisotropy, possibly influenced by differences in synthesis conditions or particle size effects.

A key distinction between the two studies is Kumar *et al.* (2023)'s<sup>59</sup> exploration of optical properties, which Sharma *et al.* (2022)<sup>53</sup> did not investigate. Photoluminescence (PL) spectra in Kumar *et al.* (2023)'s study revealed an emission peak at 481 nm, while UV-Visible spectroscopy showed a decrease in band gap energy from 2.3 eV to 1.93 eV as  $\text{Y}^{3+}$  concentration increased.<sup>59</sup> These findings indicate potential applications in optoelectronic and photocatalytic technologies, expanding the functional scope of the material beyond its magnetic properties. Furthermore, Kumar *et al.* (2023) examined the biocompatibility of  $\text{SrFe}_{12-x}\text{Y}_x\text{O}_{19}$  nanoparticles through cytotoxicity assays, demonstrating their ability to promote cell growth at lower concentrations.<sup>59</sup> This suggests potential biomedical applications such as bone replacement, magnetic drug delivery, and metal implant coatings, aspects that were not addressed in Sharma *et al.*<sup>53</sup>'s study.

While both studies provide valuable insights into the effects of  $\text{Y}^{3+}$  substitution in  $\text{SrFe}_{12-x}\text{Y}_x\text{O}_{19}$ , Kumar *et al.* (2023) extend their research beyond magnetic characterization by incorporating structural, optical, and biological analyses.<sup>59</sup> The differences in coercivity trends between the two studies highlight the need for further investigation into synthesis-dependent variations in magnetic anisotropy. Additionally, the optical and biomedical findings in Kumar *et al.*<sup>59</sup> suggest that  $\text{Y}^{3+}$ -substituted  $\text{SrFe}_{12-x}\text{Y}_x\text{O}_{19}$  nanoparticles hold promise for multifunctional applications, whereas Sharma *et al.*<sup>53</sup> focused primarily on structural and magnetic modifications. Future research could integrate insights from both studies to refine synthesis techniques and optimize the multifunctionality of these materials for diverse technological applications.

### 3.2 Structural and surface modifications

**3.2.1 Doping.** Doping is a versatile strategy to enhance the properties of materials by incorporating specific elements, tailoring them for specialized applications. Studies have explored the doping of strontium-based nanoparticles with various metals and the integration of strontium into other

materials, yielding composites with improved structural, functional, and antimicrobial properties.<sup>60,61</sup>

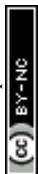
Silver doping into strontium-based materials leverages the strong antimicrobial properties of silver ions ( $\text{Ag}^+$ ). These ions disrupt microbial cell membranes, destabilize essential metabolic processes, and generate reactive oxygen species (ROS) that further damage microbial cells. By embedding silver into strontium matrices, controlled release of silver ions is achieved, providing sustained antimicrobial activity. This makes silver-doped strontium composites particularly suitable for long-term applications such as antimicrobial coatings for medical devices or water purification systems.<sup>62,63</sup>

Zinc doping has also proven effective in enhancing the antimicrobial properties of strontium-based materials. Zinc ions ( $\text{Zn}^{2+}$ ) destabilize microbial membranes, interfere with ion transport, and promote oxidative damage through ROS generation. In addition, zinc has specific antifungal properties, broadening the spectrum of antimicrobial activity. Zinc-doped strontium materials exhibit synergistic effects, targeting both bacteria and fungi, including drug-resistant strains, and are ideal for applications in healthcare settings requiring robust antimicrobial surfaces.<sup>63,64</sup>

Copper (Cu) doping has emerged as another promising avenue, where copper ions enhance antimicrobial efficacy through membrane disruption and interference with protein and enzyme activity in microbial cells. Copper's ability to generate ROS complements the intrinsic properties of strontium, creating materials with enhanced performance. Copper-doped strontium nanoparticles find applications in areas like antimicrobial coatings and environmental remediation.<sup>65</sup>

Strontium-doped materials also exhibit significant advancements in functionality. Incorporating strontium into bioactive glasses, ceramics, or other nanoparticles enhances ion exchange capabilities and facilitates a sustained release of antimicrobial ions. Strontium ions ( $\text{Sr}^{2+}$ ) have been shown to disrupt microbial metabolic pathways and inhibit biofilm formation, a critical factor in microbial resistance. These properties, combined with strontium's known benefits in promoting bone health, make strontium-doped materials highly desirable for biomedical applications, such as implant coatings that prevent infections while supporting bone regeneration.<sup>66,67</sup> Materials doped with strontium and metals like silver, zinc, or copper demonstrate enhanced photocatalytic activities, making them useful for light-activated antimicrobial applications. These materials also show improved biocompatibility, crucial for medical and environmental uses. For example, strontium's incorporation into bioactive glasses enhances osteoconductivity, while doping with silver or zinc introduces antimicrobial effects, creating multifunctional materials suitable for orthopedic implants and wound-healing applications.<sup>68,69</sup>

Doping other materials with strontium, or combining it with metals like silver, zinc, or copper, creates advanced composites with unique properties. These materials are pivotal in diverse fields, including healthcare, water treatment, environmental remediation, and food safety. Future research could focus on optimizing doping techniques, ensuring precise control over



ion release, and minimizing cytotoxic effects while exploring novel dopant combinations to unlock further potential in these multifunctional materials.<sup>70,71</sup> Strontium's multifaceted role in biomedical applications has been prominently highlighted across recent studies, underscoring its osteoinductive, antimicrobial, and synergistic properties when combined with other elements or materials. These qualities make strontium an invaluable additive in the development of next-generation biomaterials, particularly for bone regeneration and infection control.<sup>71,72</sup>

The public health implications of incorporating strontium into biomaterials are profound, given its dual role in promoting bone regeneration and mitigating infection risks. From enhancing osteogenesis to providing antimicrobial functionality, strontium-based compounds and coatings are at the forefront of innovations aimed at improving patient outcomes in orthopedic and dental applications. The following studies illuminate how strontium's unique properties contribute to these advancements while addressing critical public health challenges.<sup>73,74</sup>

Adawy and Diaz (2022) highlighted strontium's osteoinductive potential when integrated into monetite-based calcium phosphate compounds.<sup>75</sup> This study underscores strontium's ability to enhance bone growth while also providing antimicrobial effects at high concentrations. Such dual functionality is highly beneficial in clinical settings where infections and impaired bone healing often complicate recovery. For instance, strontium-doped monetite is a promising candidate for bone cement and scaffolds, particularly in procedures requiring extensive bone regeneration. By supporting the viability of osteoblast-like Soas-2 cells, strontium-doped monetite ensures biocompatibility, a critical criterion for medical applications. From a public health perspective, the deployment of such materials could significantly reduce the incidence of post-surgical infections and promote faster recovery, alleviating the burden on healthcare systems and improving patient quality of life.

Zuo *et al.* (2022) expanded this application to titanium implants, demonstrating how strontium-calcium-phosphate (SrCaP) coatings fostered osteointegration while incorporating zinc for antimicrobial efficacy.<sup>76</sup> The synergy between strontium's bioactivity and zinc's antimicrobial properties creates a comprehensive solution for implant-associated infections—a growing concern as implant usage rises globally. Strontium's contribution to structural and biological integrity in SrCaP coatings is particularly noteworthy, as it ensures that the implants not only resist bacterial colonization but also promote healthy bone integration. Public health benefits here include lower rates of implant failure, fewer revision surgeries, and reduced healthcare costs.

Similarly, Chen *et al.* (2021) developed Zn/Sr co-doped nanorod coatings that combine the osteogenic effects of strontium with the antibacterial properties of zinc.<sup>77</sup> This combination is especially effective in preventing peri-implant infections, a significant complication in dental and orthopedic implants. Strontium's role in enhancing early osteogenesis through improved cellular adhesion and proliferation of rBMSCs underscores its importance in accelerating the healing process. By synergistically inhibiting bacterial adhesion

and biofilm formation, these multifunctional coatings address two critical barriers to implant success: infection and poor bone integration. The public health implications of such materials include not only improved patient outcomes but also broader access to safer, more effective implants.

Geng *et al.* (2016) explored the co-substitution of strontium and silver in hydroxyapatite coatings, addressing the challenge of balancing antimicrobial efficacy and biocompatibility.<sup>78</sup> While silver provided robust antibacterial activity, its cytotoxicity posed limitations for safe clinical use. Strontium mitigated this toxicity, enhancing the overall biocompatibility of the coatings. The findings illustrate how strontium can serve as a stabilizing agent, enabling the integration of otherwise toxic antimicrobial components. From a public health perspective, materials like Sr/Ag-doped hydroxyapatite could reduce hospital-acquired infections, particularly in vulnerable populations, while maintaining high standards of patient safety.

Saeed and Azhdar (2020) broadened the scope of strontium's applications by introducing holmium-doped strontium hexaferrite for potential use in targeted drug delivery or bioimaging.<sup>79</sup> Although primarily focused on magnetic materials, the study highlights strontium's ability to stabilize lattice structures and refine particle morphology. These properties are essential for developing advanced biomedical technologies, such as precision imaging tools or smart drug delivery systems. Public health benefits in this context include improved diagnostic accuracy and targeted therapies, which could transform the management of chronic diseases and cancer.<sup>80</sup>

Collectively, these studies emphasize strontium's versatility in addressing pressing public health concerns. Its osteoinductive properties, when paired with antimicrobial agents like zinc and silver, provide a multifaceted approach to overcoming challenges in bone healing and infection control. Furthermore, its role in stabilizing complex material systems expands its potential applications to cutting-edge medical technologies. As the global population ages and the demand for orthopedic and dental interventions increases, optimizing strontium's integration into biomaterials will be crucial. Continued research on strontium's concentration thresholds, toxicity mitigation strategies, and synergistic interactions with other elements will ensure its safe and effective use, ultimately enhancing public health outcomes and reducing healthcare costs.

**3.2.2 Surface functionalization.** Surface functionalization of nanoparticles with polymers or peptides is a transformative strategy that addresses critical challenges in the development of nanomaterials for biomedical applications. By modifying the surface properties of nanoparticles, functionalization enhances their interaction with biological systems, thereby improving their biocompatibility, targeting capabilities, and functional efficiency.<sup>81,82</sup> This approach is especially valuable in medical contexts where the inherent properties of bare nanoparticles, such as toxicity, instability, or nonspecific interactions, could limit their therapeutic potential or lead to adverse effects.<sup>82</sup>

Polymers and peptides serve as versatile functionalization agents due to their biocompatible, biodegradable, and tunable chemical structures. When applied to nanoparticles, polymers such as dextran, polyethylene glycol (PEG), or polyvinyl alcohol



(PVA) form a protective coating that stabilizes the nanoparticles in biological environments. This stability prevents aggregation, reduces interactions with nonspecific proteins, and shields the nanoparticle core from the immune system, thereby prolonging circulation time *in vivo*. For instance, PEGylation—functionalization with PEG—has become a gold standard for increasing the biocompatibility and systemic persistence of nanoparticles used in drug delivery and imaging.<sup>83,84</sup>

Peptides, on the other hand, offer the unique advantage of specificity. Functionalizing nanoparticles with targeting peptides enables precise interaction with biological molecules or cellular receptors, enhancing the nanoparticles' ability to reach specific tissues or cellular compartments. This precision is crucial in cancer therapies, where targeted delivery can maximize therapeutic effects while minimizing off-target toxicity. For example, peptides that mimic natural ligands of cancer cell receptors can direct nanoparticles to tumor sites, enabling localized treatment and reducing systemic side effects.<sup>85–88</sup>

Surface functionalization also allows for the integration of multiple functionalities onto a single nanoparticle. This multifunctionality can combine diagnostic and therapeutic capabilities, creating theranostic platforms. For example, nanoparticles functionalized with polymers for enhanced biocompatibility can simultaneously be conjugated with peptides or antibodies for targeted therapy and fluorescent dyes or contrast agents for imaging.<sup>89,90</sup>

In addition to biocompatibility and targeting, surface functionalization with polymers or peptides can influence the pharmacokinetics and biodistribution of nanoparticles. Functionalization can alter the surface charge and hydrophilicity of nanoparticles, which affects their interaction with plasma proteins and uptake by cells. For instance, neutral or negatively charged functional groups are generally less likely to provoke unwanted interactions with negatively charged cell membranes, reducing nonspecific uptake and potential cytotoxicity.<sup>91</sup>

Importantly, functionalization provides an avenue for fine-tuning the release of therapeutic agents. For drug-loaded nanoparticles, polymers can act as stimuli-responsive coatings that release their cargo in response to environmental triggers such as pH, temperature, or enzymatic activity. Such precision in drug delivery enhances therapeutic efficacy and reduces drug wastage or unintended side effects.<sup>92</sup>

The transformative impact of surface functionalization extends beyond laboratory studies, addressing translational challenges in the clinical application of nanomaterials. Functionalized nanoparticles can meet stringent regulatory requirements for biocompatibility and safety, paving the way for their approval and adoption in real-world healthcare settings. Moreover, advances in functionalization techniques continue to expand the repertoire of polymers and peptides available, enabling the design of nanoparticles tailored to specific diseases and patient needs.<sup>93</sup>

Surface functionalization with polymers or peptides revolutionizes the use of nanoparticles in biomedicine by improving stability, biocompatibility, and specificity. This approach not only addresses the inherent limitations of bare nanoparticles

but also unlocks new possibilities for targeted therapy, diagnostics, and controlled drug delivery. As functionalization techniques evolve, they will play an increasingly vital role in the development of next-generation nanotherapeutics and their integration into precision medicine.<sup>94</sup>

For instance, the study of Thorat *et al.* (2013) provide a compelling case by synthesizing  $\text{La}_{0.7}\text{Sr}_{0.3}\text{MnO}_3$  (LSMO) nanoparticles and functionalizing them with dextran, showcasing how these strategies can significantly enhance their utility in targeted cancer therapies such as magnetic fluid hyperthermia.<sup>95</sup> The study demonstrates the benefits of dextran functionalization in stabilizing the nanoparticles, minimizing cytotoxic effects, and improving thermal efficiency, all while incorporating the unique properties of strontium within the nanoparticles.

Strontium, a key component of LSMO nanoparticles, contributes to their magnetic properties, which are crucial for applications such as hyperthermia. Strontium's substitution in the perovskite structure enhances the magnetic and thermal behaviors of LSMO nanoparticles, enabling precise and efficient heat generation under an alternating current (AC) magnetic field. This characteristic is pivotal in hyperthermia-based cancer treatment, where maintaining controlled temperatures is essential to target cancer cells while sparing healthy tissues. Strontium's role in the structural stability of LSMO further underscores its importance in biomedical applications, as it aids in maintaining the integrity of nanoparticles during synthesis and functionalization processes.

From a public health perspective, surface functionalization of strontium-containing nanoparticles, such as dextran-coated LSMO, offers several critical advantages. The biocompatibility of dextran-functionalized nanoparticles was rigorously evaluated *in vitro* using L929 and HeLa cell lines. Cytotoxicity assays demonstrated significantly reduced toxicity in dextran-coated nanoparticles compared to bare ones. The cell viability exceeded 80% even at the highest tested concentrations ( $1 \text{ mg mL}^{-1}$ ), indicating that dextran functionalization mitigates potential adverse effects on cellular health. This is particularly important for nanoparticles intended for *in vivo* applications, as minimizing toxicity is crucial for patient safety and the regulatory approval of nanoparticle-based therapies.

The study also highlighted the mechanisms by which functionalization reduces cytotoxicity. Dextran's neutral functional groups prevent nonspecific binding and clustering on negatively charged cell membranes, reducing internalization and subsequent cytotoxic effects. This is especially relevant from a public health standpoint, as nanoparticles with high cytocompatibility profiles are less likely to induce adverse systemic effects when used in therapeutic contexts. Furthermore, dextran-coated nanoparticles exhibited enhanced stability in physiological environments, ensuring consistent performance and reducing the risk of unpredictable behavior in biological systems.

The incorporation of strontium into functionalized nanoparticles also has implications for public health beyond hyperthermia. Strontium's known roles in bone health and its therapeutic potential in osteoporosis treatment suggest



additional biomedical applications for such nanoparticles, including bone-targeted drug delivery systems. However, the public health deployment of these technologies must account for potential risks, such as environmental contamination or unforeseen biological interactions, emphasizing the need for comprehensive safety evaluations.

Moreover, the magnetic fluid hyperthermia studies conducted by Thorat *et al.* revealed that dextran-coated LSMO nanoparticles achieved a specific absorption rate (SAR) of  $51 \text{ W g}^{-1}$ , compared to  $25 \text{ W g}^{-1}$  for uncoated nanoparticles.<sup>95</sup> This improvement signifies greater thermal efficiency and control, critical for clinical applications. By incorporating strontium into a biocompatible, polymer-functionalized framework, the study achieves a balance between functionality and safety, a key consideration in the public health implementation of nanoparticle-based technologies.

In a nutshell, the surface functionalization of strontium-containing nanoparticles with polymers like dextran significantly improves biocompatibility and targeting efficiency, with far-reaching implications for biomedical applications and public health. Thorat *et al.*'s<sup>95</sup> study highlights the role of strontium in enhancing the functional properties of LSMO nanoparticles and demonstrates how dextran functionalization reduces cytotoxicity and improves performance. These advancements hold promise not only for cancer therapies like magnetic fluid hyperthermia but also for broader applications in public health, such as drug delivery and regenerative medicine. Nonetheless, careful consideration of safety and environmental impacts remains essential to maximize the benefits of these innovative materials.

## 4 Molecular pathways in bone regeneration and homeostasis

### 4.1 Osteoinductive and osteogenic mechanisms

Strontium ions ( $\text{Sr}^{2+}$ ) released from strontium nanoparticles (SrNPs) promote bone regeneration by enhancing osteoblast proliferation and differentiation while inhibiting osteoclast activity.<sup>96–100</sup> These effects are mediated through two key pathways:

**4.1.1 Wnt/ $\beta$ -catenin signalling.** Strontium ions ( $\text{Sr}^{2+}$ ) play a pivotal role in bone regeneration by modulating the Wnt/ $\beta$ -catenin signaling pathway, a key regulator of osteogenesis. The activation of this pathway begins with  $\text{Sr}^{2+}$  enhancing the interaction between Wnt ligands and their respective receptors, Frizzled and LRP5/6, located on the surface of osteoblast precursor cells. This receptor–ligand binding triggers a cascade of intracellular events that stabilize  $\beta$ -catenin, a crucial signaling molecule. Stabilized  $\beta$ -catenin escapes proteasomal degradation and accumulates in the cytoplasm, eventually translocating to the nucleus.<sup>100–103</sup>

Within the nucleus,  $\beta$ -catenin acts as a transcriptional coactivator, binding to T-cell factor/lymphoid enhancer factor (TCF/LEF) transcription factors to upregulate the expression of osteogenic genes. Among these, RUNX2, COL1A1, and ALP is particularly significant. RUNX2 is a master regulator of

osteoblast differentiation, guiding progenitor cells toward an osteoblastic lineage. COL1A1 encodes type I collagen, a primary component of the bone extracellular matrix, essential for providing structural integrity and a scaffold for mineral deposition. ALP, or alkaline phosphatase, facilitates the mineralization process by hydrolyzing phosphate esters to provide inorganic phosphate necessary for hydroxyapatite crystal formation.<sup>104–107</sup>

The upregulation of these genes results in enhanced extracellular matrix production and mineralization, key processes in bone tissue development and repair. By driving these cellular and molecular activities,  $\text{Sr}^{2+}$  accelerates osteoblast proliferation and activity, promoting robust bone formation and regeneration. This makes the activation of the Wnt/ $\beta$ -catenin pathway by  $\text{Sr}^{2+}$  a cornerstone mechanism in developing therapeutic strategies for bone-related disorders and improving bone healing outcomes.<sup>108–112</sup>

For example, the following studies by Rybchyn *et al.* (2011),<sup>113</sup> Yang *et al.* (2011),<sup>114</sup> and Cui *et al.* (2019)<sup>115</sup> provide significant support for the role of  $\text{Sr}^{2+}$  in activating the Wnt/ $\beta$ -catenin signaling pathway, which is critical for osteogenesis. These studies align with the mechanistic pathway discussed earlier, showing that strontium not only enhances osteoblast activity but also influences key signaling mechanisms involved in bone formation.

Rybchyn *et al.* (2011) demonstrate that strontium exposure increases mineralization in human osteoblast cultures while decreasing the expression of sclerostin, a protein that inhibits canonical Wnt signaling.<sup>113</sup> By decreasing sclerostin levels, strontium effectively removes a negative regulator of bone formation, thus promoting Wnt/ $\beta$ -catenin signaling. Furthermore, the study highlights that strontium induces an Akt-dependent signaling cascade, which activates the nuclear translocation of  $\beta$ -catenin. This aligns with the mechanism where  $\text{Sr}^{2+}$  stabilizes  $\beta$ -catenin and facilitates its movement to the nucleus, where it regulates osteogenic gene expression. The activation of Wnt/ $\beta$ -catenin signaling in this context is presented as a crucial pathway through which strontium exerts its osteoinductive effects on osteoblasts.

Yang *et al.* (2011) further support this by demonstrating that strontium ranelate promotes osteogenic differentiation in human mesenchymal stem cells (MSCs) through the activation of the Wnt/ $\beta$ -catenin pathway.<sup>114</sup> Their study shows that strontium not only enhances osteoblast differentiation but also stimulates the expression of extracellular matrix (ECM) genes, a hallmark of osteogenesis. Importantly, they also observed increased  $\beta$ -catenin expression in newly formed bone tissue *in vivo*, suggesting that strontium's effect on Wnt/ $\beta$ -catenin signaling contributes to enhanced bone formation. This reinforces the idea that  $\text{Sr}^{2+}$  promotes osteoblast differentiation and bone regeneration by activating this key signaling pathway.

Cui *et al.* (2019) provide additional evidence by showing that strontium incorporation into bioactive borate glass cement enhances osteogenic differentiation of human bone marrow stem cells (hBMSCs) *in vitro* and supports bone regeneration *in vivo*.<sup>115</sup> They found that strontium substitution activated both the Wnt/ $\beta$ -catenin and BMP signaling pathways, further



emphasizing the role of Wnt/ $\beta$ -catenin signaling in strontium-induced osteogenesis. Their study highlights that the optimal osteogenic response was observed when the cement contained 6 mol% SrO, which effectively promoted osteoblast proliferation, differentiation, and mineralization. This suggests that the Wnt/ $\beta$ -catenin pathway is a key mediator of strontium's osteoinductive effects in various biomaterial contexts.

Collectively, these studies underscore the importance of Wnt/ $\beta$ -catenin signaling in the osteoinductive actions of strontium. They illustrate how strontium modulates key signaling pathways, such as reducing sclerostin levels, activating  $\beta$ -catenin translocation to the nucleus, and enhancing osteoblast differentiation and bone formation. This mechanistic insight reinforces the potential of strontium as an effective therapeutic agent for promoting bone healing and regeneration.

**4.1.2 RANK/RANKL/OPG system.** Strontium ( $\text{Sr}^{2+}$ ) plays a pivotal role in regulating bone metabolism by modulating the RANK/RANKL/OPG signalling pathway, which is central to osteoclastogenesis. Osteoclasts, the cells responsible for bone resorption, are regulated by the interaction of RANKL (Receptor Activator of Nuclear Factor- $\kappa$ B Ligand) with its receptor RANK, expressed on osteoclast precursors and mature osteoclasts. This interaction triggers a cascade of signaling events that leads to the differentiation and activation of osteoclasts, promoting bone resorption. The osteoblast-derived protein osteoprotegerin (OPG) functions as a decoy receptor for RANKL, binding to RANKL and preventing its interaction with RANK, thus inhibiting osteoclastogenesis.<sup>116,117</sup>

$\text{Sr}^{2+}$  has been shown to regulate this system through a dual mechanism. First,  $\text{Sr}^{2+}$  reduces the expression of RANKL, which is crucial for the activation of osteoclastogenesis. By decreasing the levels of RANKL,  $\text{Sr}^{2+}$  minimizes its availability to bind to RANK receptors on osteoclast precursors, thereby preventing the initiation of the signaling cascade that leads to osteoclast differentiation. Second,  $\text{Sr}^{2+}$  upregulates the secretion of OPG from osteoblasts. Elevated OPG levels increase the binding of OPG to RANKL, further limiting RANKL's ability to activate RANK and suppressing osteoclast differentiation. This combined effect—reduced RANKL expression and enhanced OPG secretion—ultimately leads to a decrease in osteoclastogenesis, thereby inhibiting excessive bone resorption.<sup>118,119</sup>

In addition to modulating the RANK/RANKL/OPG pathway,  $\text{Sr}^{2+}$  also exerts direct effects on osteoclast activity. It has been shown to reduce the expression of key osteoclast markers, including tartrate-resistant acid phosphatase (TRAP) and Cathepsin K, both of which are critical for osteoclast function. TRAP is a well-established marker of osteoclast differentiation and activity, and its downregulation by  $\text{Sr}^{2+}$  leads to a reduction in osteoclast activity. Similarly, Cathepsin K, a protease involved in the degradation of the bone matrix by osteoclasts, is also downregulated in response to  $\text{Sr}^{2+}$  treatment, further limiting osteoclast-mediated bone resorption.<sup>120,121</sup>

Together, these actions of  $\text{Sr}^{2+}$  provide a comprehensive approach to regulating bone resorption. By decreasing RANKL expression and increasing OPG secretion,  $\text{Sr}^{2+}$  not only prevents osteoclast differentiation but also ensures that the osteoclasts

that do form are less active. This dual action of  $\text{Sr}^{2+}$  in suppressing osteoclastogenesis and inhibiting osteoclast function helps to maintain bone homeostasis, preventing excessive bone loss while promoting the preservation of bone structure. Furthermore, this regulatory role of  $\text{Sr}^{2+}$  is crucial in both physiological and pathological conditions, such as osteoporosis and osteoarthritis, where controlling bone resorption and supporting bone formation is essential for maintaining skeletal health.

The following studies provide valuable insights into the mechanism by which  $\text{Sr}^{2+}$  regulates the RANK/RANKL/OPG signaling axis to suppress osteoclast activity, thereby supporting its role in inhibiting osteoclastogenesis while promoting bone formation. A detailed discussion of these studies is presented below:

The following studies provide compelling evidence supporting the role of strontium ( $\text{Sr}^{2+}$ ) in regulating the RANK/RANKL/OPG signalling axis, which is critical for osteoclastogenesis and bone metabolism.  $\text{Sr}^{2+}$ 's effects are characterized by a dual mechanism: suppression of osteoclast differentiation and activity, coupled with the promotion of osteoblast function and bone formation. The studies reviewed below highlight key molecular pathways through which  $\text{Sr}^{2+}$  exerts these effects, offering a cohesive understanding of its role in bone homeostasis.

Sun *et al.* (2018) investigated the impact of  $\text{Sr}^{2+}$  on osteoclastogenesis, particularly through its regulation of the RANK/RANKL/OPG pathway.<sup>122</sup> The authors demonstrated that  $\text{Sr}^{2+}$  treatment led to a reduction in RANKL levels, a crucial mediator of osteoclast differentiation. This reduction in RANKL expression directly supports the suppression of osteoclast activity by limiting the signaling that triggers osteoclastogenesis. Additionally,  $\text{Sr}^{2+}$  was shown to enhance the LRP6/ $\beta$ -catenin/OPG signaling pathway in MC3T3-E1 osteoblast-like cells. This pathway promotes the upregulation of OPG, which subsequently binds to RANKL, preventing its interaction with the RANK receptor on osteoclast precursors. These findings align with the proposed mechanism where  $\text{Sr}^{2+}$  both reduces RANKL expression and upregulates OPG to inhibit osteoclastogenesis while promoting bone formation. Furthermore,  $\text{Sr}^{2+}$  also modulated osteoclast activity through direct regulation of markers like miR-181d-5p, which is involved in OPG expression, further supporting its anti-resorptive effects.

Atkins *et al.* (2009) explored the effects of strontium ranelate (SR) on the OPG/RANKL system and its influence on osteoblastic function.<sup>123</sup> SR treatment promoted osteoblast maturation and osteocyte differentiation, accompanied by an increase in OPG secretion. This enhancement in the OPG/RANKL ratio was associated with a reduction in osteoclastogenesis. By increasing OPG levels, SR reduced the availability of RANKL to bind to RANK receptors on osteoclast precursors, thereby inhibiting osteoclast differentiation and resorptive activity. This study reinforces the mechanism proposed by Sun *et al.* (2018),<sup>122</sup> where  $\text{Sr}^{2+}$  regulates the RANK/RANKL/OPG system to suppress osteoclast activity and bone resorption while supporting osteoblast maturation and mineralization.



Peng *et al.* (2011) further elucidated the role of Sr<sup>2+</sup> in enhancing OPG secretion in osteoblasts.<sup>124</sup> The study demonstrated that SrCl<sub>2</sub> treatment of MC3T3-E1 cells increased OPG expression, which played a critical role in inhibiting osteoclastogenesis. Notably, neutralization of OPG reversed Sr<sup>2+</sup>'s effects on osteoclast differentiation, highlighting the centrality of the OPG/RANKL pathway in mediating Sr<sup>2+</sup>'s anti-resorptive effects. These findings complement the earlier studies by confirming that Sr<sup>2+</sup> promotes OPG secretion from osteoblasts, thereby inhibiting osteoclastogenesis by preventing RANKL from interacting with RANK receptors. Additionally, Sr<sup>2+</sup> treatment led to a decrease in osteoclast activity, further substantiating its dual action in regulating bone resorption and formation.

Tat *et al.* (2011) investigated the effects of strontium ranelate (SR) on osteoblasts from human osteoarthritic (OA) subchondral bone.<sup>125</sup> They found that SR treatment significantly increased OPG production while reducing RANKL expression, particularly the RANKL isoforms involved in osteoclast activation. This was coupled with a reduction in membranous RANKL, further inhibiting osteoclastogenesis. The study also observed a decrease in bone resorption, as evidenced by reduced resorbed surface area. These results are particularly relevant in pathological conditions like osteoarthritis, where Sr<sup>2+</sup> not only regulates the OPG/RANKL axis to inhibit osteoclast activity but also promotes osteoblast function and bone formation.

Collectively, these studies provide strong evidence that Sr<sup>2+</sup> modulates bone metabolism through its regulation of the RANK/RANKL/OPG system. Sr<sup>2+</sup> reduces RANKL expression, upregulates OPG secretion, and inhibits osteoclast differentiation and activity. This dual mechanism—directly suppressing osteoclastogenesis and indirectly promoting osteoblast differentiation and OPG secretion—prevents excessive bone resorption while supporting bone formation. Therefore, Sr<sup>2+</sup> emerges as a crucial modulator of bone homeostasis, with significant implications for both healthy bone remodelling and the treatment of pathological bone conditions such as osteoarthritis and osteoporosis.

## 5 Biomedical applications of strontium-based nanomaterials in orthopedic implants

SrNPs have been widely integrated into various biomedical platforms such as scaffolds, hydrogels, and surface coatings for orthopedic implants, demonstrating their multifaceted role in enhancing bone repair and regeneration. These applications leverage the osteoconductive and osteoinductive properties of Sr ions, which promote osteoblast activity and suppress osteoclast-mediated bone resorption.<sup>126,127</sup>

In scaffolds, SrNPs are often incorporated to improve mechanical strength, biocompatibility, and osteogenic potential. These scaffolds provide structural support while actively participating in bone regeneration by releasing Sr ions that stimulate bone tissue growth. Hydrogels containing SrNPs serve as injectable systems or 3D matrices, offering both a conducive environment for cellular activities and the gradual release of

bioactive ions to encourage bone healing. Similarly, SrNPs have been used as coatings for orthopedic implants to enhance surface bioactivity, minimize implant-associated inflammation, and promote direct bone-implant integration.<sup>128–131</sup>

These platforms collectively exemplify the versatility of SrNPs in addressing critical challenges in orthopedic treatments, including poor integration of implants, insufficient mechanical support, and the need for sustained bioactivity. Specific applications range from non-load-bearing bone repair to enhancing the performance of load-bearing implants in complex fractures or bone defects. Examples include their integration into polymeric scaffolds, hybrid composites, and bioactive coatings, demonstrating their efficacy in both *in vitro* and *in vivo* studies.

### 5.1 Strontium-doped hydroxyapatite (HA) nanoparticles

The incorporation of strontium (Sr) into hydroxyapatite (HA) nanoparticles has proven to be a promising approach in advancing scaffold technology for bone tissue engineering. Sr-doped HA exhibits unique bioactive properties that significantly enhance the biological and mechanical performance of scaffolds. On the biological front, Sr ions are known to stimulate osteoblast activity, promote alkaline phosphatase (ALP) expression, and encourage extracellular matrix mineralization.<sup>132,133</sup> These effects are crucial for initiating and sustaining osteogenesis, making Sr-doped HA a favourable choice for bone regeneration applications. Additionally, Sr is recognized for its capacity to inhibit osteoclast-mediated bone resorption, which helps to maintain bone integrity during the healing process.<sup>134</sup>

In terms of mechanical strength, the doping of Sr into HA improves the crystallinity and stability of the material, making it more robust under physiological conditions. This is particularly beneficial for scaffolds designed to bear the mechanical loads of bone tissue, as it addresses one of the major limitations of conventional HA-based scaffolds, which often lack sufficient compressive strength. By optimizing the doping concentration and combining Sr-doped HA with other reinforcing materials, scaffolds can achieve a balanced profile of high porosity for cell infiltration and adequate mechanical support for tissue regeneration.<sup>135,136</sup>

Moreover, Sr-doped HA nanoparticles have demonstrated versatility in their integration into composite scaffolds. These composites often combine Sr-doped HA with polymers, ceramics, or other bioactive materials to create hybrid scaffolds with enhanced properties. For example, incorporating Sr-doped HA into biopolymeric matrices not only improves the structural integrity but also allows for controlled ion release, promoting sustained osteogenic activity. This synergy between the components of the composite scaffolds contributes to their multifunctionality, addressing challenges such as poor mechanical performance, limited osteoconductivity, and the need for vascularization.<sup>137,138</sup>

Recent advancements have explored strategies such as coupling Sr-doped HA with nanostructured elements or functional additives, which further enhance scaffold properties. These developments are pivotal in aligning scaffold design with



the complex demands of bone tissue engineering, including osteogenesis, angiogenesis, and long-term structural support. Sr-doped HA scaffolds have shown potential in various applications, from non-load-bearing bone repair to supporting more dynamic and mechanically demanding environments.<sup>138–140</sup>

The progress in Sr-doped HA nanoparticle-based scaffolds underscores the material's potential to bridge the gap between biocompatibility and mechanical performance. By leveraging the osteogenic and anti-resorptive properties of Sr with the structural advantages of HA, these scaffolds represent a significant step forward in designing bioactive and mechanically resilient materials for clinical applications. The ongoing optimization of these systems continues to open new avenues in the field of bone tissue engineering, promising improved patient outcomes in the treatment of bone defects and fractures.<sup>140–142</sup>

Li *et al.* (2018) explored the incorporation of strontium-substituted hydroxyapatite (Sr-HA) nanoparticles into poly(propylene fumarate) (PPF)-based scaffolds to enhance their mechanical strength and osteoinductive properties for bone tissue engineering applications.<sup>143</sup> The study aimed to investigate the effect of varying strontium contents (0%, 5%, 10%, and 20% Sr substitution) in Sr-HA on the structural characteristics, mechanical properties, and biological responses of the composite scaffolds. These scaffolds were fabricated as two-dimensional disks using a thermal cross-linking method, and their structure and surface morphology were thoroughly analyzed using scanning electron microscopy (SEM), transmission electron microscopy (TEM), atomic force microscopy (AFM), and energy-dispersive X-ray spectroscopy (EDS).

The study focused on evaluating cellular responses *in vitro* by culturing MC3T3-E1 cells on the different PPF/Sr-HA composite scaffolds. Cell viability, morphology, and proliferation were assessed over various time points. Among the four different Sr-HA composites, the PPF/Sr10-HA group exhibited the highest cell density after 24 hours, as shown in the confocal laser scanning electron microscopy (CLSM) images (Fig. 18). This result suggested that the 10% Sr content in the composite scaffold provided an optimal environment for cell survival, while the PPF/Sr20-HA group exhibited the lowest viable cell density, indicating potential cytotoxic effects at higher Sr concentrations. This observation highlighted the importance of Sr content in tailoring the biological activity of the scaffold materials.

Further SEM analysis at 5 days post-seeding revealed that MC3T3-E1 cells adhered to all four types of scaffolds, displaying typical elongated spindle-like morphology. The PPF/Sr10-HA group showed the most pronounced cell attachment and proliferation, with more cells and cellular processes evident compared to the other groups (Fig. 19). This finding suggests that the PPF/Sr10-HA composite scaffold provided superior conditions for cellular attachment, likely due to enhanced surface interactions resulting from the Sr-HA incorporation. In contrast, the PPF/Sr20-HA scaffold exhibited fewer attached cells, possibly due to the excessive Sr content affecting cell adhesion.

The osteogenic differentiation of MC3T3-E1 cells was assessed using alkaline phosphatase (ALP) live staining and

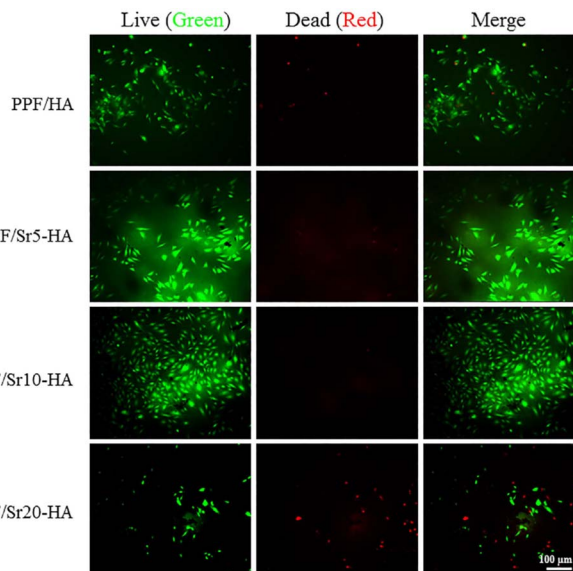


Fig. 18 Live/dead cell viability assay images of MC3T3-E1 cells after 24 h seeding on PPF/HA, PPF/Sr5-HA, PPF/Sr10-HA, and PPF/Sr20-HA scaffolds. Cell density on PPF/Sr10-HA nanocomposite scaffolds was the highest ( $p < 0.05$ ) among the groups. Green color indicates live cells; red indicates dead cells.<sup>143</sup>

enzyme activity measurements. ALP staining revealed increased accumulation of green particles in the cytoplasm of cells cultured on the PPF/Sr10-HA scaffold, indicating stronger osteogenic differentiation compared to the other groups (Fig. 20A–D). Quantitative ALP activity measurements (Fig. 20E) confirmed that the PPF/Sr10-HA scaffold significantly enhanced ALP activity at 14 days of culture, with levels remaining elevated at 21 days, indicating sustained osteogenic potential. Osteocalcin content, a late marker of osteogenic differentiation, was also significantly higher in the PPF/Sr10-HA group at each time point, further supporting its superior osteoinductive properties (Fig. 20F).

The study's results underscore the importance of the Sr content in Sr-HA nanoparticles, with the 10% Sr-substituted HA formulation (PPF/Sr10-HA) showing the most favorable biological responses in terms of cell viability, attachment, proliferation, and osteogenic differentiation. These findings align with previous research suggesting that Sr-HA can enhance osteogenesis by promoting cell adhesion and inducing osteoblastic differentiation. The study also highlights the critical role of scaffold composition in modulating cellular behavior and osteogenic activity, with PPF/Sr10-HA offering a promising material for bone tissue engineering applications. The incorporation of Sr-HA nanoparticles into PPF-based scaffolds not only enhanced the mechanical properties but also significantly promoted osteogenesis, making it an ideal candidate for applications in bone regeneration and repair.

Wang *et al.* (2018) explored the potential of Sr-doped, Zn-doped, and Sr/Zn-codoped hydroxyapatite (HA) porous scaffolds in enhancing the biological properties required for bone regeneration applications.<sup>144</sup> The study addressed the inherent limitations of HA scaffolds, specifically their insufficient



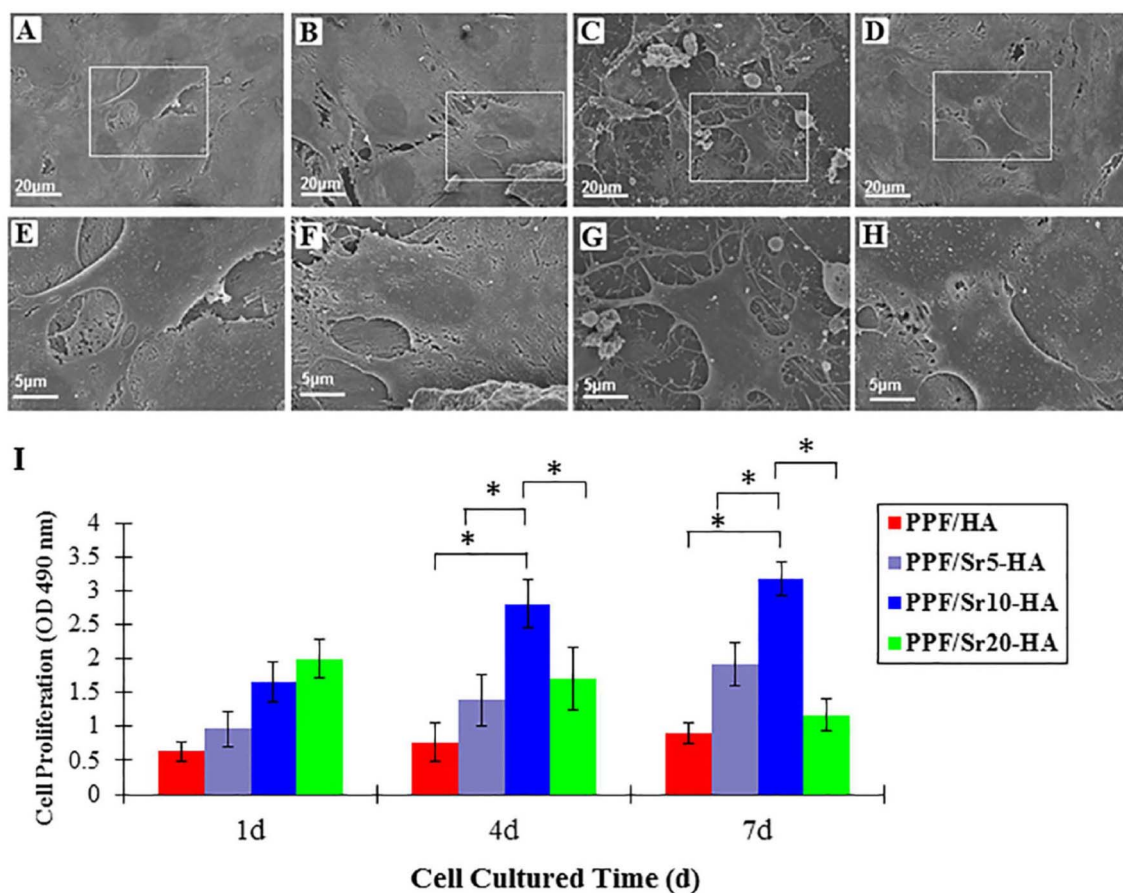


Fig. 19 SEM images of MC3T3-E1 cells after 5 days of culture on PPF/HA (A and E), PPF/Sr5-HA (B and F), PPF/Sr10-HA (C and G), and PPF/Sr20-HA (D and H) scaffolds. MTS assay analysis of cell proliferation (I) on PPF/HA and PPF/Sr-HA samples at 1, 4, and 7 days ( $*p < 0.05$ ).<sup>143</sup>

antibacterial properties and osteoinductivity, which hinder their broader clinical use. Through the use of ion-exchange and foaming methods, the researchers successfully integrated Sr and Zn into the HA lattice, altering the material's lattice parameters and thereby enhancing its properties. The results, supported by density functional theory (DFT) and experimental data, demonstrated that Sr and Zn doping significantly improved the mechanical strength, biocompatibility, and osteoinductive potential of the HA scaffolds. Importantly, the Sr-doped and codoped scaffolds promoted the differentiation of bone marrow stromal cells (BMSCs), while both Zn-doped and codoped scaffolds exhibited superior antibacterial activity. These findings suggest that the codoped HA scaffolds, with their enhanced mechanical properties, biocompatibility, and antibacterial capabilities, hold great promise as an effective material for bone tissue regeneration. They could provide a reliable solution for bone repair, mitigating microbial infections and promoting the healing process. The study, as depicted in Fig. 21, emphasizes the significant potential of Sr/Zn codoped HA porous scaffolds for clinical applications as bone replacement materials.

Panzavolta *et al.* (2018) investigated the incorporation of strontium-doped hydroxyapatite (SrHA) into gelatin-based

scaffolds, aiming to enhance scaffold biocompatibility and mechanical strength while leveraging strontium's role in bone remodeling.<sup>145</sup> Strontium is well-known for its beneficial effects in treating bone resorption-related pathologies like osteoporosis, and this study explored the potential of SrHA as a strontium delivery system using 3D porous gelatin scaffolds. The scaffolds were created *via* freeze-drying, with the incorporation of approximately 30% SrHA or pure hydroxyapatite (HA). The study revealed that these scaffolds exhibited impressive porosity and interconnected pore structures, which are essential for tissue engineering applications.

The incorporation of SrHA into the scaffolds did not significantly alter the interconnectivity, which remained at 100%, but did result in a slight decrease in average pore size. This modification did not hinder the porosity but suggested a finer dispersion of inorganic particles within the scaffolds. The mechanical properties of the scaffolds also improved with reinforcement, as indicated by increased values for elastic modulus and stress when compared to unreinforced scaffolds. These improvements were attributed to the crosslinking of gelatin and the reduction in pore size induced by the addition of gelatin, which acted as a stiffening agent. The mechanical testing showed that the reinforced scaffolds, as shown in



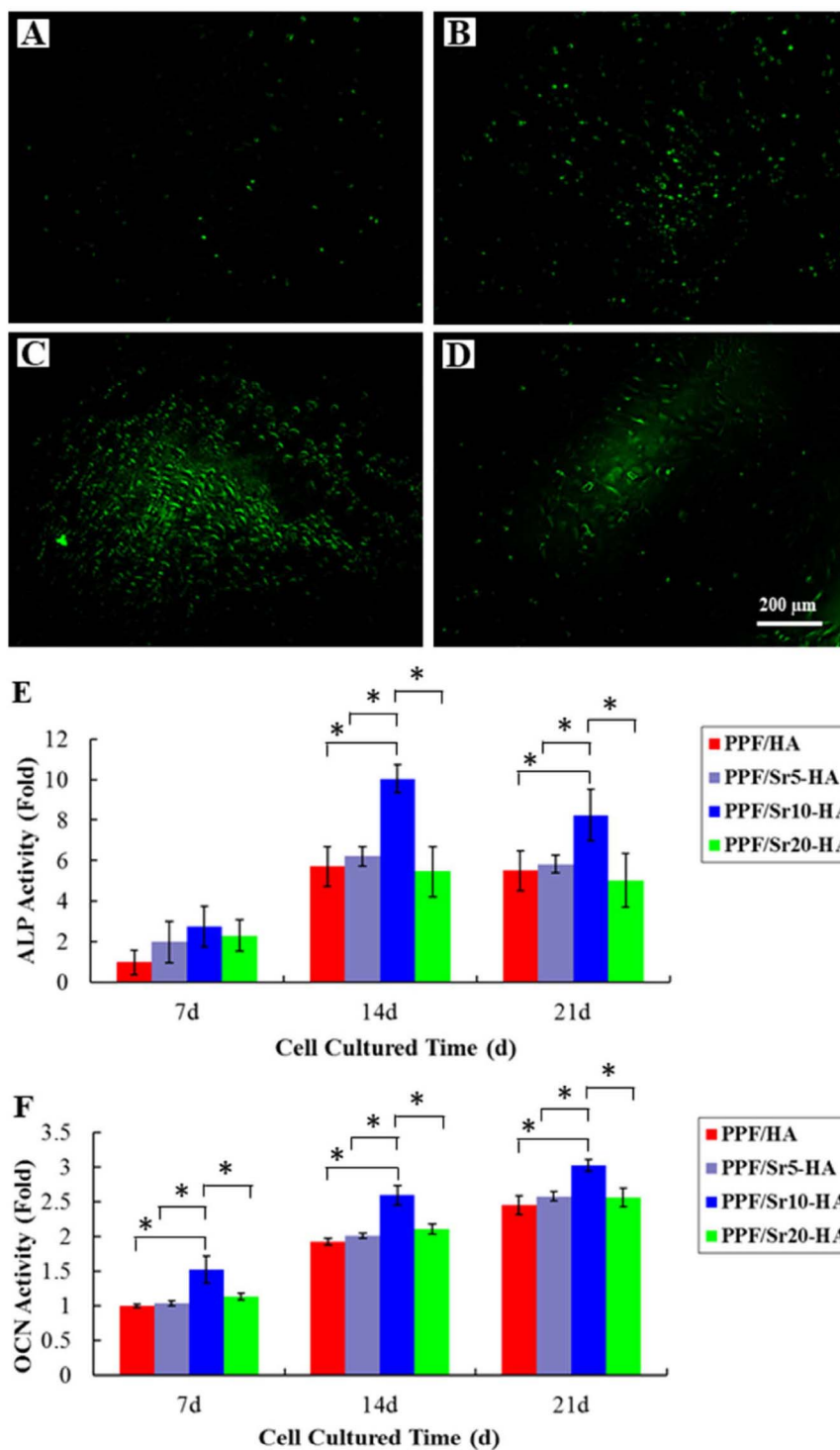


Fig. 20 ALP live staining images showing the number of green particles in the cytoplasm of MC3T3-E1 cells after 10 days of culture on PPF/Sr10-HA scaffolds (C) was significantly higher ( $p < 0.05$ ) than the other groups of (A) PPF/HA, (B) PPF/Sr5-HA, and (D) PPF/Sr20-HA. ALP (E) and osteocalcin (F) quantification at 7, 14, and 21 days after cell seeding ( $*p < 0.05$ ).<sup>143</sup>

Fig. 22, had higher values for compressive strength and elastic modulus, highlighting the positive effect of gelatin reinforcement on scaffold stability and mechanical performance.

Strontium release from the scaffolds in phosphate-buffered saline (PBS) was sustained over a period of 14 days, with only

14% of the initial content released from the unreinforced scaffolds and 18% from the reinforced scaffolds, indicating a controlled release profile. This suggests that the SrHA-containing scaffolds could effectively serve as a local delivery system for strontium in areas of excessive bone resorption. In





Fig. 21 Sr/Zn codoped hydroxyapatite (HA) porous scaffold: enhanced antibacterial properties and osteoinductive potential for bone regeneration applications.<sup>144</sup>

addition to the physical and mechanical properties, biological studies indicated that the SrHA scaffolds promoted osteoblast viability and activity when compared to HA scaffolds. Coculture experiments of osteoblasts and osteoclasts further revealed that the SrHA scaffolds inhibited osteoclast differentiation and osteoclastogenesis, which is crucial for preventing excessive bone resorption.

The X-ray diffraction analysis confirmed that SrHA maintained the crystal structure of hydroxyapatite, with slight shifts in the diffraction peaks, indicating the substitution of calcium ions by strontium. The scaffolds displayed significant bioactivity, and the combination of gelatin, HA, and SrHA made the

material suitable for bone tissue engineering applications, particularly in scenarios where bone resorption is excessive. The study's  $\mu$ -CT analysis, shown in Fig. 23, illustrated the high porosity and interconnectivity of the scaffolds, further supporting their suitability for cell migration and tissue ingrowth, which are critical for bone regeneration.

The study of Panzavolta *et al.* (2018)<sup>145</sup> demonstrated that SrHA-doped gelatin scaffolds offer a promising approach for enhancing the mechanical properties and biological performance of bone scaffolds, with the added benefit of strontium's anti-osteoporotic properties. This work provides a comprehensive look at the potential of such scaffolds for local strontium delivery and their application in bone regeneration therapies.

Strontium-doped hydroxyapatite (SrHA) has been widely studied for its potential to enhance bone regeneration due to its favourable osteoconductivity and high alkaline phosphatase (ALP) activity. However, a challenge persists in improving the mechanical strength of SrHA scaffolds to meet the high compressive modulus required for bone repair. Wu *et al.* (2020) addressed this limitation by incorporating graphene oxide (GO)-reinforced SrHA nanoparticles into chitosan-based scaffolds.<sup>146</sup> The inclusion of GO not only provided nucleation sites for hydroxyapatite growth but also contributed to the mechanical strengthening of the scaffold. The resulting scaffold exhibited a four-fold increase in compressive modulus compared to unreinforced scaffolds, alongside enhanced ALP activity and *in vitro* mineralization. This demonstrates that SrHA, when modified with reinforcing agents like GO, can achieve the desired mechanical properties while retaining its osteoconductive benefits, making it suitable for bone tissue engineering.

Further exploring the role of Sr in scaffold development, Scalera *et al.* (2019) synthesized magnesium-strontium hydroxyapatite (HAMgSr) nanocrystals to fabricate thermally stable, highly porous scaffolds.<sup>147</sup> These scaffolds showed improved thermal stability and mechanical properties when doped with Mg and Sr, which are known to promote osteogenesis. The HAMgSr scaffolds demonstrated good biocompatibility, supporting osteoblast proliferation, which underscores the synergistic effect of Sr and Mg in enhancing bone tissue regeneration. This study supports the idea that Sr-doped materials can be fine-

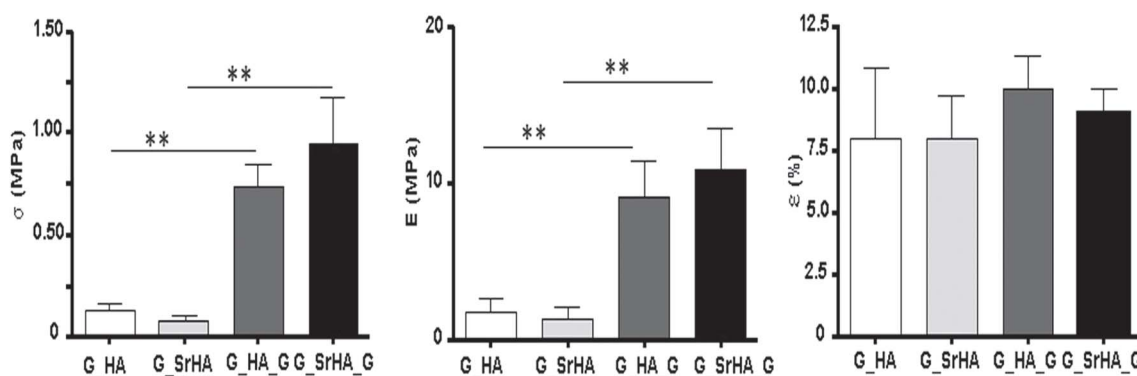


Fig. 22 Mean values of collapse stress ( $\sigma$ ), linear elastic modulus ( $E$ ), and strain ( $\epsilon$ %) of the different scaffolds. Each value is the mean of six determinations and is reported with its standard deviation (\*\* $p < 0.001$ ). Stress: \*\*G\_HA versus G\_HA\_G; G\_SrHA versus G\_SrHA\_G. Elastic modulus: \*\*G\_HA versus G\_HA\_G; G\_SrHA versus G\_SrHA\_G.<sup>145</sup>



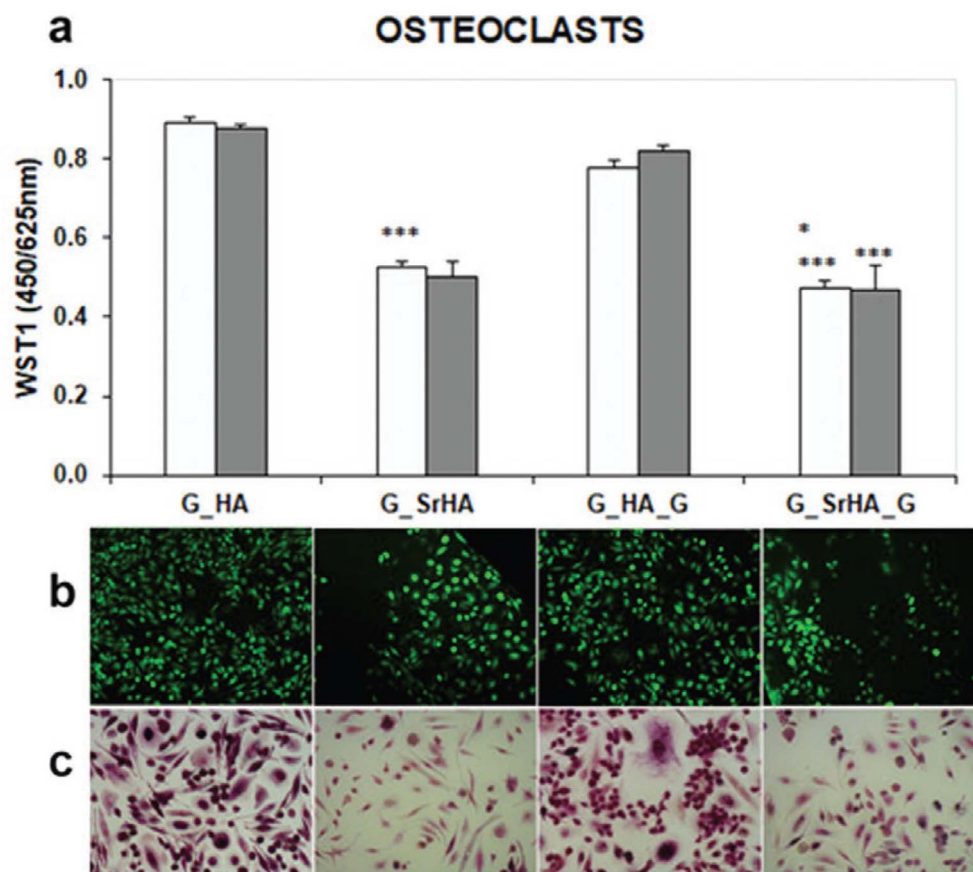


Fig. 23 Osteoclast viability and differentiation after coculture with osteo-blast on the different samples. (a) Osteoclast viability after 7 (light bars) and 14 (dark bars) days of culture by WST1 reagent test. Statistical analysis is reported in the figure (\* $p < 0.05$ , \*\* $p < 0.005$ , \*\*\* $p < 0.0005$ ): 7 days, \*G\_SrHA\_G versus G\_SrHA; 7 and 14 days \*\*\*G\_SrHA, G\_SrHA\_G versus G\_HA, G\_HA\_G. (b) Live&dead significant images of osteoclasts grown around material samples (magnification 10 $\times$ ). (c) TRAP staining of osteoclasts (magnification 20 $\times$ ) after 14 days of coculture with osteoblast: considering G\_HA as 100%, G\_SrHA, G\_HA\_G, and G\_SrHA\_G were 32, 89, and 24%, respectively.<sup>145</sup>

tuned with other elements to further improve scaffold properties, such as thermal stability and mechanical strength, making them more effective for clinical applications.

Zhang *et al.* (2019) introduced a biocomposite scaffold incorporating strontium-substituted hydroxyapatite (Sr-HAP) alongside cellulose nanocrystals (CNCs) and carboxymethyl chitosan (CMCS).<sup>148</sup> The composite scaffolds exhibited increased compressive strength compared to pure chitosan-based scaffolds, with a significant enhancement in osteogenic gene expression and ALP activity. The addition of Sr-HAP promoted osteoblast differentiation and protein adsorption, demonstrating the potential of Sr-doped scaffolds in enhancing osteogenic responses. The combination of Sr-HAP with other materials like CNCs not only improves mechanical properties but also supports the biological functions essential for bone repair, emphasizing the versatility of Sr-doped HA scaffolds in various biomaterial formulations.

In a more advanced approach, Borciani *et al.* (2024) developed a composite material combining strontium-enriched mesoporous bioactive glasses with hydroxyapatite nanoparticles and collagen type I for bone tissue engineering.<sup>149</sup> These 3D-printed scaffolds, crosslinked with genipin for improved stability,

significantly enhanced osteoblast activity and reduced osteoclast differentiation. The presence of Sr in the scaffold promoted a positive cellular response, boosting alkaline phosphatase activity and supporting the proliferation of bone cells. This study highlights how Sr doping can improve both the mechanical and biological properties of scaffolds, making them suitable for bone regeneration applications.

Finally, Li *et al.* (2023) demonstrated the potential of Sr-doped scaffolds for vascularized bone regeneration by incorporating Sr<sup>2+</sup> and simvastatin (SIM)-loaded hydroxyapatite microspheres into a poly( $\epsilon$ -caprolactone) (PCL) matrix.<sup>150</sup> These scaffolds exhibited enhanced osteogenic differentiation of mesenchymal stem cells (BMSCs) and promoted vascular network formation, which is crucial for successful bone regeneration. The dual-loading strategy of Sr<sup>2+</sup> and SIM further facilitated osteogenesis and angiogenesis, underscoring the importance of Sr in promoting both bone formation and vascularization. This study emphasizes that Sr-doped scaffolds, when combined with growth factors or drugs, can further enhance their regenerative potential.

In a nutshell, these studies collectively highlight the potential of Sr-doped hydroxyapatite scaffolds to significantly



improve the mechanical strength, osteoconductivity, and biocompatibility required for effective bone tissue engineering. Through various strategies such as incorporating reinforcing agents, combining Sr with other bioactive ions, and dual-loading with drugs, Sr-doped scaffolds have become increasingly optimized for clinical use in bone repair and regeneration.

## 5.2 Bioactive coatings: reduction of implant-associated infections and promotion of osseointegration

Strontium-based nanoparticles have gained significant attention for their potential to address two critical challenges in orthopedic and dental implants: reducing implant-associated infections and promoting osseointegration. Strontium, known for its osteoinductive properties, can enhance bone formation and remodeling by stimulating osteoblast activity and inhibiting osteoclast differentiation. When incorporated into nanoparticle formulations, strontium can be effectively delivered to implant surfaces, creating a favorable environment for bone growth while simultaneously combating bacterial colonization.<sup>151,152</sup>

The antimicrobial properties of strontium nanoparticles, particularly when combined with other agents like silver, offer a dual benefit—enhancing the antibacterial efficacy of implants while ensuring biocompatibility. These nanoparticles can be applied to titanium surfaces using various coating techniques, such as sol-gel or plasma immersion ion implantation, which allow for the controlled release of strontium ions over time. This slow-release mechanism not only reduces the risk of infection but also provides sustained osteogenic effects, promoting faster and more stable osseointegration.<sup>153,154</sup>

In addition to reducing bacterial adhesion, strontium-based nanoparticles support cellular adhesion and proliferation, further facilitating the integration of the implant into the surrounding bone tissue. As a result, strontium nanoparticles represent a promising strategy for improving the long-term success of implant surgeries by addressing both infection prevention and bone healing simultaneously.<sup>155,156</sup>

For instance, let's examine the use of strontium and silver coatings on titanium surfaces as a case study to reduce implant-associated infections and enhance osseointegration. Strontium-based nanoparticles have emerged as a focal point in the design of functionalized titanium implant surfaces due to their dual functionality in promoting osteoinduction and combating bacterial infections.<sup>151-153</sup> Combining strontium (Sr) with silver (Ag) on titanium surfaces offers a promising strategy to address the persistent challenge of optimizing osseointegration while mitigating infection risks. This delicate balance is necessary as most antibacterial materials exhibit cytotoxicity at high concentrations, and excessive use of osteoinductive agents may compromise cell viability. The synergistic effects of Sr and Ag, as highlighted in recent systematic reviews, demonstrate the potential for enhanced implant performance through innovative surface modifications.<sup>154-157</sup>

Various strategies for modifying titanium surfaces with Sr/Ag combinations have been explored, including plasma immersion ion implantation and sol-gel chemistry. These methods not only ensure superficial modifications but also allow deeper

alterations to the material layers, enhancing their applicability to diverse biomedical materials. Importantly, the release kinetics of ions from these surfaces typically follow zero- or first-order patterns, avoiding the burst release that could otherwise lead to cytotoxic effects or reduced antibacterial efficacy. This controlled release is a significant advantage, ensuring prolonged therapeutic effects while minimizing risks to surrounding tissues. Studies consistently report that the biocompatibility of Sr/Ag coatings is comparable to Sr-only surfaces and superior to Ag-only surfaces, highlighting Sr's role in mitigating Ag's cytotoxicity.<sup>158,159</sup>

The antimicrobial properties of Sr/Ag coatings are primarily attributed to Ag ions, which disrupt bacterial membranes, generate reactive oxygen species (ROS), and impair essential cellular functions, ultimately causing bacterial death.<sup>160,161</sup> The addition of Sr further enhances antibacterial efficacy through mechanisms that may include environmental modifications, such as pH changes or increased membrane permeability, although the exact processes remain unclear.<sup>162</sup> Notably, studies have observed antibacterial effects in Sr-only groups, indicating a potential intrinsic antimicrobial activity of Sr, particularly against pathogens like *S. aureus* and MRSA.<sup>64</sup>

Fig. 24 illustrates the multifaceted mechanisms underlying the antibacterial and osteogenic effects of Sr/Ag-modified titanium surfaces. Ag ions directly target bacterial structures and processes, while Sr contributes to enhanced osteogenic outcomes by promoting bone marrow stromal cell (BMSC) adhesion, proliferation, and differentiation. These effects are mediated through signaling pathways such as ERK1/2 and NF- $\kappa$ B, which are crucial for osteogenic gene expression and mineralization.<sup>163,164</sup> The integration of nanostructures into these coatings, as demonstrated by Pan *et al.* (2020), further enhances surface hydrophilicity, reducing bacterial adhesion and promoting osseointegration.<sup>165</sup>

Despite these advances, the clinical translation of Sr/Ag-modified surfaces faces challenges. The critical period for preventing implant infections, particularly the immediate post-surgery phase, requires reliable antibacterial activity. Studies suggest that Ag ion release is most effective during this early period, with its efficacy diminishing over time. To ensure sustained antibacterial effects, innovative strategies such as incorporating cross-linking agents like silk fibroin or hierarchical micro/nanostructures have been employed to modulate ion release kinetics.<sup>166-168</sup>

The variability in bacterial sensitivity to Ag, as seen in studies comparing *E. coli* and *S. aureus*, underscores the need for tailored approaches based on the clinical context. While most research has focused on single-species bacterial strains, the complexity of multispecies biofilms associated with infections such as dental peri-implantitis remains underexplored.<sup>169</sup> Future investigations should prioritize biofilm models and clinically relevant bacterial communities to enhance the applicability of findings.

From a public health perspective, the development of Sr/Ag-coated implants addresses two critical concerns: the increasing prevalence of implant-related infections and the growing demand for durable, biocompatible orthopedic and dental



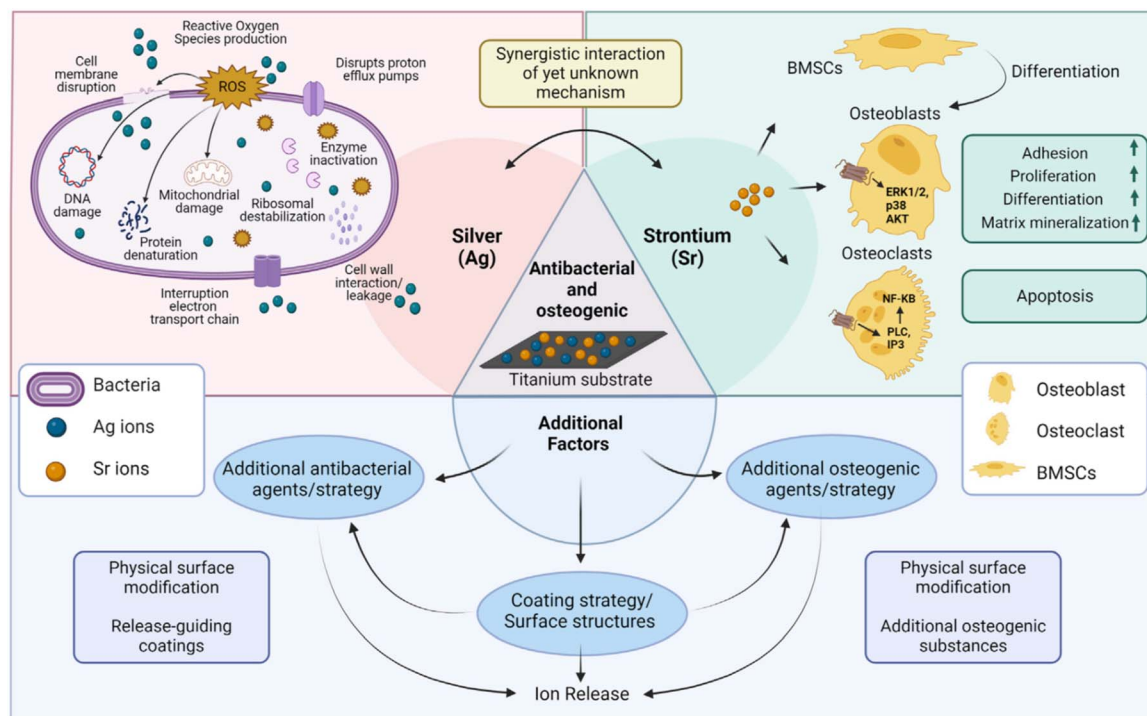


Fig. 24 Schematic illustration of possible mechanisms related to antibacterial/osteogenic titanium surfaces in the included studies. Abbreviations: BMSCs, bone marrow stromal cells; ERK1/2, extracellular signal-regulated kinases 1/2; NF-KB, nuclear factor *k*-light-chain-enhancer of activated B cells.<sup>60</sup>

solutions. The ability of these coatings to reduce infection rates while promoting bone healing has significant implications for reducing healthcare costs and improving patient outcomes. However, the potential environmental impact of silver ion release and the long-term effects on human health warrant further investigation.<sup>60,170</sup>

In general, Sr/Ag-modified titanium surfaces offer a promising solution for dual-functionality in medical implants, achieving both osteogenic and antibacterial outcomes. While the biocompatibility and controlled ion release of these coatings are promising, further studies are needed to unravel the underlying mechanisms, optimize their long-term performance, and address public health and environmental concerns. The integration of advanced surface modification techniques with a deeper understanding of biological interactions will be crucial for the successful clinical translation of these innovative biomaterials.

Kuo *et al.* (2022) present a detailed investigation into poly-electrolyte multilayer (PEM) coatings doped with mesoporous bioactive glass (MBG), specifically incorporating strontium (Sr) and silver (Ag) ions, to address implant-associated challenges.<sup>171</sup> The study demonstrates how such coatings can mitigate risks like infections and insufficient osseointegration, thereby aligning closely with the concept of bioactive coatings aimed at reducing implant-related infections while promoting tissue integration.

The PEM coatings evaluated in this study exhibit significant potential to enhance implant biocompatibility and

functionality. Sr ions, a trace element in human bone, are shown to enhance osteoblast activity, promote angiogenesis, and stimulate osseointegration without compromising cellular viability. On the other hand, Ag ions, incorporated as an antimicrobial agent, effectively disrupt bacterial cell membranes, reducing the likelihood of infections. However, the cytotoxicity associated with higher Ag concentrations necessitates careful optimization. As demonstrated by the cytotoxicity assays (Fig. 25), 1 mol% Ag in SrMBG exhibited a balance between antibacterial properties and cell viability, making it suitable for PEM preparation.

The structural and physical modifications of the PEM coatings also contribute to their bioactive capabilities. Scanning Electron Microscopy (SEM) imaging (Fig. 26) reveals a wrinkled surface morphology with distinct particle formations that improve surface roughness and hydrophilicity. These attributes facilitate cell adhesion, proliferation, and differentiation. The enhanced wettability of the PEM/SrMBG and PEM/AgSrMBG coatings, as evidenced by reduced contact angles, further underscores their ability to create a favorable microenvironment for tissue integration.

Mechanical property assessments reveal that while the PEM coatings reduce the surface hardness and Young's modulus of stainless-steel substrates, these changes bring the mechanical properties closer to those of natural bone. This compatibility supports osteoblast proliferation and attachment, a critical factor in osseointegration. The MTT assay results also confirm the coatings' ability to sustain high cell viability across extended



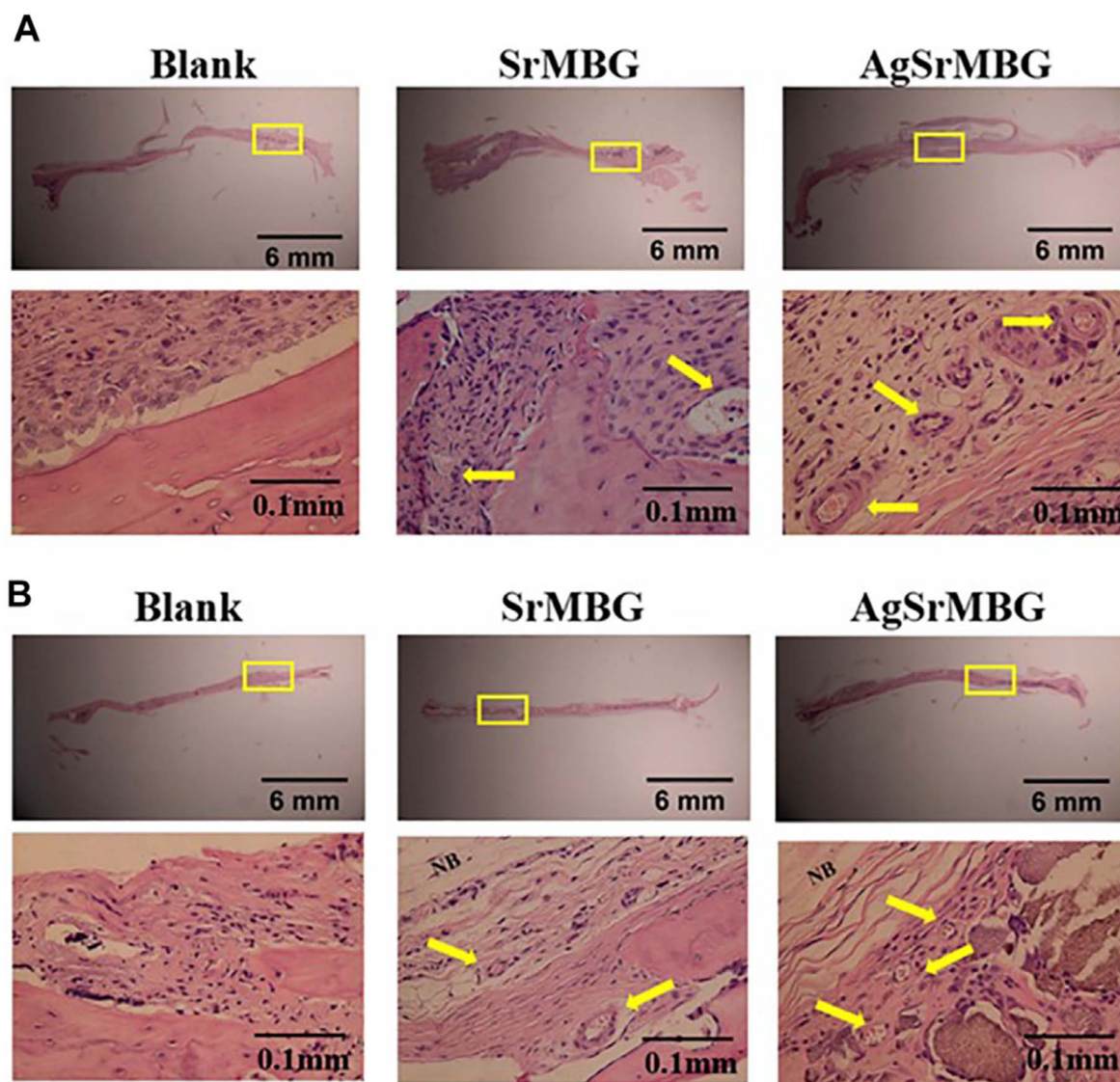


Fig. 25 The H&E staining *in vivo* results of packed SrMBG and AgSrMBG discs for (A) 1 week and (B) 3 weeks after implantation into the skull defects of Sprague-Dawley rats. The yellow square represents the implantation site, yellow arrow is the site of new blood vessel formation, and NB indicates new bone formation ( $n = 5$ ).<sup>171</sup>

culture periods, further validating their suitability for orthopedic applications.

In a recent study, Kuo *et al.* (2022) demonstrate that PEM coatings embedded with SrMBG and AgSrMBG provide a multifaceted approach to enhancing implant efficacy.<sup>171</sup> By combining antimicrobial activity with enhanced osteogenic properties, these coatings address two critical challenges in implant surgery: infection control and osseointegration. Fig. 25 and 26 effectively illustrate the cytotoxicity and structural enhancements, respectively, highlighting the functional synergy of Sr and Ag in the bioactive coatings. This research lays a strong foundation for developing next-generation biomaterials with tailored properties for clinical applications.

The study by Mao *et al.* (2018) presents a comprehensive strategy for addressing two critical challenges associated with

orthopedic implants: reducing implant-associated infections and promoting osseointegration.<sup>172</sup> This aligns directly with the goals of bioactive coatings designed to improve clinical outcomes in orthopedic and dental implants.

Bone infections, particularly in cases of long open fractures (4–64%) and joint-related surgeries (approximately 1%), remain significant complications. To address these, Mao *et al.* developed a multifunctional system combining strontium ranelate-loaded poly(lactic-co-glycolic acid) microspheres (SR-PM) with assembled silver nanoparticles (AgNPs) and hydroxyapatite nanoparticles (HANPs) using a novel solid-in-oil nano-suspension (S/O/N) technique. The schematic of this experimental protocol is depicted in Fig. 27, emphasizing the integration of antibacterial and osteoinductive components in a single platform. This dual functionality is critical in



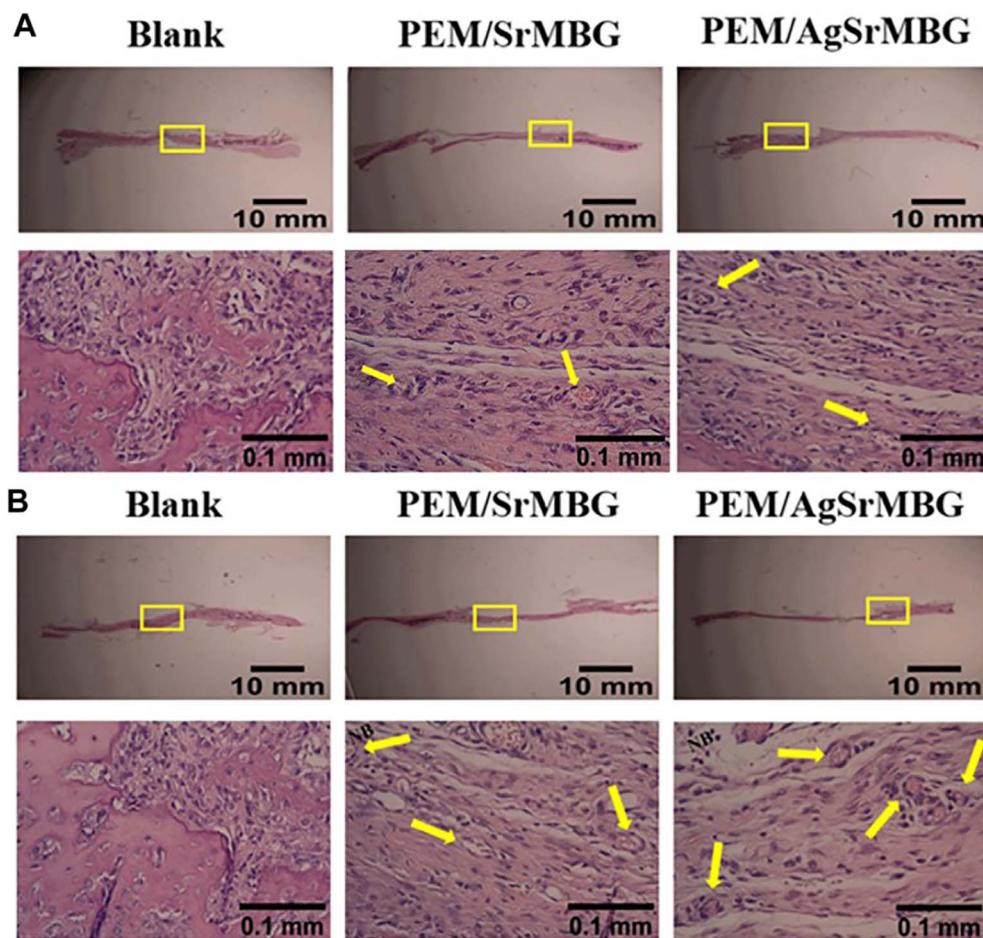


Fig. 26 The H&E staining *in vivo* results of PEM/SrMBG and PEM/AgSrMBG (A) 1 week and (B) 3 weeks of implantation in Sprague-Dawley rat skull defects. The yellow square represents the implantation site, yellow arrows indicate new blood vessel formation sites, and NB represents new bone formation ( $n = 5$ ).<sup>171</sup>

minimizing post-surgical infections while enhancing bone repair and regeneration.

The microspheres exhibited promising drug release profiles, with cumulative release reaching approximately 90% within 22 days. This sustained release is beneficial for long-term therapeutic effects, particularly in managing infections and supporting bone tissue repair. The inclusion of strontium ranelate notably enhanced MC3T3-E1 cell proliferation compared to microspheres without it, suggesting improved biocompatibility and cellular response.

*In vitro* evaluations demonstrated that SR-PM-Ag-HA microspheres significantly promoted osteogenic differentiation of MC3T3-E1 cells, as evidenced by enhanced alkaline phosphatase (ALP) activity and upregulated expression of osteogenic marker genes, including ALP, Col I, OCN, and RunX-2. The results, as shown in ALP staining, highlight the superior osteoinductive capacity of SR-PM-Ag-HA compared to other formulations. This enhanced differentiation is pivotal for achieving robust osseointegration, ensuring the stability and longevity of implants.

Antibacterial activity, a cornerstone of implant-associated infection prevention, was also robustly addressed. The SR-PM-

Ag-HA formulation effectively reduced colony-forming units (CFUs) of bacterial strains and inhibited biofilm formation on titanium surfaces. As demonstrated in biofilm assays (Fig. 28), co-culturing with SR-PM-Ag-HA led to significantly fewer viable bacteria and diminished biofilm intensity. These results underscore the potent antibacterial properties conferred by the incorporated silver nanoparticles, a key component in combating implant-associated infections.

By integrating osteoinductive and antibacterial properties, the SR-PM-Ag-HA microspheres developed by Mao *et al.* (2018)<sup>172</sup> represent a promising advancement in bioactive coatings. The combination of sustained drug release, enhanced cell proliferation, osteogenic differentiation, and strong antibacterial activity positions this system as a potential solution for improving implant outcomes in clinical settings. The study underscores the importance of multifunctional materials in modern implant technology, paving the way for reduced infection rates and improved bone healing.

Geng *et al.* (2022) address the critical challenge of implant-associated infections and the promotion of osseointegration in the osteoporotic microenvironment by utilizing strontium (Sr)-doped nanocoatings on titanium (Ti) implant surfaces.<sup>173</sup>



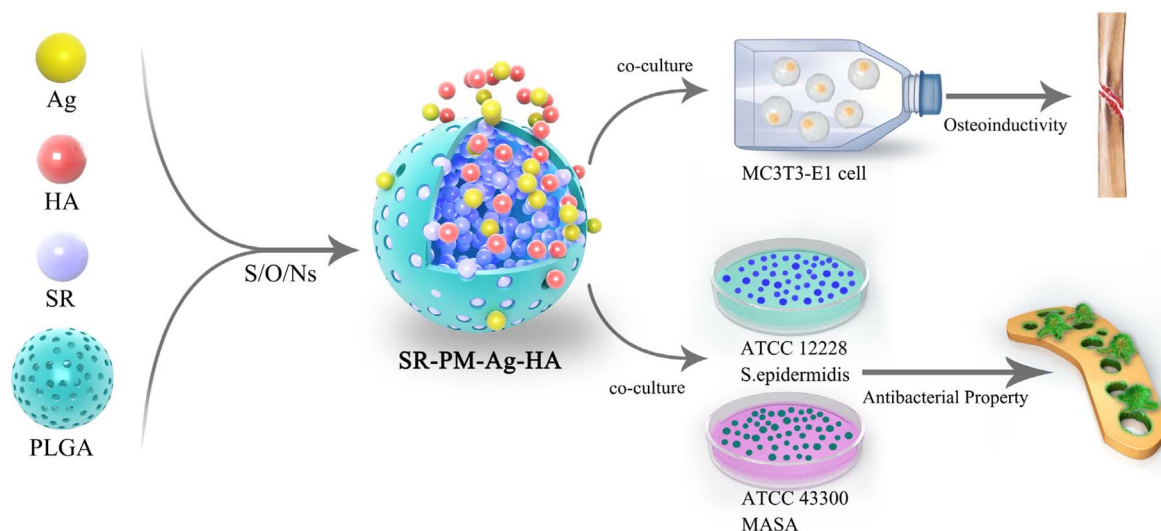


Fig. 27 Schematic diagram of the overall experimental protocol.<sup>172</sup>

Osteoporosis, a condition characterized by reduced bone density and impaired bone healing, significantly compromises the effectiveness of oral implants. To overcome this, the study employed hydrothermal treatment to fabricate Sr-doped nano-coatings (AHT-Sr) on Ti implants, aiming to enhance the bone-binding properties of implants in osteoporotic conditions. Sr ions, known for their osteogenic properties, were integrated into nanoscale surface features, effectively improving biological functionality.

*In vitro* assessments demonstrated that AHT-Sr coatings significantly promoted the osteogenic differentiation of bone marrow mesenchymal stem cells (OVX-BMSCs) derived from osteoporotic models. Alkaline phosphatase (ALP) activity, a marker of early osteogenic differentiation, was markedly higher on AHT-Sr surfaces compared to AHT coatings, as evidenced by more intense purple staining (Fig. 29A). Additionally, gene expression analysis revealed substantial upregulation of key osteogenic markers such as ALP, BMP-2, COL-1, OCN, OPN, and BSP in OVX-BMSCs cultured on AHT-Sr coatings (Fig. 29B). These findings underscore the ability of Sr-doped coatings to stimulate early-stage osteogenesis through the sustained release of Sr ions.

*In vivo* studies further validated the superior performance of AHT-Sr implants in enhancing osseointegration. Micro-computed tomography (micro-CT) analysis was used to evaluate primary bone healing, comparing AHT-Sr implants with AHT-treated controls. The AHT-Sr implants showed significantly enhanced bone formation, with higher bone volume, greater trabecular thickness and number, and reduced trabecular spacing around the implants after two and four weeks (Fig. 30). The 3D reconstruction images (Fig. 30A) vividly illustrated these improvements, highlighting the transformative potential of Sr-doped coatings in promoting bone integration in osteoporotic environments.

This study offers a robust approach to surface modification for dental and orthopedic implants, emphasizing the dual

benefits of reducing implant-associated infections and enhancing osseointegration. By integrating Sr ions into nanoscale coatings, the AHT-Sr implants effectively address the challenges posed by osteoporosis, offering a promising avenue for improving implant outcomes in vulnerable populations.

Shen *et al.* (2022) investigated the impact of oxidative stress (OS), induced by excessive reactive oxygen species (ROS), on titanium implants in osteoporotic environments and the potential for strontium (Sr)-doped titanium coatings to address these challenges.<sup>174</sup> They fabricated titanium implants with varying Sr content (Sr0%, Sr25%, Sr50%, Sr75%, and Sr100%) using the micro-arc oxidation (MAO) technique, which creates a porous oxide layer with enhanced bonding strength and biocompatibility. Importantly, these Sr-doped coatings maintained similar physicochemical properties such as morphology, roughness, crystal structure, and wettability, enabling a focused study on the biological effects of Sr doping levels under normal and OS conditions.

Under normal conditions, the Sr25% group demonstrated superior osteogenesis, consistent with previous findings that bioactivity is highly dose dependent. However, under OS conditions, higher Sr content (Sr75% and Sr100%) outperformed Sr25% in promoting osteogenic differentiation of MC3T3-E1 cells and M2 macrophage polarization. These effects were attributed to the upregulation of antioxidant enzymes catalase (CAT) and superoxide dismutase (SOD), reducing ROS levels and mitigating OS-induced damage. This mechanism was confirmed through *in vitro* cell co-culture studies and *in vivo* implantation procedures, where high Sr-doped samples, particularly Sr100%, exhibited enhanced osteoimmunomodulation and promoted early osseointegration.

The composition analysis revealed the presence of SrO, Sr<sub>3</sub>(PO<sub>4</sub>)<sub>2</sub>, and SrTiO<sub>3</sub> in the coatings, with the ratio of SrO increasing alongside Sr content. The gradual release of Sr<sup>2+</sup> from these coatings was identified as a critical factor in their bioactivity. Sr<sup>2+</sup> not only supported osteogenesis but also



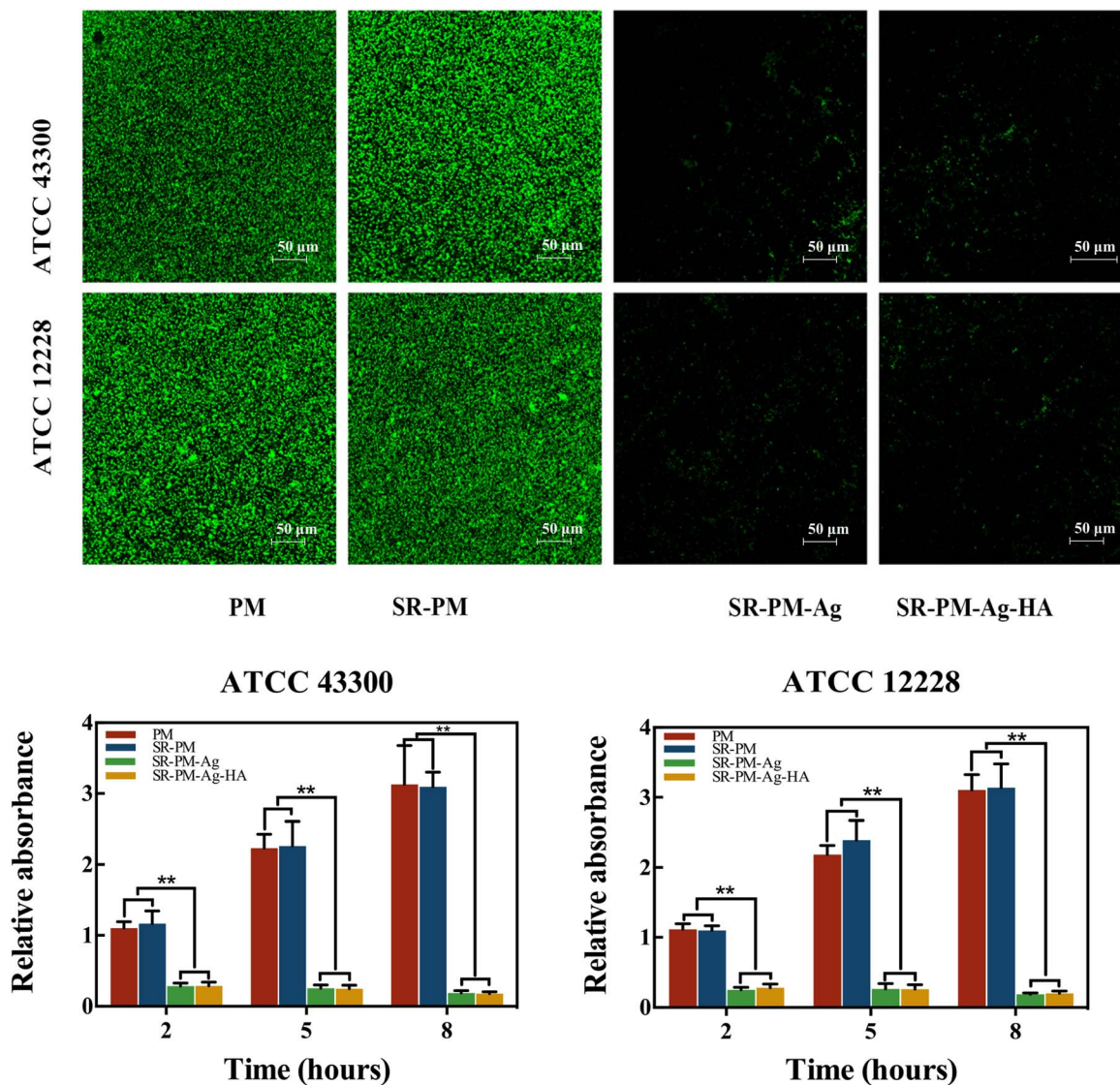


Fig. 28 Confocal laser scanning microscopy (CLSM) images depict biofilm development by two bacterial strains on titanium (Ti) disks following co-culture with four distinct microspheres formulations. Quantitative examination of biofilm formation using crystal violet staining shows biofilm absorption intensity for ATCC43300 and ATCC12228 over 2, 5, and 8 hours of co-culture. Results are presented as mean  $\pm$  standard deviation ( $M \pm SD$ ), with statistical significance indicated ( $*P < 0.01$ ).<sup>172</sup>

induced M2 macrophage polarization, which is vital for creating an anti-inflammatory and regenerative microenvironment. This dual action facilitated both the reduction of OS and the enhancement of bone formation at the implant site.

Furthermore, Shen *et al.* (2022) illustrated the comprehensive process by which high Sr-incorporated samples inhibit ROS-mediated injury and promote new bone formation, as depicted in Fig. 31.<sup>174</sup> The schematic highlights how Sr<sup>2+</sup> enhances CAT and SOD activity in osteoblasts, regulates macrophage polarization to the M2 phenotype, and stimulates osteogenesis through the secretion of osteogenic cytokines such as TGF- $\beta$ 1 and BMP-2. This integration of antioxidant and osteogenic mechanisms underscores the potential of Sr-doped coatings to improve implant performance in challenging osteoporotic environments.

The findings by Shen *et al.*<sup>174</sup> provide compelling evidence for the utility of Sr-doped titanium implants in mitigating OS and promoting osseointegration. These results pave the way for further research into Sr-doped coatings as a promising strategy to reduce implant-associated infections and enhance bone regeneration in patients with osteoporosis.

Wang *et al.* (2021) demonstrated the potential of silk fibroin-silver (SF-Ag) coatings incorporated into strontium (Sr)-loaded titanium dioxide nanotubes (SFAGSTN). This hybrid system leverages the osteogenic and antibacterial properties of Sr and Ag, respectively, with silk fibroin acting as a stabilizer to ensure a sustained release of silver ions, minimizing cytotoxicity while maintaining antibacterial efficacy.<sup>160</sup> Their *in vitro* and *in vivo* results highlighted enhanced osteoblast adhesion, proliferation, and differentiation alongside significant antibacterial



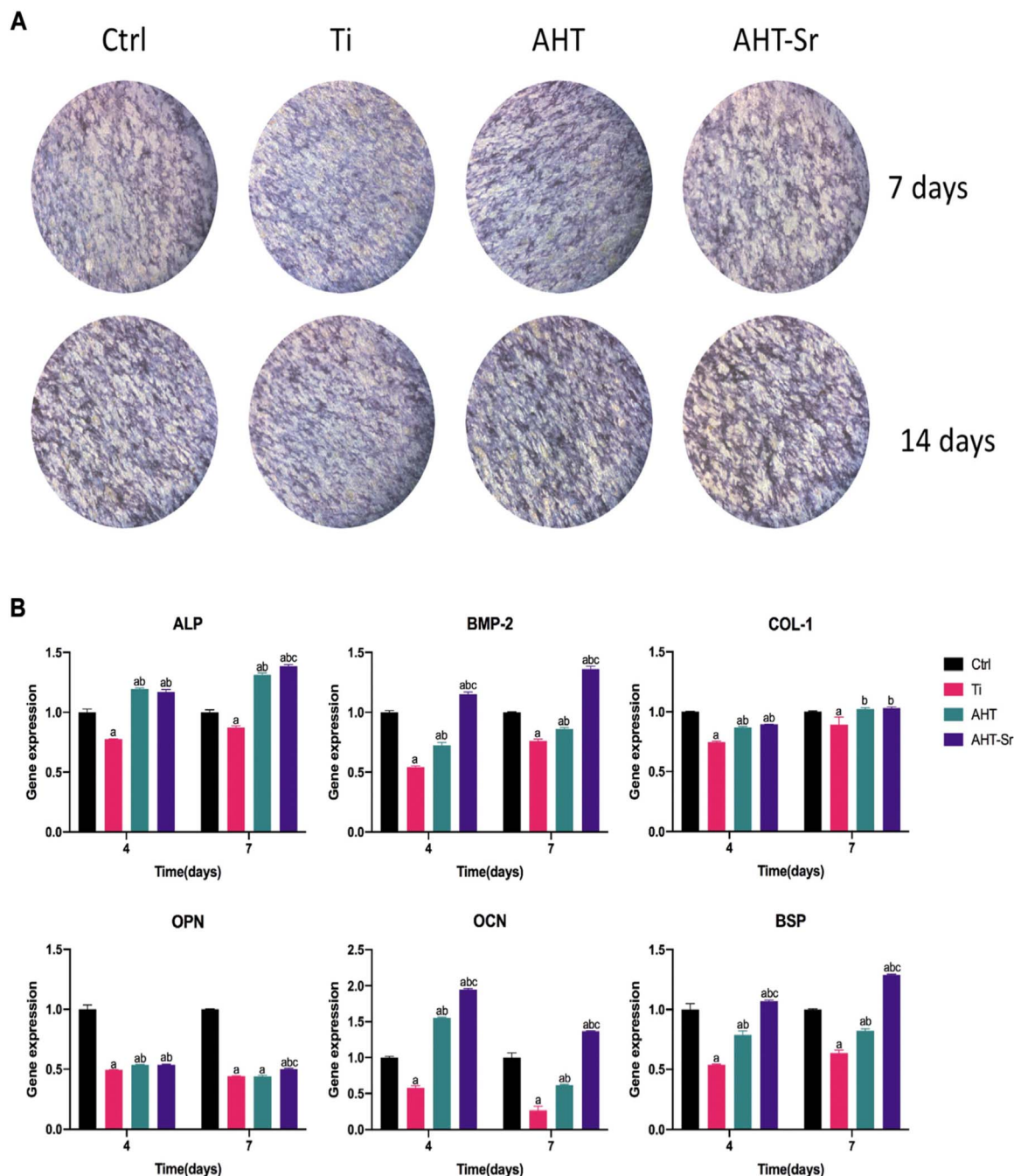


Fig. 29 AHT-Sr promoted osteogenic differentiation of OVX-BMSCs. (A) ALP staining of H-BMSCs and OVX-BMSCs cultured on Ti, AHT and AHT-Sr disks for 4 and 7 days. Representative images of three separate experiments. (B) mRNA expression of selected osteogenic markers in H-BMSCs and OVX-BMSCs that were cultured on different Ti disks for 4 and 7 days. Error bars indicate the SD of three separate experiment. \* $p < 0.05$ .<sup>173</sup>

activity against *E. coli* and *S. aureus*, underscoring SFAgSTN's multifunctionality as a bone repair implant.

Building on the role of strontium, Qiao *et al.* (2019) explored a gallium-doped polydopamine-functionalized SrTiO<sub>3</sub> nanotube (PDA-SrTiO<sub>3</sub> NT) coating.<sup>175</sup> By combining the bioactivity of strontium with gallium's antibacterial and osteogenic properties, this coating exhibited sustained ion release with negligible cytotoxicity. The synergistic effects significantly inhibited *E. coli* and *S. aureus* growth while promoting osteoblast activity and

osseointegration in rabbit bone defect models. The gallium doping enhanced osteoinductivity, demonstrating that such coatings could serve as promising candidates for long-term infection resistance and bone regeneration.

Wu *et al.* (2023) introduced an innovative spatiotemporal immunomodulatory approach using Cu-Sr bilayer bioactive glass nanoparticles (CS-BGNs) on polyetheretherketone (PEEK) surfaces.<sup>176</sup> By regulating the sequential release of Cu<sup>2+</sup> and Sr<sup>2+</sup>, the coating modulated macrophage polarization, initiating



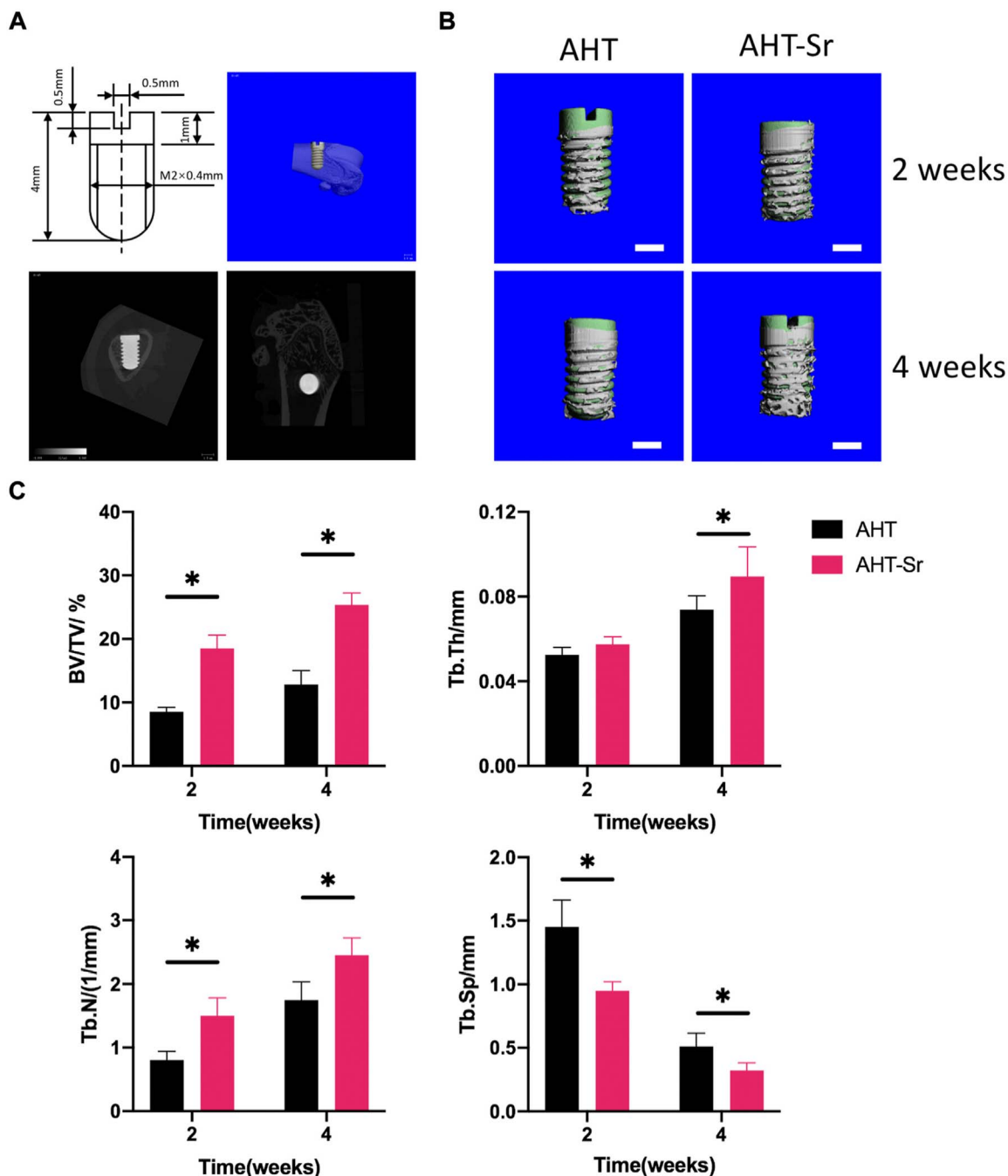


Fig. 30 Osseointegration of AHT and AHT-Sr implants was measured by micro-CT. (A) Schematic of the surgery. (B) Reconstructed pictures of AHT implants (control) and AHT-Sr implants at 2- and 4-weeks post surgery. Scale bar representing 1 mm;  $n = 5$  per group. (C) BV/TV, Tb.Th, Tb.N, and Tb.Sp were measured.  $n = 5$ . \* $p < 0.05$ .<sup>173</sup>

early-stage M1 phenotypes for antibacterial effects and transitioning to M2 phenotypes to support tissue repair. This dual-phase immunomodulation facilitated early bacterial inhibition and long-term osseointegration, offering a novel design framework for next-generation biomaterials tailored for orthopedic applications.

Further advancing bioactive coatings, Wang *et al.* (2024) developed a “pneumatic nanocannon” system for titanium

implants, combining SrTiO<sub>3</sub> nanotubes with on-demand antibiotic release triggered by near-infrared irradiation.<sup>177</sup> This approach achieved robust antibacterial activity against planktonic and biofilm pathogens while ensuring continuous Sr ion release for enhanced osteogenic differentiation. *In vivo* studies confirmed significant reductions in infection and improved bone-to-implant integration, showcasing the potential of dynamic, responsive coatings in complex surgical scenarios.



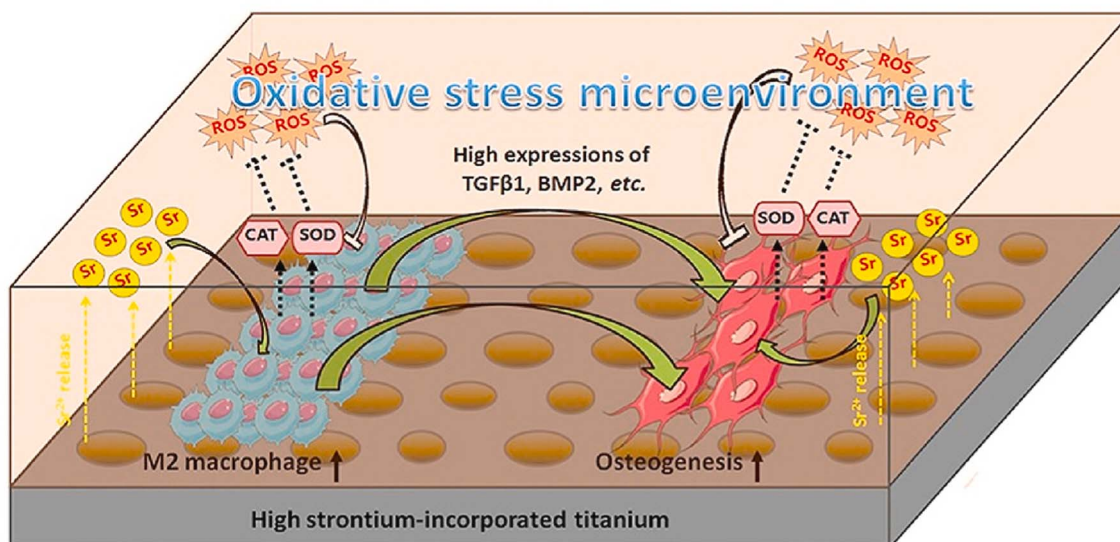


Fig. 31 Schematic representation of high Sr-incorporated samples promoting early osseointegration under oxidative stress (OS) conditions. Released  $\text{Sr}^{2+}$  enhances catalase (CAT) and superoxide dismutase (SOD) activity, reducing excessive endogenous reactive oxygen species (ROS) in osteoblasts, thereby improving osteoinductive and antioxidative properties.  $\text{Sr}^{2+}$  also regulates macrophage morphology and CAT/SOD activity, mitigating OS and inflammation to facilitate macrophage polarization from M0 to M2. M2 macrophages overexpress osteogenic cytokines, such as TGF- $\beta$ 1 and BMP-2, significantly enhancing osteogenesis.<sup>174</sup>

Chen *et al.* (2021) focused on the co-incorporation of zinc (Zn) and Sr into a nanorod coating on sandblasted and acid-etched titanium (SLA-Zn/Sr).<sup>178</sup> This dual-doped system significantly reduced biofilm formation by downregulating *icaA* gene expression in *S. aureus*, leading to diminished polysaccharide intercellular adhesion. Concurrently, the coating enhanced rBMSCs adhesion, proliferation, and osteogenic differentiation, positioning SLA-Zn/Sr as a multifunctional platform for dental implant applications.

Offermanns *et al.* (2018) emphasized the sustained-release capabilities of a strontium-functionalized titanium (Ti-Sr-O) coating prepared *via* magnetron sputtering.<sup>179</sup> *In vivo* studies revealed accelerated bone-to-implant contact (BIC) and enhanced bone formation (BF) after both two and twelve weeks of implantation in a rabbit femur model. The localized release of Sr provided substantial benefits in osseointegration without systemic effects, underscoring its osteoinductive potential for endosseous implants.

Liu *et al.* (2015) investigated the dual osteogenic and anti-bacterial effects of strontium-substituted bioactive glasses.<sup>180</sup> Their findings highlighted that a 5% Sr-substituted glass (5Sr) significantly promoted alkaline phosphatase activity, cell proliferation, type I collagen synthesis, and mineral nodule formation in MC3T3-E1 osteoblast-like cells. Furthermore, the material exhibited dose-dependent antibacterial activity against *Aggregatibacter actinomycetemcomitans* and *Porphyromonas gingivalis*, key pathogens implicated in dental infections. This dual functionality underscores the potential of Sr-substituted bioactive glasses in scenarios where rapid bone formation and infection prevention are critical, such as dental bone defect repair.

Building on this, Lu *et al.* (2022) demonstrated that Sr-incorporated micro/nano titanium surfaces (SLA-Sr) not only

improved osteogenic activity but also facilitated angiogenesis through upregulation of HIF-1 $\alpha$  protein expression and Erk1/2 phosphorylation.<sup>181</sup> Additionally, SLA-Sr coatings induced macrophage polarization toward the M2 phenotype, promoting a pro-healing environment. The synergistic effects of angiogenesis and immunomodulation were further evidenced by early vascularized osseointegration and type H vessel formation *in vivo*. These findings illustrate the multifaceted benefits of Sr modifications in implant surfaces, aligning with the broader goal of enhancing implant integration while minimizing inflammatory complications.

Cheng *et al.* (2023) expanded on the use of Sr in the context of critical-size bone defects, which pose a significant challenge in clinical practice.<sup>182</sup> By incorporating Sr ions into nano-hydroxyapatite (nHA)/chitosan microspheres using polydopamine (PDA) as a chelating agent, the study achieved a controlled release system that enhanced both osteogenic differentiation and vascularization. *In vivo* experiments involving cranial defects in rats demonstrated effective bone regeneration facilitated by the composite microspheres. This approach highlights the importance of integrating bioactive ions like Sr into scaffolds to provide sustained biological cues for bone repair.

The benefits of Sr substitution extend to orthopedic applications, as evidenced by Geng *et al.* (2020), who fabricated Sr-substituted apatite coatings *via* electrochemical deposition.<sup>183</sup> These coatings not only supported mesenchymal stem cell adhesion, proliferation, and differentiation but also inhibited osteoclast activity, a key factor in counteracting osteoporosis-associated implant loosening. *In vivo* studies revealed that nano-needle-like Sr-substituted coatings promoted new bone formation and improved implant-bone integration. This



demonstrates the potential of Sr to address the unique challenges posed by osteoporotic bone conditions.

Hayann *et al.* (2024) took a complementary approach by developing a porous polymethylmethacrylate (pPMMA) cement enriched with Sr-based nanoparticles.<sup>184</sup> These nanoparticles, which mimicked the structure of bone apatite, significantly enhanced osteoblast activity, as evidenced by upregulated TNAP activity, Runx2 expression, and matrix mineralization. *In vivo* implantation in rabbit femurs confirmed the cement's ability to promote osteointegration and apatite mineral formation. The use of pPMMA cement highlights how Sr nanoparticles can be leveraged to enhance the bioactivity of traditionally inert materials, addressing long-term implant stability and integration.

Zhang *et al.* (2016) further emphasized the role of Sr in enhancing rapid osseointegration through the development of a novel strontium-incorporated nanoporous coating (MAO-Sr) for titanium implants.<sup>185</sup> This coating significantly enhanced bone marrow stromal cell (BMSC) adhesion and osteogenic differentiation while promoting angiogenic growth factor secretion to recruit endothelial cells. The involvement of MAPK/Erk and PI3K/Akt signaling pathways was identified as a key mechanism underlying these effects. *In vivo*, the MAO-Sr coating demonstrated rapid bone formation and osseointegration comparable to commercial implants, underscoring its clinical potential.

Together, these studies illustrate the diverse strategies employed to integrate Sr into bioactive coatings and scaffolds. By promoting osteogenesis, angiogenesis, and immunomodulation while simultaneously reducing infection risks, Sr-based materials address critical barriers in implant technology. This body of work not only underscores the therapeutic potential of Sr but also highlights its versatility in various material platforms, paving the way for innovations in reducing implant-associated infections and enhancing osseointegration.

## 6 Antimicrobial properties

### 6.1 Mechanisms of action

Strontium nanoparticles (SrNPs) exhibit antimicrobial activity through a multifaceted mechanism that targets key aspects of bacterial survival and function, making them effective against a broad range of pathogenic microorganisms. A primary mode of action involves membrane disruption.<sup>186,187</sup> Upon contact with bacterial cells, SrNPs interact with the cell wall and membrane, compromising their structural integrity. This destabilization leads to leakage of intracellular contents, depletion of essential ions, and ultimately, bacterial cell lysis. By dismantling the membrane, SrNPs not only disrupt critical cellular processes but also prevent the microorganism from initiating self-repair, leading to its complete eradication.<sup>187</sup>

Each study discussed below elaborates on how SrNPs, synthesized through various methodologies, achieve this antimicrobial action.

Hamarawf *et al.* (2023) explored the antibacterial properties of strontium manganese hexaferrite nanoparticles (SMHFs) synthesized through chemical and green sol-gel auto-

combustion routes.<sup>188</sup> Among the variants tested, SMHF-P, synthesized using pomegranate extract, exhibited superior antibacterial activity. The study suggests that SMHF-P's high magnetic characteristics, mesoporosity, and large surface area enhance its interaction with bacterial cell walls. When SMHF-P comes into contact with bacterial membranes, its small particle size enables penetration into the lipid bilayer, disrupting the membrane's structural integrity. This interaction results in cytoplasmic leakage, as indicated by the well diffusion assay, and leads to bacterial cell death. The combination of physical membrane disruption and the intrinsic properties of SMHF-P underscores its potent bactericidal mechanism.

Similarly, Ilavenil *et al.* (2023) reported the antimicrobial efficacy of strontium oxide nanoparticles (SrONPs) synthesized using *Lantana camara* leaf extract.<sup>189</sup> These SrONPs showed substantial antibacterial activity, particularly against *E. coli* and *S. aureus*, with zones of inhibition reaching 28 mm. The researchers observed that SrONPs at higher concentrations effectively penetrated the bacterial cell walls, compromising the polysaccharide and peptidoglycan layers. The nanoparticles caused irreversible damage by weakening the electrostatic interactions that maintain membrane integrity. This breakdown not only allowed the nanoparticles to breach the bacterial cells but also facilitated the release of intracellular contents, culminating in the cessation of bacterial growth and metabolism.

Kasthuri and Pandian (2023) extended these findings by synthesizing SrONPs using *Solanum nigrum* leaf extract.<sup>187</sup> These nanoparticles demonstrated significant antibacterial activity, with zones of inhibition as large as 33 mm for *E. coli*. The study highlighted that phytochemical, including flavonoids and tannins present in the extract, synergize with SrONPs to enhance their membrane-disruptive capabilities. These bioactive compounds destabilize the lipid bilayer, allowing SrONPs to penetrate and disrupt the membrane. The subsequent leakage of cellular components, coupled with impaired replication, underscores the bactericidal potential of these nanoparticles. The researchers further noted the pronounced vulnerability of Gram-negative bacteria, such as *E. coli*, due to their thinner and less rigid cell walls, making them more susceptible to membrane disruption by SrONPs.

Swain and Rautray (2021) investigated strontium bismuth titanate nanoparticles (SBT NPs), which also demonstrated robust antibacterial activity.<sup>190</sup> The polarized SBT specimens exhibited enhanced efficacy, with a zone of inhibition of 28 mm against *Staphylococcus aureus*. The researchers attributed this activity to electroporation, a phenomenon where an externally induced electric field creates pores in bacterial membranes. This membrane perforation facilitates ion and molecular leakage, severely compromising bacterial viability. The bismuth component in SBT NPs further contributes to this bactericidal action by interacting with bacterial surface proteins, amplifying the destabilization of the cell membrane.

Collectively, these studies emphasize that the antimicrobial efficacy of SrNPs fundamentally hinges on their ability to disrupt bacterial membranes. The physical interaction of SrNPs with cell walls destabilizes the membrane, initiating a cascade



of events, including the loss of essential ions, leakage of intracellular components, and eventual bacterial cell lysis. Factors such as nanoparticle size, surface area, charge, and the presence of bioactive capping agents significantly influence this mechanism, enhancing the penetration and destabilization of bacterial membranes. This membrane-targeting strategy underscores the potential of SrNPs as effective antimicrobial agents against a broad spectrum of bacterial pathogens.

Another key mechanism underlying the antimicrobial activity of SrNPs is the generation of reactive oxygen species (ROS). These nanoparticles enhance ROS production, leading to extensive oxidative damage to essential cellular components. Highly reactive molecules such as superoxide radicals, hydrogen peroxide, and hydroxyl radicals inflict significant harm on bacterial DNA, proteins, and lipids. The resulting oxidative stress overwhelms the bacteria's intrinsic defense mechanisms, including antioxidant enzymes and repair systems, leaving them unable to mitigate the damage. This disruption ultimately leads to cellular dysfunction and bacterial death due to the accumulation of oxidative injuries.<sup>191,192</sup>

The antimicrobial efficacy of SrNPs, particularly through ROS generation, is underscored in the work of Gao *et al.* (2021) involving the design and application of zirconium-doped strontium titanate (ZSTO) nanofibrous membranes modified

with silver phosphate (AZSTO).<sup>193</sup> The study meticulously reveals how these nanofibrous membranes leverage ROS generation to achieve remarkable antibacterial effects against Gram-positive and Gram-negative bacteria. This mechanism is pivotal to their enhanced bactericidal performance.

The fabrication of AZSTO membranes through a combination of sol-gel and electrospinning methods endowed the materials with excellent structural flexibility and porosity. Importantly, the doping with silver phosphate significantly amplified their photocatalytic and antibacterial activities under visible light. The membranes exhibited over 99.99% bacterial inhibition rates, attributed to synergistic effects between ROS, such as superoxide radicals and photogenerated holes, and the release of silver ions.

The study revealed that in dark environments, the antibacterial effects stem primarily from  $\text{Ag}^+$ , which interferes with bacterial enzymatic systems and other cellular processes. However, under visible light, the membranes' bactericidal efficiency increased significantly due to the generation of ROS. These reactive species, generated in the valence and conduction bands of the AZSTO membranes, were released into the bacterial suspension, where they penetrated bacterial cells, inflicting oxidative damage on DNA, RNA, and proteins. This oxidative stress led to cellular dysfunction and eventual bacterial death.

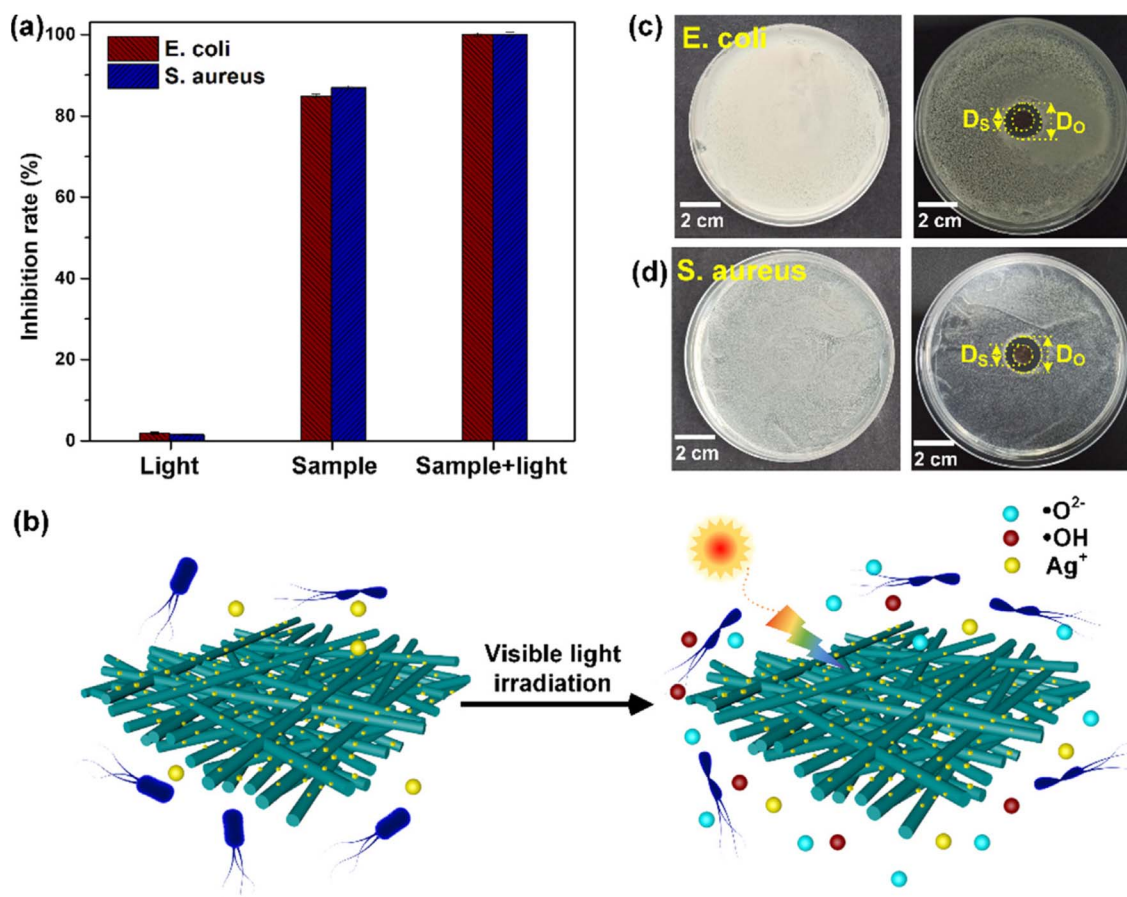


Fig. 32 (a) The inhibition rate of AZSTO nanofibrous membranes against *E. coli* and *S. aureus* under different conditions. (b) Schematic illustrating the disinfection mechanism of AZSTO nanofibrous membranes. Optical profiles showing the inhibition zone test against (c) *E. coli* and (d) *S. aureus*: unprocessed (left) and treated with AZSTO nanofibrous membranes under visible-light irradiation (right).<sup>193</sup>



Fig. 32 provides a mechanistic illustration of the antibacterial action. It depicts how the AZSTO nanofibrous membranes, upon visible-light irradiation, generate free radicals that induce severe oxidative damage. This figure supports the assertion that the interaction between ROS and bacterial cellular components, facilitated by the AZSTO membranes, overwhelms bacterial defense mechanisms, resulting in their inactivation.

Additionally, the inhibition zone method demonstrated the practical application of AZSTO membranes. The calculated inhibition zone widths for *S. aureus* (3.5 mm) and *E. coli* (3.4 mm) exceeded ISO 20645:2004 standards for “good effect,” further validating their potent antimicrobial properties. These results emphasize that the ROS-mediated pathways, augmented by  $\text{Ag}^+$ , play a critical role in the observed antimicrobial efficacy, aligning closely with the described oxidative mechanisms in SrNPs.

This comprehensive analysis not only confirms the potential of AZSTO membranes in antibacterial applications but also highlights their robustness under harsh environmental conditions, suggesting superior adaptability compared to traditional polymeric antibacterial materials. The findings bridge fundamental ROS-driven antimicrobial pathways with practical implementations, marking a significant advance in nanomaterial-based antibacterial strategies.

The study by Aloufi (2023) highlights the critical role of reactive oxygen species (ROS) generation in the antimicrobial activity of Sr-doped tin dioxide ( $\text{SrSnO}_2$ ) nanoparticles synthesized through a green approach using *Mahonia bealei* leaf extract.<sup>194</sup> The  $\text{SrSnO}_2$  nanoparticles were characterized for their structural, compositional, and functional properties, and their effectiveness against Gram-positive and Gram-negative pathogens was attributed significantly to ROS-mediated mechanisms.

ROS molecules, including superoxide radicals, hydrogen peroxide, and hydroxyl radicals, are known to induce oxidative damage to bacterial cells. In the study, photoluminescence (PL) spectroscopy confirmed the presence of surface defects and oxygen vacancies in  $\text{SrSnO}_2$  nanoparticles. These oxygen vacancies are critical active sites for ROS production, as they enhance the interaction of the nanoparticles with molecular oxygen and water, leading to the generation of ROS under appropriate conditions. These ROS then attack essential cellular components of the bacteria, including DNA, proteins, and lipids, resulting in oxidative stress that overwhelms the bacteria's intrinsic defense systems. The disruption of antioxidant enzymes and repair pathways ensures that bacteria cannot mitigate this damage, culminating in cellular dysfunction and eventual death.

The antimicrobial activity of  $\text{SrSnO}_2$  nanoparticles against various human pathogens, as demonstrated in the study, underscores the potency of ROS-induced oxidative stress. The Gram-positive and Gram-negative bacteria treated with  $\text{SrSnO}_2$  nanoparticles exhibited significant growth inhibition, which can be directly linked to the ability of these nanoparticles to generate ROS. This aligns with the fundamental pathway described, where the accumulation of ROS-induced injuries to critical cellular machinery irreparably damages bacterial cells.

The green synthesis approach employed by Aloufi (2023)<sup>194</sup> adds an eco-friendly dimension to the development of  $\text{SrSnO}_2$  nanoparticles while maintaining their functional efficacy. This method not only supports sustainable nanoparticle production but also retains the structural and chemical properties essential for ROS generation and the resulting antimicrobial activity. The results of this study solidify the centrality of ROS as a mechanism of action for Sr-doped nanoparticles, offering insights into their potential applications in healthcare as antimicrobial agents.

The study by Dapporto *et al.* (2022) underscores the critical role of bioactive strontium ions released from SrCPC formulations in enhancing therapeutic outcomes.<sup>195</sup> Strontium ions, known for their dual functionality in bone regeneration and antimicrobial activity, are released during the degradation of SrCPCs into the surrounding environment. This release mechanism is evident from the degradation tests, which demonstrated a measurable release of calcium and strontium ions over 35 days (Fig. 33A).

Strontium ions interfere with bacterial metabolic processes by disrupting enzymatic activities essential for survival. Once released, these ions can bind to critical bacterial enzymes and cofactors, altering their structure and functionality. This disruption cascades into impairments in nutrient absorption and ion homeostasis, effectively inhibiting bacterial growth and reproduction. These findings highlight the antimicrobial efficacy of SrCPCs, particularly formulations containing NP-TC, which further optimize the release kinetics of therapeutic agents while supporting ion-mediated bacterial inhibition.

Moreover, the release of strontium ions also aligns with the broader biological functionality of SrCPCs in bone regeneration. By contributing to the osteointegrative potential of the material, the ions create a synergistic effect, coupling the antibacterial properties with bone-healing capabilities. The steady ion release, observed alongside the slow TC release profile from NP-TC-loaded formulations, reinforces the multifaceted utility of SrCPCs in treating complex bone defects and infection-prone environments.

In summary, the bioactive strontium ions released from SrCPCs play a pivotal role in their functionality, particularly by modulating bacterial metabolism and enhancing therapeutic efficacy. Fig. 33A provides a clear depiction of the ion release dynamics, supporting the study's conclusions on the material's antimicrobial and regenerative potential.

The study by Kumar *et al.* (2023) provides significant insights into the antimicrobial properties of strontium and copper co-doped hydroxyapatite nanoparticles ( $\text{SrCuHA}$  NPs) incorporated into orthodontic composites.<sup>59</sup> The results demonstrate that  $\text{SrCuHA}$  NPs enhance antimicrobial efficacy by leveraging the dual action of copper and strontium ions, particularly against *Streptococcus mutans* (*S. mutans*), a primary contributor to white spot lesions (WSLs) during orthodontic treatments. Strontium ions, released from these nanoparticles, likely contribute to the observed antimicrobial activity by interfering with bacterial metabolism and disrupting enzymatic activities critical to bacterial survival.



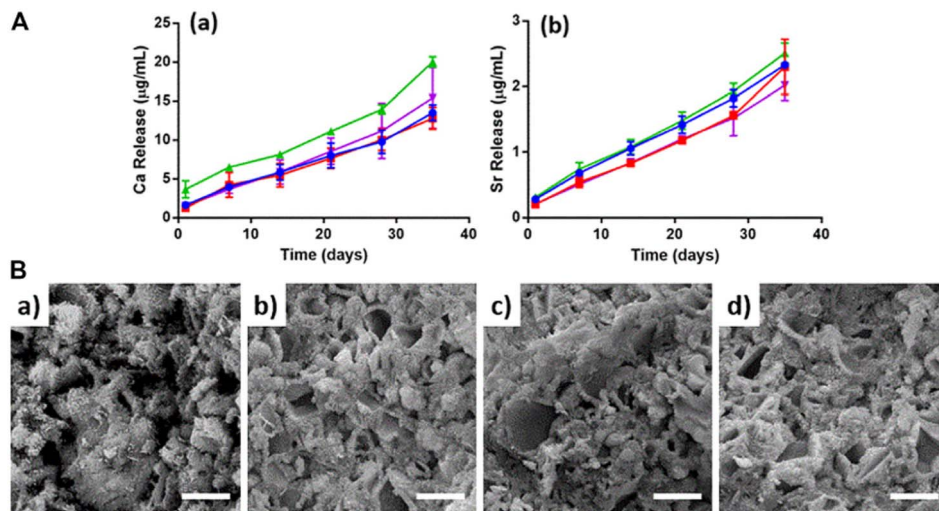


Fig. 33 (A) Ion releases up to 35 days: (a) calcium, (b) strontium. SrCPC (blue), SrCPC\_NP (red), SrCPC\_TC (green), SrCPC\_NP-TC (violet); (B) SEM micrographs of cements: CPC (a), CPC\_TC (b), CPC\_NP (c), CPC\_NP-TC (d). Scale bar = 5 µm.<sup>195</sup>

Strontium ions, upon release into the surrounding environment, may bind to essential bacterial enzymes and cofactors, altering their structural integrity and functionality. This action potentially inhibits metabolic pathways necessary for bacterial growth, such as nutrient absorption and ion homeostasis. The study's findings align with these mechanisms, as the SrCuHA NP-incorporated composite demonstrated a marked zone of inhibition (ZOI) against *S. mutans*. This activity highlights the role of bioactive strontium ions in impairing the bacterial metabolic processes, thereby reducing the viability of cariogenic pathogens.

Further characterization of SrCuHA NPs using EDAX, FTIR, and SEM confirmed successful nanoparticle synthesis and incorporation into orthodontic composites. These nanoparticles showed concentration-dependent antimicrobial activity, with higher concentrations leading to enhanced ZOI, particularly against *S. mutans*. This outcome underscores the importance of optimizing nanoparticle content in clinical materials to achieve maximal antibacterial efficacy.

Copper ions, also released from SrCuHA NPs, complement the antimicrobial effects of strontium by disrupting bacterial cell membranes and generating reactive oxygen species, which further enhance bactericidal activity. These combined effects not only inhibit bacterial growth but also prevent biofilm formation on orthodontic composites, reducing the risk of enamel demineralization and WSLs. Additionally, the study corroborates findings from previous research that demonstrated the enhanced antimicrobial properties of metal-doped hydroxyapatite nanoparticles, particularly in combating *Escherichia coli* and *Staphylococcus aureus*.

Kumar *et al.* (2023) successfully synthesized SrCuHA NPs and demonstrated their potential in orthodontic composites to mitigate WSLs by leveraging the antimicrobial properties of strontium and copper ions.<sup>59</sup> This study emphasizes the importance of bioactive ions in disrupting bacterial metabolic pathways and highlights the promising role of SrCuHA NPs in advancing orthodontic materials. These findings contribute to

the growing body of evidence supporting the use of nanotechnology in preventing bacterial infections associated with dental treatments.

The study conducted by Alshammari *et al.* (2024) highlights the significant antimicrobial potential of strontium (Sr)-functionalized wafers in combating bacteria commonly associated with peri-implant infections.<sup>196</sup> The wafers, coated with a strontium titanium oxygen (Sr-Ti-O) layer, were evaluated for their bacteriostatic and bactericidal effects on both mono-species and multispecies biofilms over varying time intervals. The findings underscore the efficacy of Sr-functionalized wafers in reducing bacterial viability, colony-forming units (CFUs), and enzymatic activity, notably gingipain, in biofilms.

Key results demonstrated that Sr-functionalized wafers led to a statistically significant reduction in viable cells compared to titanium (Ti) control wafers, as evidenced by bacterial viability assays and CFU plate counting methods. For mono-species biofilms, Sr-functionalized wafers showed pronounced reductions in viable cells for *Staphylococcus aureus* and *Escherichia coli* within 2 hours, with similar trends observed for *Porphyromonas gingivalis* after 24 hours (Fig. 34). In multispecies biofilms, a marked decrease in total biomass and viable cells was observed across various bacterial consortia, including those containing *P. gingivalis*, *S. aureus*, and *E. coli*, over six days (Fig. 35). Notably, *P. gingivalis* was undetectable in Sr-functionalized wafers at all time points, contrasting with its persistence in control samples, where it constituted up to 15% of the total biofilm by Day 6.

The antimicrobial action of Sr-functionalized wafers is attributed to their ability to release bioactive strontium ions into the surrounding environment. These ions disrupt bacterial metabolism by interfering with enzymatic activities essential for bacterial survival. Strontium ions can bind to critical bacterial enzymes and cofactors, altering their structure and functionality, thereby impairing key metabolic pathways such as nutrient absorption and ion homeostasis. These disruptions



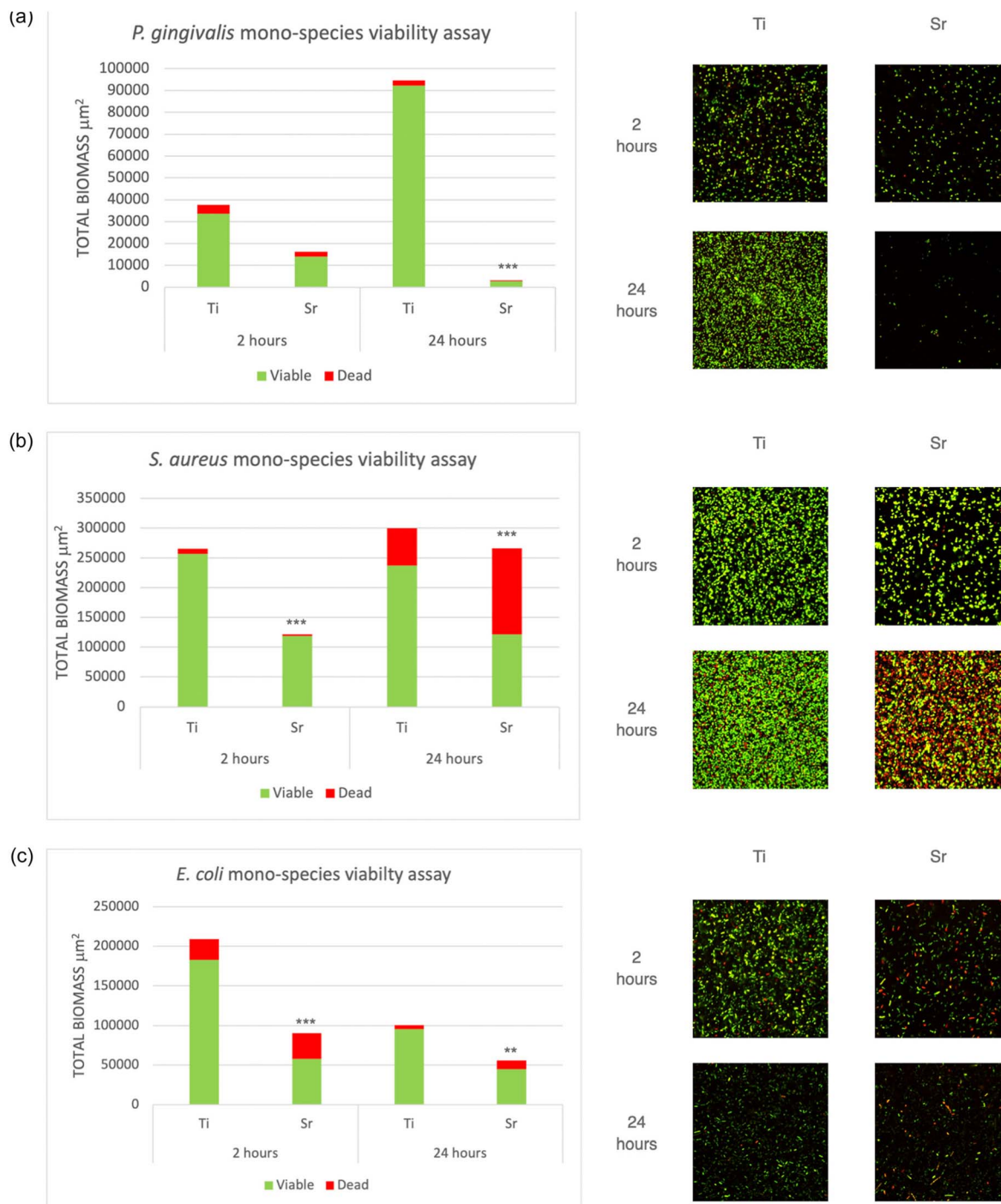


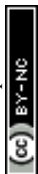
Fig. 34 Bar graph showing the results of mono-species viability assay showing total biomass, viable (green) and dead (red) cells, and CSLM images of both Sr-functionalized and Ti control wafers tested against *Porphyromonas gingivalis* (a), *Staphylococcus aureus* (b), and *Escherichia coli* (c).  $**p < 0.01$  compared to Ti control.  $***p < 0.001$  compared to Ti control.<sup>196</sup>

inhibit bacterial growth and reproduction, amplifying the antimicrobial efficacy of Sr-functionalized wafers.

Additionally, Sr-functionalized wafers exhibited a significant reduction in gingipain activity, an enzyme produced by *P. gingivalis* that plays a critical role in peri-implantitis. Lower gingipain activity was consistently observed in biofilms grown on Sr-functionalized wafers compared to Ti control wafers. This

reduction aligns with the suppression of *P. gingivalis* viability and indicates the broader potential of Sr-functionalized surfaces to modulate biofilm-associated virulence factors.

These findings align with previous studies demonstrating the antimicrobial properties of Sr coatings. The sustained bacteriostatic and bactericidal effects observed in this study further emphasize the prolonged antimicrobial efficacy of Sr ion



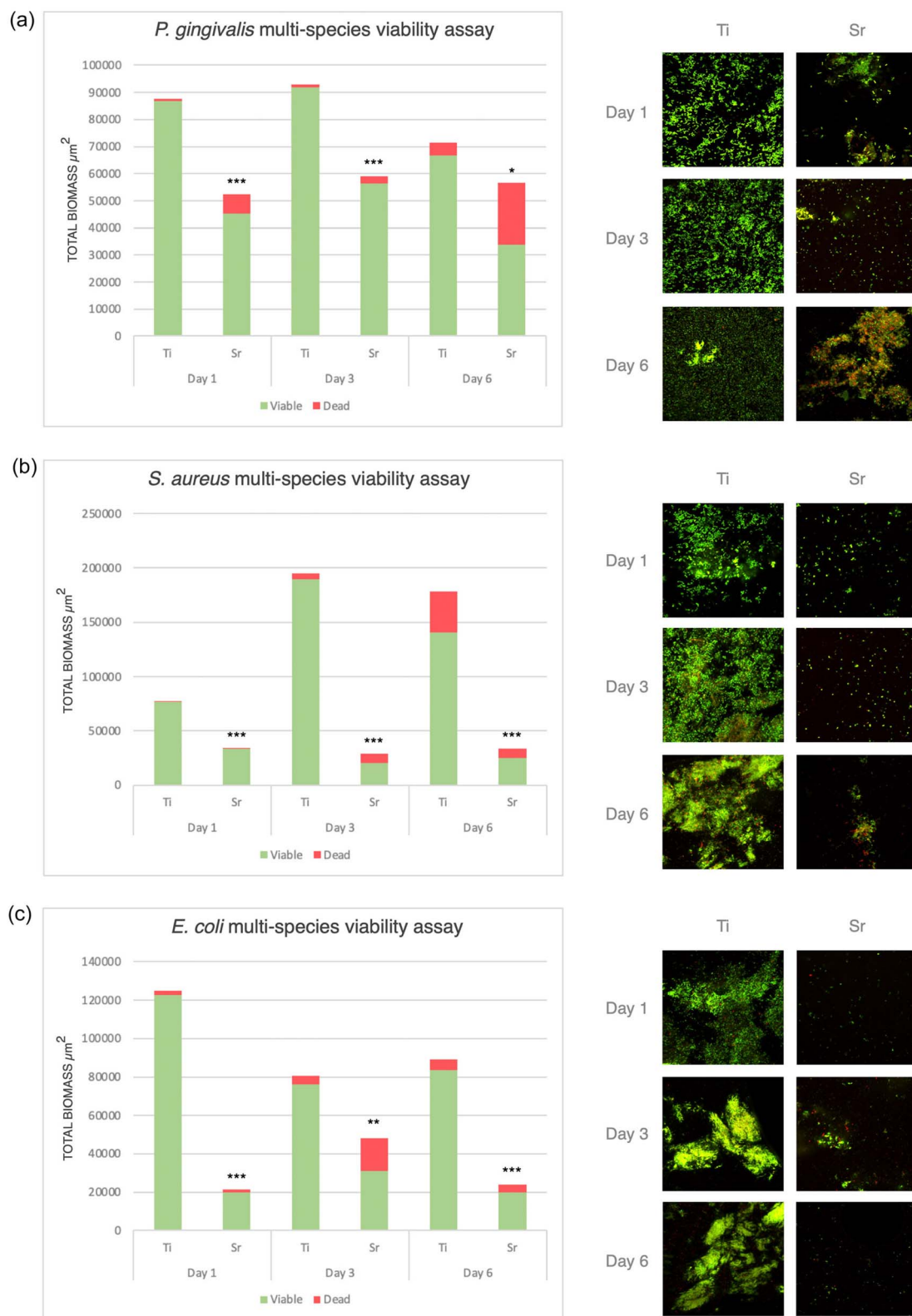


Fig. 35 Bar graph showing the results of multispecies viability assay showing total biomass, viable (green) and dead (red) cells, and CSLM images of both Sr-functionalized and Ti control wafers tested against *Porphyromonas gingivalis* multispecies (a), *Staphylococcus aureus* multispecies (b) and *Escherichia coli* multispecies consortia (c). \* $p < 0.05$  compared to Ti control. \*\* $p < 0.01$  compared to Ti control. \*\*\* $p < 0.001$  compared to Ti control.<sup>196</sup>



release over six days. The study also suggests that the formation of  $\text{Sr}(\text{OH})_2$ , due to Sr ions reacting with water, may contribute to localized pH changes, which in turn enhance antimicrobial activity.

In a nutshell, the study by Alshammari *et al.* (2024) demonstrates that Sr-functionalized wafers are effective in significantly reducing bacterial viability, inhibiting biofilm formation, and mitigating virulence factors in mono- and multispecies biofilms.<sup>196</sup> These findings underscore the potential of Sr-functionalized surfaces in preventing and managing peri-implant infections, particularly through their capacity to release bioactive ions that disrupt bacterial metabolism and growth.

The combined action of membrane disruption, ROS generation, and ion-mediated metabolic interference ensures that SrNPs attack bacteria through multiple fronts, reducing the likelihood of resistance development. This comprehensive approach makes SrNPs highly effective against both planktonic bacterial cells and biofilm-associated communities. By leveraging these synergistic mechanisms, SrNPs emerge as a versatile and potent antimicrobial agent capable of addressing a broad spectrum of pathogens, including drug-resistant strains. These characteristics highlight their potential as a powerful tool in the fight against microbial infections, particularly in settings where conventional antibiotics are becoming less effective.

## 6.2 Synergistic effects with antibiotics

SrNPs also enhance the efficacy of antibiotics, particularly in combating multidrug-resistant (MDR) pathogens such as *Staphylococcus aureus* and *Pseudomonas aeruginosa*. Their synergistic effects stem from their ability to disrupt biofilms—complex bacterial communities that act as a physical and chemical barrier against antibiotic penetration.<sup>195,197</sup> By breaking down biofilms, SrNPs expose the embedded bacteria, increasing their susceptibility to antibiotics. Additionally, SrNPs sensitize resistant strains by targeting resistance mechanisms, such as inhibiting efflux pumps or reducing enzymatic degradation of antibiotics. Studies have highlighted the enhanced antibacterial potency of antibiotics when combined with SrNPs, with significant improvements in treatment outcomes against MDR strains. This synergy underscores the potential of SrNPs as valuable adjuncts in antimicrobial therapy, addressing the critical challenge of antibiotic resistance in modern medicine.<sup>195,198–201</sup>

For example, the study by Dapporto *et al.* (2022) highlights the potential of strontium-doped calcium phosphate cements (SrCPCs) in bone regeneration and antibacterial applications, with an emphasis on their synergistic effects when functionalized with hydroxyapatite nanoparticles loaded with tetracycline (NP-TC).<sup>195</sup> A key aspect of this synergy involves the enhancement of antibiotic efficacy, particularly against resistant pathogens such as *Staphylococcus aureus* and *Escherichia coli*.

SrNPs and SrCPC formulations play a crucial role in disrupting biofilms, which are structured bacterial communities that protect pathogens from antibiotics. Biofilms often act as formidable barriers, limiting antibiotic penetration and

fostering resistance. The study demonstrates that SrCPC formulations enriched with NP-TC not only inhibit bacterial growth but also facilitate the breakdown of biofilms, exposing previously shielded bacteria to the effects of antibiotics. This disruption, coupled with the bacteriostatic and bactericidal properties of NP-TC, creates a conducive environment for antibiotics to function more effectively.

Moreover, SrNPs enhance antibiotic sensitivity by targeting specific resistance mechanisms in bacteria. By interfering with bacterial metabolic activities and potentially inhibiting efflux pumps—key components in antibiotic resistance—SrNPs make resistant strains more susceptible to treatment. The study provides empirical evidence that combining NP-TC-loaded SrCPCs with antibiotics results in significantly improved antibacterial outcomes, as observed in microbiological tests.

Another critical contribution of SrCPCs to the synergistic effect is the sustained release of tetracycline from NP-TC formulations. The study shows that the inclusion of NP-TC slows down the release profile of tetracycline, ensuring a steady and prolonged antibacterial effect. This controlled release mechanism enhances the long-term efficacy of antibiotic therapy, particularly in treating infections associated with bone defects.

Furthermore, degradation tests of SrCPCs demonstrate the release of calcium and strontium ions over time, which not only supports bone regeneration but also contributes to the antibacterial activity by altering the local environment to deter bacterial growth. The combination of ion release, biofilm disruption, and antibiotic sensitization underscores the multifaceted role of SrCPC formulations in addressing the challenges of multidrug-resistant pathogens.

Overall, the findings by Dapporto *et al.*<sup>195</sup> illustrate the promise of SrCPCs as a platform for synergistic antibiotic therapy. By integrating the bioactive properties of SrNPs with the controlled drug delivery capabilities of NP-TC, these formulations address critical challenges in antimicrobial therapy, particularly in combating antibiotic resistance and enhancing treatment outcomes.

The studies by Alkhraisat *et al.* (2010)<sup>202</sup> and Jayasree *et al.* (2018)<sup>203</sup> also provided valuable insights into the synergistic effects of strontium (Sr) substitution in calcium phosphate cements (CPCs) for antibiotic delivery, demonstrating enhanced therapeutic potential for managing bone infections.

In Alkhraisat *et al.* (2010), a novel Sr-substituted CPC loaded with doxycycline hyclate (DOXY-h) was developed to explore the influence of Sr substitution on antibiotic adsorption and release.<sup>202</sup> The results highlighted that Sr incorporation significantly improved the cement's capacity to adsorb DOXY-h, attributed to better accessibility to drug-binding sites. The study revealed that the method of antibiotic loading—whether through adsorption from drug-containing solutions or using antibiotic solution as the cement's liquid phase—had a profound impact on the release profile. Cement prepared with Sr-substituted  $\beta$ -tricalcium phosphate (Sr- $\beta$ -TCP) exhibited a faster release rate when loaded with DOXY-h solution, pointing to Fickian diffusion as the primary release mechanism. This tunability in drug release profiles, ranging from rapid to



prolonged, underscores the potential of Sr-substituted CPCs as an efficient drug delivery system, enhancing local antibiotic efficacy in bone defects.

Jayasree *et al.* (2018) further advanced the concept by incorporating Sr<sup>2+</sup> ions into tetracalcium phosphate (TTCP)-based cements designed to release both Sr<sup>2+</sup> ions and the antibiotic ornidazole.<sup>203</sup> The study demonstrated that Sr substitution not only improved the physicochemical properties of CPCs, such as complete hydroxyapatite (HA) formation within a week but also accelerated the release of ornidazole. The dual-action CPCs exhibited sustained antibacterial activity against *E. coli* from day one, with needle-shaped HA crystals observed in Sr-substituted formulations. Moreover, the biocompatibility of the Sr-substituted CPCs with skeletal myoblast (L6) cells underscored their suitability for clinical applications in bone infection treatment. The study's findings highlight the role of Sr in enhancing both the structural and antimicrobial properties of CPCs, making them effective for localized drug delivery and promoting bone regeneration.

Together, these studies demonstrate that Sr substitution in CPCs not only facilitates improved antibiotic delivery through enhanced adsorption and tailored release mechanisms but also synergistically combines antimicrobial efficacy with osteogenic benefits, offering a promising strategy for treating infected bone defects. The incorporation of Sr enables CPCs to act as dual-action materials, capable of addressing infection while simultaneously promoting bone healing, thus addressing critical clinical challenges in orthopedic applications.

## 7 Public health implications

### 7.1 Addressing bone disorders

The application of strontium nanoparticles (SrNPs) in the treatment of osteoporosis and bone infections represents a groundbreaking advancement in modern medicine.<sup>172</sup> Osteoporosis, characterized by reduced bone mass and structural deterioration, often leads to fractures and long-term disabilities, while bone infections such as osteomyelitis pose significant challenges in terms of treatment and recovery. SrNPs offer a unique dual-action capability: they not only enhance osteogenesis by stimulating bone regeneration but also exert potent antimicrobial effects to mitigate infections.<sup>204,205</sup> This combination makes SrNPs particularly valuable in orthopedic and dental treatments, where the risk of infection often complicates the healing process. By promoting bone density, accelerating fracture healing, and providing an antimicrobial shield, SrNP-based therapies hold the potential to substantially enhance patient outcomes, improve mobility, and reduce the prevalence of chronic complications associated with bone disorders.<sup>205</sup>

From an economic perspective, integrating SrNP-based treatments into mainstream healthcare systems could significantly alleviate financial burdens. Osteoporosis and bone infections impose substantial costs due to prolonged hospitalizations, complex surgical interventions, and extensive rehabilitation programs.<sup>206,207</sup> For instance, the treatment of hip fractures alone represents a considerable financial strain on both patients and healthcare systems worldwide. SrNPs, by

offering an efficient and potentially cost-effective alternative, could reduce these expenses. Their ability to expedite healing and reduce the incidence of complications may also help decrease readmission rates and the need for additional interventions, further contributing to cost savings.<sup>184</sup>

However, realizing the full potential of SrNP-based therapies requires overcoming significant barriers. Scaling up the production of SrNPs is a crucial step to meet the demands of widespread clinical use. Advances in nanotechnology manufacturing must focus on cost-effective methods that maintain the therapeutic efficacy of SrNPs. Equally important is the establishment of streamlined distribution networks to ensure timely and equitable access to these treatments, especially in resource-limited settings where advanced medical technologies remain scarce.<sup>208–210</sup>

Addressing these challenges demands a concerted effort from multiple stakeholders. International collaborations between governments, research institutions, and healthcare providers could drive innovation and facilitate the sharing of resources and expertise. Public–private partnerships are also critical in bridging the gap between research and commercialization, ensuring that SrNP-based treatments reach the global market efficiently. Furthermore, policies that prioritize affordable healthcare and the inclusion of advanced therapies in insurance coverage plans are essential for reducing disparities in access.<sup>211–213</sup>

By addressing these systemic challenges, SrNPs have the potential to revolutionize the treatment landscape for bone-related disorders, improving patient outcomes while simultaneously reducing the economic strain on healthcare systems. Through collaborative efforts, SrNP-based therapies could become a cornerstone of orthopedic and dental care, offering hope to millions of patients worldwide.

### 7.2 Combating antimicrobial resistance (AMR)

The rise of antimicrobial resistance (AMR) has emerged as one of the most pressing challenges in global public health, threatening to render many conventional antibiotics ineffective and leaving infections increasingly difficult to treat. This crisis necessitates the development of innovative solutions that go beyond traditional approaches to combat resistant pathogens. Strontium nanoparticles (SrNPs) present a promising alternative, leveraging their unique antimicrobial properties to inhibit the growth and proliferation of multidrug-resistant organisms.<sup>214,215</sup> Unlike conventional antibiotics, which often target specific cellular processes, SrNPs employ a multifaceted mechanism of action. They disrupt bacterial metabolic pathways, impair enzymatic functions critical for survival, and generate reactive oxygen species (ROS) that compromise bacterial cell membranes. These combined effects not only enhance their antimicrobial efficacy but also reduce the likelihood of resistance development, making SrNPs a valuable tool in mitigating the AMR crisis.<sup>216</sup>

However, the successful deployment of SrNP-based antimicrobial strategies requires a comprehensive and integrated approach to their development, regulation, and implementation. Public health policies must prioritize the establishment of



stringent guidelines that ensure the safe synthesis, application, and disposal of SrNPs. This is essential to mitigate potential risks, such as environmental contamination or unintended health effects, that could arise from the widespread use of nanomaterials.<sup>217,218</sup> Collaborative efforts between regulatory agencies, researchers, and industry stakeholders are needed to standardize safety protocols and promote the responsible use of SrNPs in healthcare settings.

Investing in research and development (R&D) is equally critical to unlocking the full potential of SrNPs. R&D initiatives should focus on optimizing nanoparticle formulations to enhance their antimicrobial spectrum and efficacy while minimizing cytotoxicity to human cells. Advanced characterization techniques and preclinical studies can help refine their design, enabling the creation of SrNP-based antimicrobials tailored to combat a diverse array of pathogens, including bacteria, fungi, and viruses. Furthermore, exploring synergies between SrNPs and existing antibiotics could pave the way for combination therapies that restore the efficacy of drugs rendered ineffective by resistance.<sup>194,217</sup>

Integrating SrNPs into national and global AMR mitigation programs could significantly bolster efforts to address this growing threat. Such integration would involve incorporating SrNP-based solutions into treatment guidelines and protocols for resistant infections, ensuring their availability and proper use in clinical practice. Public awareness campaigns are also crucial for fostering acceptance and uptake of nanoparticle-based antimicrobials. By educating healthcare providers and the public about the safety, efficacy, and benefits of SrNPs, these campaigns can address potential concerns and accelerate their adoption.<sup>218–222</sup>

Ultimately, the judicious implementation of SrNPs in clinical and public health settings, underpinned by robust evidence-based policies, has the potential to revolutionize the fight against AMR. By reducing reliance on conventional antibiotics and curbing the emergence of resistant strains, SrNPs can play a pivotal role in safeguarding global health and ensuring the continued effectiveness of antimicrobial therapies for future generations.

## 8 Challenges

The application of strontium nanoparticles (SrNPs) in healthcare and other sectors holds immense promise, but several critical challenges must be addressed to ensure their safe, effective, and equitable deployment. These challenges span toxicological concerns, scalability, cost, and regulatory and ethical considerations. Tackling these issues will require a multidisciplinary effort involving scientists, industry stakeholders, policymakers, and ethicists.

### 8.1 Toxicological concerns

One of the most significant challenges in the development and application of strontium nanoparticles (SrNPs) is understanding their potential impact on human health and the environment. While SrNPs exhibit promising therapeutic and

antimicrobial properties, the long-term consequences of exposure remain insufficiently explored. Thorough investigation is essential to address the possible risks associated with their use.<sup>7</sup>

A primary concern is cytotoxicity, as SrNPs may interact with human cells in unintended ways, potentially causing cellular damage or death. It is imperative to evaluate the dose-dependent effects of SrNPs on various cell types to establish safe exposure limits and minimize harm. These studies will provide crucial insights into the safe application of SrNPs, particularly in medical and pharmaceutical contexts.<sup>223</sup>

Another critical area is genotoxicity, which involves the potential of SrNPs to induce genetic mutations or DNA damage. This concern is particularly relevant for scenarios involving repeated or chronic exposure to SrNPs. Rigorous preclinical testing is needed to assess these risks and ensure that SrNP-based technologies do not pose a threat to genetic stability or long-term human health.<sup>224,225</sup>

Additionally, immunogenicity presents a challenge, as nanoparticles can trigger immune responses that lead to inflammation or hypersensitivity. Understanding how SrNPs interact with the immune system is vital for preventing adverse effects, especially in clinical applications where biocompatibility is a top priority. Investigating these impacts will help guide the development of SrNP formulations that minimize immune-related complications.<sup>226,227</sup>

The environmental impact of SrNPs is another pressing issue. Once released into the environment, SrNPs could accumulate in ecosystems, potentially affecting aquatic organisms and soil microorganisms. Comprehensive studies are necessary to understand the environmental fate of SrNPs, including their bioaccumulation potential and long-term ecological effects. These findings will help inform strategies to mitigate environmental risks.<sup>228,229</sup>

To address these concerns, preclinical and clinical studies must prioritize extensive toxicological evaluations. Advanced analytical techniques, such as omics-based analyses, can offer valuable insights into the molecular mechanisms underlying SrNP interactions with biological systems. Furthermore, regulatory agencies need to collaborate with researchers to establish standardized safety assessment protocols. By addressing these challenges proactively, the development and application of SrNPs can be guided toward safe and sustainable use.

### 8.2 Scalability and cost

The transition from laboratory-scale research to industrial-scale production of strontium nanoparticles (SrNPs) presents a series of challenges that must be addressed to ensure their successful integration into various applications. One of the primary difficulties is maintaining consistent quality, uniform size distribution, and high purity during large-scale manufacturing. Current synthesis methods often depend on expensive reagents, intricate procedures, or advanced and specialized equipment, all of which limit their scalability and affordability. These challenges hinder the broader adoption of SrNP technologies in real-world applications, especially in resource-constrained settings.<sup>230,231</sup>



To overcome these barriers and ensure the efficient, affordable, and sustainable large-scale production of SrNPs, several strategies must be prioritized. One promising avenue is green synthesis, which involves the development of environmentally friendly and sustainable methods for producing SrNPs. Using plant extracts, biopolymers, or other natural materials as reducing and stabilizing agents can significantly lower costs while minimizing environmental risks associated with conventional chemical synthesis methods. This approach not only reduces reliance on expensive and hazardous reagents but also aligns with sustainability goals and eco-friendly manufacturing processes.<sup>231</sup>

Another critical strategy is process optimization, which focuses on technological improvements to enhance production yield and ensure quality control. Advances in process engineering, such as the implementation of automated systems and continuous production techniques, can streamline SrNP synthesis by reducing variability, improving efficiency, and enabling consistent production at scale. Innovations in these areas could lead to more predictable and cost-effective manufacturing processes that address both industry and environmental standards.<sup>232</sup>

Furthermore, achieving economies of scale will be vital for overcoming the financial hurdles associated with SrNP production. Collaborative efforts between academia and industry can foster partnerships that promote the development of cost-effective production methods and shared technological resources. Such collaborations can drive innovation while ensuring that SrNP-based technologies become more affordable and accessible to a broader range of end-users, particularly in regions where affordability and resource availability are major concerns.

Investing in these approaches—green synthesis, process optimization, and collaborative efforts for economies of scale—will be essential to enable the widespread adoption of SrNPs across diverse applications. Addressing these challenges will not only ensure the cost-effective production of SrNPs but also make them more readily available for critical applications in biomedical, environmental, and technological fields, especially in resource-limited areas where access to advanced medical and technological interventions can be restricted.<sup>230</sup>

### 8.3 Regulatory and ethical considerations

The lack of standardized guidelines for evaluating and utilizing strontium nanoparticles (SrNPs) represents a considerable obstacle to their safe, ethical, and effective deployment in various applications. The establishment of clear and comprehensive regulatory frameworks is essential to ensure consistency, safety, and efficacy across the growing range of SrNP technologies while addressing broader ethical and societal concerns. Without such guidelines, variations in SrNP production, testing, and application could lead to unintended consequences, including safety risks, environmental concerns, and inequitable access to these advanced technologies. Therefore, addressing these gaps requires a multifaceted approach that

incorporates regulatory standards, ethical considerations, environmental sustainability, and public engagement.<sup>189,233</sup>

One of the primary areas of focus is regulatory standards. Comprehensive guidelines for the characterization, toxicity testing, and clinical evaluation of SrNPs are vital for assessing their safety and efficacy in various contexts. These standards should be developed collaboratively with international organizations, such as the World Health Organization (WHO) and other regulatory bodies, to ensure global harmonization. Such harmonization would facilitate uniformity in the assessment of SrNPs across different regions, allowing for their safe and effective application worldwide. Regulatory bodies must also consider a variety of risk factors, such as dose–response relationships, potential for immunogenic responses, and long-term environmental effects, during their development of these standards.<sup>18,194</sup>

Another critical ethical consideration involves accessibility and equity. As advancements in nanotechnology bring transformative solutions, it is imperative to ensure that access to SrNP-based treatments and technologies does not widen health disparities. Ethical frameworks must address challenges associated with ensuring equitable distribution, particularly in low- and middle-income countries, where healthcare infrastructure may be limited. Policymakers, healthcare providers, and industry leaders have a shared responsibility to create strategies that ensure SrNP technologies are affordable, accessible, and integrated into health systems without discriminating against vulnerable or underserved populations.

Furthermore, environmental sustainability must be prioritized in the development and regulation of SrNPs. Regulations should mandate lifecycle assessments to evaluate the environmental footprint of SrNPs from their synthesis through disposal. This includes analyzing their potential for bioaccumulation, persistence, and ecological disruption. Policies promoting the use of green synthesis techniques and the adoption of environmentally responsible manufacturing and waste management strategies can further support sustainability goals. These actions would minimize the ecological risks associated with the production, use, and disposal of SrNPs while maintaining their therapeutic and technological benefits.<sup>234–237</sup>

Lastly, public engagement is vital for fostering trust, transparency, and inclusivity in the development and implementation of SrNP technologies. Public concerns about the safety, efficacy, and ethical implications of novel nanotechnologies must be addressed through clear, transparent, and accessible communication. Building trust requires open dialogue between scientists, policymakers, and the public, ensuring that stakeholders—ranging from patients to community representatives—are actively involved in decision-making processes. By integrating diverse perspectives into the conversation, policymakers can ensure that the societal impacts of SrNP technologies are thoughtfully considered, resulting in broader acceptance and ethical use.

In a nutshell, addressing the challenges associated with the lack of standardized guidelines for SrNP evaluation and application requires a comprehensive and multidisciplinary approach. Establishing regulatory standards, ensuring



equitable access, prioritizing environmental sustainability, and fostering public engagement will be essential in enabling the ethical, safe, and effective deployment of SrNP technologies. Such efforts will help ensure that SrNPs fulfill their promise of addressing critical health and technological needs while minimizing risks and promoting fairness and sustainability.

## 9 Future directions

Tackling the challenges related to the development, production, and use of strontium nanoparticles (SrNPs) will demand a unified and multidisciplinary approach. Considering the intricate interactions of SrNPs with biological systems, the environment, and societal factors, it is crucial for researchers, policymakers, and industry leaders to collaborate in creating and implementing strategies that guarantee their ethical, safe, and sustainable use. A focused and collective effort is necessary to emphasize research, foster innovation, strengthen regulatory frameworks, and ensure equitable access to SrNP technologies.

One key research focus should be advancing our understanding of SrNP interactions with biological and environmental systems. This can be achieved through the use of advanced analytical techniques, such as omics-based methodologies, high-resolution imaging, and computational modeling. These tools can uncover the molecular and cellular mechanisms through which SrNPs interact with human cells, environmental agents, and ecosystems. Understanding these interactions will clarify potential risks, mechanisms of toxicity, and opportunities for optimizing SrNP design for targeted applications. Such insights would also support risk assessment and the development of safer SrNP formulations.

Another critical area is developing innovative and sustainable synthesis methods. Current methods for synthesizing SrNPs can be costly, require specialized infrastructure, or rely on non-eco-friendly reagents and processes. To ensure the large-scale production of SrNPs while minimizing environmental impact, research efforts should focus on creating scalable, cost-effective, and environmentally friendly synthesis routes. Green synthesis methods—utilizing renewable resources such as plant extracts, biopolymers, or other natural reducing agents—could play a pivotal role. Optimizing these methods will lower costs, enhance accessibility, and align production with environmental sustainability goals.

Moreover, strengthening regulatory frameworks and fostering international cooperation is vital for the standardized evaluation and use of SrNPs across borders. Establishing clear, transparent, and internationally harmonized guidelines for the characterization, testing, clinical evaluation, and application of SrNPs will ensure safety and efficacy while reducing risks associated with their use. Collaborative efforts between governments, international organizations, and research institutions can streamline these guidelines and provide the necessary oversight to monitor SrNP development and use. Additionally, these international partnerships can enhance knowledge sharing and resource allocation, particularly for regions that lack access to the infrastructure and expertise needed to evaluate SrNPs.

Equally important is promoting equitable access to SrNP-based solutions, particularly for underserved or low-resource populations. Barriers to accessibility—ranging from high costs to limited healthcare infrastructure—could prevent the full societal benefits of SrNP technologies from being realized. Public-private partnerships can play a vital role in addressing these inequities by pooling expertise, resources, and funding to scale production, improve distribution networks, and integrate SrNP solutions into health systems. Targeted funding initiatives and strategic collaborations can ensure that advancements in SrNP technology do not exacerbate existing global health disparities.

Overcoming the complex challenges associated with the development and application of strontium nanoparticles (SrNPs) will demand a coordinated and multidisciplinary approach. The scientific and medical communities must focus on a comprehensive research agenda that explores biological and environmental interactions, develops scalable and sustainable synthesis methods, and establishes robust regulatory and ethical frameworks. By fostering innovation, promoting international collaboration, and ensuring equitable access, we can fully realize the transformative potential of SrNPs. This strategic approach will guarantee their ethical, safe, and sustainable use while addressing pressing global challenges, including improving health outcomes, combating antimicrobial resistance, and mitigating environmental and technological concerns.

## 10 Conclusion

Strontium-based nanoparticles (SrNPs) hold immense potential as multifunctional nanomaterials in addressing pressing healthcare challenges, particularly in bone regeneration and combating antimicrobial resistance (AMR). Their ability to enhance bone density, accelerate fracture healing, and target multidrug-resistant pathogens highlights their versatility as both orthopedic and antimicrobial therapeutic agents. The synthesis methods discussed—co-precipitation, hydrothermal synthesis, and sol-gel techniques—demonstrate effective strategies for controlling SrNPs' size, shape, and functionality, with considerations for scalability, environmental sustainability, and cost-effectiveness. Furthermore, the exploration of toxicological risks and environmental fate underscores the importance of conducting rigorous preclinical and clinical evaluations to ensure the safe application of SrNPs. Addressing regulatory and ethical challenges, such as the establishment of global safety standards and equitable access, is crucial for supporting the responsible development and application of these nanomaterials. This review provides a comprehensive perspective on the opportunities and challenges associated with SrNPs, emphasizing their potential to revolutionize bone regenerative therapies and the fight against AMR. Moving forward, strategic investments in research, technological innovation, and international collaboration will be vital to unlock their full capabilities while ensuring their ethical, safe, and sustainable deployment.



## Informed consent statement

On behalf of all authors, the corresponding author states that informed consent was obtained from all participants involved in the study.

## Data availability

This study is a review and does not include primary data. All data supporting the findings and conclusions of this review are drawn from previously published works, which are appropriately cited within the manuscript. The references for these works are included in the article.

## Author contribution

Uchenna Uzoma Akobundu led the conceptualization of the review topic, coordinated the overall structure, and contributed to drafting the manuscript. Ikhazuagbe H. Ifijen conducted the first drafting of the manuscript, provided critical oversight of the manuscript's direction, and performed in-depth editing. Prince Duru conducted an extensive literature search on clinical implications and synthesized key findings into relevant sections. Juliet C. Igboanugo assisted in compiling and organizing references, created visual aids, and formatted the manuscript according to journal guidelines. Innocent Ekanem reviewed and validated synthesized findings, ensuring accuracy and coherence across all sections. Moshood Fagbolade contributed to the critical analysis and interpretation of the reviewed literature on strontium-based nanoparticles. Abiola Samuel Ajayi focused on the antimicrobial aspects, providing expert commentary and reviewing relevant subsections. Mayowa George drafted and refined sections discussing bone regeneration mechanisms and applications. Best Atoe conducted additional literature reviews to fill gaps and ensured the integrity of cross-referenced materials. John Tsado Matthews managed project administration, coordinated correspondence, and performed final proofreading to ensure consistency and quality. All authors actively contributed to the manuscript, reviewed the final version, and approved its submission.

## Conflicts of interest

On behalf of all authors, the corresponding author states that there is no conflict of interest.

## References

- 1 K. E. Mokobia, I. H. Ifijen and E. U. Ikhuoria, ZnO-NPs-coated implants with osteogenic properties for enhanced osseointegration, in *TMS 2023 152nd Annual Meeting & Exhibition Supplemental Proceedings. TMS 2023. The Minerals, Metals & Materials Series*, Springer, Cham, 2023, DOI: [10.1007/978-3-031-22524-6\\_27](https://doi.org/10.1007/978-3-031-22524-6_27).
- 2 E. M. Jonathan, A. O. Ohifuemen, J. N. Jacob, *et al.*, Polymeric biodegradable biomaterials for tissue bioengineering and bone rejuvenation, in *TMS 2023 152nd Annual Meeting & Exhibition Supplemental Proceedings. The Minerals, Metals & Materials Series*, Springer, Cham, 2023, DOI: [10.1007/978-3-031-22524-6\\_25](https://doi.org/10.1007/978-3-031-22524-6_25).
- 3 C. O. Okereke, J. O. Onaifo, S. O. Omorogbe, *et al.*, Bioactive glasses for bone repair application: A review of osteointegration and controlled ion release capabilities, in *TMS 2024 153rd Annual Meeting & Exhibition Supplemental Proceedings. The Minerals, Metals & Materials Series*, Springer, Cham, 2024, DOI: [10.1007/978-3-031-50349-8\\_28](https://doi.org/10.1007/978-3-031-50349-8_28).
- 4 E. M. Jonathan, O. E. Oghama, *et al.*, Biodegradable polymers for 3D printing of tissue engineering scaffolds: Challenges and future directions, in *TMS 2024 153rd Annual Meeting & Exhibition Supplemental Proceedings. The Minerals, Metals & Materials Series*, Springer, Cham, 2024, DOI: [10.1007/978-3-031-50349-8\\_40](https://doi.org/10.1007/978-3-031-50349-8_40).
- 5 B. Atoe, I. H. Ifijen, I. P. Okiemute, O. I. Emmanuel and M. Maliki, Silk biomaterials in wound healing: Navigating challenges and charting the future of regenerative medicine, in *TMS 2024 153rd Annual Meeting & Exhibition Supplemental Proceedings. The Minerals, Metals & Materials Series*, Springer, Cham, 2024, DOI: [10.1007/978-3-031-50349-8\\_78](https://doi.org/10.1007/978-3-031-50349-8_78).
- 6 I. H. Ifijen, M. Maliki, I. J. Odiachi, *et al.*, Performance of metallic-based nanomaterials doped with strontium in biomedical and supercapacitor electrodes: A review, *Biomed. Mater. & Devices*, 2023, **1**, 402–418, DOI: [10.1007/s44174-022-00006-3](https://doi.org/10.1007/s44174-022-00006-3).
- 7 S. Mukherjee and M. Mishra, Application of strontium-based nanoparticles in medicine and environmental sciences, *Nanotechnol. Environ. Eng.*, 2021, **6**, 25, DOI: [10.1007/s41204-021-00115-2](https://doi.org/10.1007/s41204-021-00115-2).
- 8 P. Wei, W. Jing, Z. Yuan, Y. Huang, B. Guan, W. Zhang, *et al.*, Vancomycin- and strontium-loaded microspheres with multifunctional activities in antibacteria, angiogenesis and osteogenesis for enhancing infected bone regeneration, *ACS Appl. Mater. Interfaces*, 2019, **11**, 30596–30609, DOI: [10.1021/acsami.9b10219](https://doi.org/10.1021/acsami.9b10219).
- 9 A. Elumalai and D. Mills, An eco-friendly, simple, and inexpensive method for metal-coating strontium onto halloysite nanotubes, *J. Compos. Sci.*, 2022, **6**, 276, DOI: [10.3390/jcs6090276](https://doi.org/10.3390/jcs6090276).
- 10 J. Du, L. Fan, J. Razal, S. Chen, H. Zhang, H. Yang, *et al.*, Strontium-doped mesoporous bioglass nanoparticles for enhanced wound healing with rapid vascularization, *J. Mater. Chem. B*, 2023, **11**, 7364–7377, DOI: [10.1039/d3tb01256e](https://doi.org/10.1039/d3tb01256e).
- 11 S. Meka, S. Jain and K. Chatterjee, Strontium eluting nanofibers augment stem cell osteogenesis for bone tissue regeneration, *Colloids Surf., B*, 2016, **146**, 649–656, DOI: [10.1016/j.colsurfb.2016.07.012](https://doi.org/10.1016/j.colsurfb.2016.07.012).
- 12 S. Afewerki, N. Bassous, S. Harb, C. Palo-Nieto, G. Ruiz-Esparza, F. Marciano, *et al.*, *Advances in antimicrobial and osteoinductive biomaterials*, 2020, pp. 3–34, DOI: [10.1007/978-3-030-34471-9\\_1](https://doi.org/10.1007/978-3-030-34471-9_1).
- 13 D. Ibrahim, E. Sani, A. Soliman, N. Zandi, E. Mostafavi, A. Youssef, *et al.*, Bioactive and elastic nanocomposites with antimicrobial properties for bone tissue regeneration, *ACS Appl. Bio Mater.*, 2020, **3**(5), 3313–3325, DOI: [10.1021/acsabm.0c00250](https://doi.org/10.1021/acsabm.0c00250).



- 14 Y. Qian, X. Zhou, F. Zhang, T. Diekwisch, X. Luan and J. Yang, Triple PLGA/PCL scaffold modification including silver-impregnation, collagen-coating, and electrospinning significantly improve biocompatibility, antimicrobial, and osteogenic properties for oro-facial tissue regeneration, *ACS Appl. Mater. Interfaces*, 2019, **11**, 37381–37396, DOI: [10.1021/acsami.9b07053](https://doi.org/10.1021/acsami.9b07053).
- 15 J. You, Y. Zhang and Y. Zhou, Strontium functionalized in biomaterials for bone tissue engineering: A prominent role in osteoimmunomodulation, *Front. Bioeng. Biotechnol.*, 2022, **10**, DOI: [10.3389/fbioe.2022.928799](https://doi.org/10.3389/fbioe.2022.928799).
- 16 Q. Wang, P. Li, P. Tang, X. Ge, F. Ren, C. Zhao, *et al.*, Experimental and simulation studies of strontium/fluoride-codoped hydroxyapatite nanoparticles with osteogenic and antibacterial activities, *Colloids Surf., B*, 2019, **182**, 110359, DOI: [10.1016/j.colsurfb.2019.110359](https://doi.org/10.1016/j.colsurfb.2019.110359).
- 17 M. Frasnelli, F. Cristofaro, V. Sglavo, S. Diré, E. Callone, R. Ceccato, *et al.*, Synthesis and characterization of strontium-substituted hydroxyapatite nanoparticles for bone regeneration, *Mater. Sci. Eng., C*, 2017, **71**, 653–662, DOI: [10.1016/j.msec.2016.10.047](https://doi.org/10.1016/j.msec.2016.10.047).
- 18 M. Karimi, S. Hesarakhi and N. Nezafati, In vitro biodegradability–bioactivity–biocompatibility and antibacterial properties of SrF2 nanoparticles synthesized by one-pot and eco-friendly method based on ternary strontium chloride-choline chloride-water deep eutectic system, *Ceram. Int.*, 2018, **44**, 12877–12885, DOI: [10.1016/J.CERAMINT.2018.04.098](https://doi.org/10.1016/J.CERAMINT.2018.04.098).
- 19 Y. Ebrahimi, A. Alvani, A. Sarabi, H. Sameie, R. Salimi, M. Alvani, *et al.*, A comprehensive study on the magnetic properties of nanocrystalline SrCo<sub>0.2</sub>Fe<sub>11.8</sub>O<sub>19</sub> ceramics synthesized via diverse routes, *Ceram. Int.*, 2012, **38**, 3885–3892, DOI: [10.1016/J.CERAMINT.2012.01.040](https://doi.org/10.1016/J.CERAMINT.2012.01.040).
- 20 T. Akhtar and M. Anis-Ur-Rehman, Conductivity relaxations and phase purity in strontium cobalt oxides prepared by numerous chemical routes, *J. Dispersion Sci. Technol.*, 2020, **42**, 1936–1949, DOI: [10.1080/01932691.2020.1791717](https://doi.org/10.1080/01932691.2020.1791717).
- 21 S. Ueno, K. Nakashima, Y. Sakamoto and S. Wada, Synthesis of Silver-Strontium Titanate Hybrid Nanoparticles by Sol-Gel-Hydrothermal Method, *Nanomaterials*, 2015, **5**, 386–397, DOI: [10.3390/nano5020386](https://doi.org/10.3390/nano5020386).
- 22 S. Fuentes, R. Zárate, E. Chávez, P. Muñoz, D. Díaz-Droguett and P. Leyton, Preparation of SrTiO<sub>3</sub> nanomaterial by a sol-gel-hydrothermal method, *J. Mater. Sci.*, 2010, **45**, 1448–1452, DOI: [10.1007/S10853-009-4099-Y](https://doi.org/10.1007/S10853-009-4099-Y).
- 23 T. Akhtar, O. Farooq and M. Anis-Ur-Rehman, Structural and Electrical Properties of Barium Strontium Cobaltite Nanoparticles Synthesized by Wet Chemical Methods, *Key Eng. Mater.*, 2018, **778**, 151–157, DOI: [10.4028/www.scientific.net/KEM.778.151](https://doi.org/10.4028/www.scientific.net/KEM.778.151).
- 24 M. Iqbal and M. Ashiq, Comparative studies of Sr<sub>2</sub>xMnxFe<sub>12–2x</sub>O<sub>19</sub> nanoparticles synthesized by co-precipitation and sol-gel combustion methods, *Scr. Mater.*, 2007, **56**, 145–148, DOI: [10.1016/J.SCRIPTAMAT.2006.09.005](https://doi.org/10.1016/J.SCRIPTAMAT.2006.09.005).
- 25 M. Iqbal, M. Ashiq and I. Gul, Physical, electrical and dielectric properties of Ca-substituted strontium hexaferrite (SrFe<sub>12</sub>O<sub>19</sub>) nanoparticles synthesized by co-precipitation method, *J. Magn. Magn. Mater.*, 2010, **322**, 1720–1726, DOI: [10.1016/J.JMMM.2009.12.013](https://doi.org/10.1016/J.JMMM.2009.12.013).
- 26 E. El-Ghazzawy and M. Amer, Structural, elastic and magnetic studies of the as-synthesized Co<sub>1–x</sub>Sr<sub>x</sub>Fe<sub>2</sub>O<sub>4</sub> nanoparticles, *J. Alloys Compd.*, 2017, **690**, 293–303, DOI: [10.1016/J.JALLCOM.2016.08.135](https://doi.org/10.1016/J.JALLCOM.2016.08.135).
- 27 A. Turkey, M. Rashad, A. Hassan, E. Elnaggar and M. Bechelany, Tailoring optical, magnetic and electric behavior of lanthanum strontium manganite La<sub>1–x</sub>Sr<sub>x</sub>MnO<sub>3</sub> (LSM) nanopowders prepared via a co-precipitation method with different Sr<sup>2+</sup> ion contents, *RSC Adv.*, 2016, **6**, 17980–17986, DOI: [10.1039/C5RA27461C](https://doi.org/10.1039/C5RA27461C).
- 28 X. Hu, H. Yang, T. Guo, D. Shu, W. Shan, G. Li, *et al.*, Preparation and properties of Eu and Dy co-doped strontium aluminate long afterglow nanomaterials, *Ceram. Int.*, 2018, **44**, 7535–7544, DOI: [10.1016/J.CERAMINT.2018.01.157](https://doi.org/10.1016/J.CERAMINT.2018.01.157).
- 29 M. Yousefi and M. Ranjbar, Ultrasound and Microwave-Assisted Co-precipitation Synthesis of La<sub>0.75</sub>Sr<sub>0.25</sub>MnO<sub>3</sub> Perovskite Nanoparticles from a New Lanthanum(III) Coordination Polymer Precursor, *J. Inorg. Organomet. Polym. Mater.*, 2017, **27**, 633–640, DOI: [10.1007/s10904-017-0504-1](https://doi.org/10.1007/s10904-017-0504-1).
- 30 F. Kiani, U. Shamraiz, A. Badshah, S. Tabassum, M. Ambreen and J. Patujo, Optimization of Ag<sub>2</sub>O nanostructures with strontium for biological and therapeutic potential, *Artif. Cells, Nanomed., Biotechnol.*, 2018, **46**, 1083–1091, DOI: [10.1080/21691401.2018.1529678](https://doi.org/10.1080/21691401.2018.1529678).
- 31 K. Mohammadi, M. Sadeghi and R. Azimirad, Facile synthesis of SrFe<sub>12</sub>O<sub>19</sub> nanoparticles and its photocatalyst application, *J. Mater. Sci.:Mater. Electron.*, 2017, **28**, 10042–10047, DOI: [10.1007/s10854-017-6763-3](https://doi.org/10.1007/s10854-017-6763-3).
- 32 S. R. Ali, R. Kumar, A. Kalam, *et al.*, Effect of strontium doping on the band gap of nanoparticles synthesized using facile co-precipitation, *Arabian J. Sci. Eng.*, 2019, **44**(9), 6295–6302, DOI: [10.1007/s13369-018-03700-x](https://doi.org/10.1007/s13369-018-03700-x).
- 33 T. Huynh, H. Nersisyan, S. Hong and J. Lee, Co-Precipitation Synthesis and Characterization of Strontium Lanthanum Vanadate Nanoparticles, *Korean J. Mater. Res.*, 2021, **31**, 209–218, DOI: [10.3740/MRSK.2021.31.4.209](https://doi.org/10.3740/MRSK.2021.31.4.209).
- 34 S. Vallimeena and B. Helina, Cauliflower-like strontium-doped SnO<sub>2</sub> nanoparticles for photocatalytic degradation, *Mater. Sci. Technol.*, 2023, **39**, 2277–2285, DOI: [10.1080/02670836.2023.2197725](https://doi.org/10.1080/02670836.2023.2197725).
- 35 Y. Li, W. Wang, J. Han, Z. Li, Q. Wang, X. Lin, *et al.*, Synthesis of Silver- and Strontium-Substituted Hydroxyapatite with Combined Osteogenic and Antibacterial Activities, *Biol. Trace Elem. Res.*, 2021, **200**, 931–942, DOI: [10.1007/s12011-021-02697-z](https://doi.org/10.1007/s12011-021-02697-z).
- 36 F. Oztekin, T. Gurgenc, S. Dundar, I. Ozercan, M. Eskibağlar, E. Ozcan, *et al.*, In Vivo Effects of Nanotechnologically Synthesized and Characterized Fluoridated Strontium Apatite Nanoparticles in the Surgical Treatment of Endodontic Bone Lesions, *Crystals*, 2022, **12**, 1192, DOI: [10.3390/cryst12091192](https://doi.org/10.3390/cryst12091192).



- 37 D. Primc, M. Drogenik and D. Makovec, Low-Temperature Hydrothermal Synthesis of Ultrafine Strontium Hexaferrite Nanoparticles, *Eur. J. Inorg. Chem.*, 2011, **2011**, 3802–3809, DOI: [10.1002/EJIC.201100326](https://doi.org/10.1002/EJIC.201100326).
- 38 D. Alby, F. Salles, A. Geneste, B. Prélôt, J. Zajac and C. Charnay, Microwave-assisted hydrothermal synthesis of manganese nanoflowers for selective retention of strontium, *J. Hazard. Mater.*, 2019, **368**, 661–669, DOI: [10.1016/j.jhazmat.2019.01.064](https://doi.org/10.1016/j.jhazmat.2019.01.064).
- 39 G. Canu, M. T. Buscaglia, V. Buscaglia, M. Viviani, N. Masó and A. R. West, Modified processing conditions to enhance properties of strontium titanate ceramics, *Acta Mater.*, 2004, **52**(12), 3747–3758, DOI: [10.1016/j.actamat.2004.04.036](https://doi.org/10.1016/j.actamat.2004.04.036).
- 40 Y. Zhang, L. Zhong, D. Duan, X. Gao, J. Jing and X. Hao, Single-step hydrothermal synthesis of strontium titanate nanoparticles from crystalline anatase titanium dioxide, *Ceram. Int.*, 2015, **41**, 13516–13524, DOI: [10.1016/J.CERAMINT.2015.07.145](https://doi.org/10.1016/J.CERAMINT.2015.07.145).
- 41 Z. Zhou, Q. Wang, X. Ge and Z. Li, Strontium Doped Hydroxyapatite Nanoparticles: Synthesis, Characterization and Simulation, *J. Inorg. Mater.*, 2020, DOI: [10.15541/jim20190439](https://doi.org/10.15541/jim20190439).
- 42 R. Boulkroune, M. Sebais, Y. Messai, R. Bourzami, M. Schmutz, C. Blanck, *et al.*, Hydrothermal synthesis of strontium-doped ZnS nanoparticles: structural, electronic and photocatalytic investigations, *Bull. Mater. Sci.*, 2019, **42**, 223, DOI: [10.1007/s12034-019-1905-2](https://doi.org/10.1007/s12034-019-1905-2).
- 43 B. Phoon, C. Lai, G. Pan, T. Yang and J. Juan, One-pot hydrothermal synthesis of strontium titanate nanoparticles photoelectrode using electrophoretic deposition for enhancing photoelectrochemical water splitting, *Ceram. Int.*, 2018, **44**, 9923–9933, DOI: [10.1016/J.CERAMINT.2018.03.017](https://doi.org/10.1016/J.CERAMINT.2018.03.017).
- 44 Y. Devi, P. Rajasekaran, K. Vijayakumar, A. Nedunchezian, D. Sidharth, G. Anbalagan, *et al.*, Enhancement of thermoelectric power factor of hydrothermally synthesised SrTiO<sub>3</sub> nanostructures, *Mater. Res. Express*, 2020, **7**, 015094, DOI: [10.1088/2053-1591/ab6c96](https://doi.org/10.1088/2053-1591/ab6c96).
- 45 Q. Rahman, S. Hasan, A. Ali, S. Mehta, M. Raja, N. Ahmad, *et al.*, Synthesis and Characterizations of Nitrogen (N) Doped Strontium Titanate (SrTiO<sub>3</sub>) Nanoparticles for Enhanced Visible Light Driven Photocatalytic Degradation, *J. Nanosci. Nanotechnol.*, 2020, **20**(10), 6475–6481, DOI: [10.1166/jnn.2020.18591](https://doi.org/10.1166/jnn.2020.18591).
- 46 L. Schmidt, F. Emmerling, H. Kirmse and E. Kemnitz, Sol-gel synthesis and characterisation of nanoscopic strontium fluoride, *RSC Adv.*, 2014, **4**, 32–38, DOI: [10.1039/C3RA43769H](https://doi.org/10.1039/C3RA43769H).
- 47 S. Alamolhoda, S. Mirkazemi, Z. Ghiami and M. Niyafar, Structure and magnetic properties of Zr–Mn substituted strontium hexaferrite Sr(Zr,Mn)<sub>x</sub>Fe<sub>12–2x</sub>O<sub>19</sub> nanoparticles synthesized by sol–gel auto-combustion method, *Bull. Mater. Sci.*, 2016, **39**, 1311–1318, DOI: [10.1007/s12034-016-1262-3](https://doi.org/10.1007/s12034-016-1262-3).
- 48 N. Khamehashari, S. Hassanzadeh-Tabrizi and A. Bigham, Effects of strontium adding on the drug delivery behavior of silica nanoparticles synthesized by P123-assisted sol-gel method, *Mater. Chem. Phys.*, 2018, **205**, 283–291, DOI: [10.1016/J.MATCHEMPHYS.2017.11.034](https://doi.org/10.1016/J.MATCHEMPHYS.2017.11.034).
- 49 G. Hernández-Alvarado, S. Montemayor, I. Moggio, E. Arias, E. Trujillo-Vázquez, J. Díaz-Guillén, *et al.*, Synthesis at room atmosphere conditions of phosphorescent emitter SrAlO:Eu,Dy, *Ceram. Int.*, 2018, DOI: [10.1016/J.CERAMINT.2018.04.085](https://doi.org/10.1016/J.CERAMINT.2018.04.085).
- 50 L. García-Cerda, O. Rodríguez-Fernández and P. Reséndiz-Hernández, Study of SrFe<sub>12</sub>O<sub>19</sub> synthesized by the sol-gel method, *J. Alloys Compd.*, 2004, **369**, 182–184, DOI: [10.1016/J.JALLCOM.2003.09.099](https://doi.org/10.1016/J.JALLCOM.2003.09.099).
- 51 E. Romańczuk-Ruszk, B. Sztorch, Z. Oksiuta and R. Przekop, Metallic Strontium as a Precursor of the Al<sub>2</sub>O<sub>3</sub>/SrCO<sub>3</sub> Xerogels Obtained by the One-Pot Sol-Gel Method, *Gels*, 2022, **8**, 473, DOI: [10.3390/gels8080473](https://doi.org/10.3390/gels8080473).
- 52 M. Rehman, M. Akram and I. Gul, Improved Electrical Properties of Strontium Hexaferrite Nanoparticles by Co<sup>2+</sup> Substitutions, *ACS Omega*, 2022, **7**, 43432–43439, DOI: [10.1021/acsomega.2c03256](https://doi.org/10.1021/acsomega.2c03256).
- 53 M. Sharma, D. Kumar, J. Gewali and A. Thakur, Yttrium doped strontium nano hexaferrites: Influence of yttrium on the structural and magnetic properties of sol-gel synthesized nanocrystalline strontium hexaferrite, *J. Phys.: Conf. Ser.*, 2022, **2267**, 012024, DOI: [10.1088/1742-6596/2267/1/012024](https://doi.org/10.1088/1742-6596/2267/1/012024).
- 54 Á. Leite, A. Gonçalves, M. Rodrigues, M. Gomes and J. Mano, Strontium-Doped Bioactive Glass Nanoparticles in Osteogenic Commitment, *ACS Appl. Mater. Interfaces*, 2018, **10**(27), 23311–23320, DOI: [10.1021/acsomega.2c03256](https://doi.org/10.1021/acsomega.2c03256).
- 55 W. Zhang, N. Cao, Y. Chai, X. Xu and Y. Wang, Synthesis of nanosize single-crystal strontium hydroxyapatite via a simple sol-gel method, *Ceram. Int.*, 2014, **40**, 16061–16064, DOI: [10.1016/J.CERAMINT.2014.07.103](https://doi.org/10.1016/J.CERAMINT.2014.07.103).
- 56 L. Schmidt, F. Emmerling, H. Kirmse and E. Kemnitz, Sol-gel synthesis and characterisation of nanoscopic strontium fluoride, *RSC Adv.*, 2014, **4**, 32–38, DOI: [10.1039/C3RA43769H](https://doi.org/10.1039/C3RA43769H).
- 57 A. Youssef, H. Farag, A. El-Kheshen and F. Hammad, Synthesis of Nano-Structured Strontium Titanate by Sol-Gel and Solid State Routes, *Silicon*, 2018, **10**, 1225–1230, DOI: [10.1007/s12633-017-9596-z](https://doi.org/10.1007/s12633-017-9596-z).
- 58 A. Alimuddin and M. Rafeeq, Synthesis and Characterization of Strontium Oxide Nano Particle by Sol-Gel Method, *Orient. J. Chem.*, 2021, **37**, 177–180, DOI: [10.13005/OJC/370124](https://doi.org/10.13005/OJC/370124).
- 59 S. Kumar, R. Singh, P. Kumari, N. Ranga, A. Manash and R. Kumari, Structural, ferromagnetic, ferroelectric, and bio-medical behaviour of yttrium doped strontium hexaferrite nanoparticles synthesized by sol-gel auto-combustion method, *Ceram. Int.*, 2023, DOI: [10.1016/j.ceramint.2023.01.241](https://doi.org/10.1016/j.ceramint.2023.01.241).
- 60 M. Kheirmand-Parizi, K. Doll-Nikutta, A. Gaikwad, H. Denis and M. Stiesch, Effectiveness of strontium/silver-based titanium surface coatings in improving antibacterial and osteogenic implant characteristics: a systematic review of in-vitro studies, *Front. Bioeng. Biotechnol.*, 2024, **12**, DOI: [10.3389/fbioe.2024.1346426](https://doi.org/10.3389/fbioe.2024.1346426).



- 61 C. Sullivan, L. Neill, N. O'Leary, J. Gara, A. Crean and K. Ryan, Osteointegration, antimicrobial and antibiofilm activity of orthopaedic titanium surfaces coated with silver and strontium-doped hydroxyapatite using a novel blasting process, *Drug Delivery Transl. Res.*, 2021, **11**, 702–716, DOI: [10.1007/s13346-021-00946-1](https://doi.org/10.1007/s13346-021-00946-1).
- 62 A. Cochis, J. Barberi, S. Ferraris, M. Miola, L. Rimondini, E. Verné, *et al.*, Competitive surface colonization of antibacterial and bioactive materials doped with strontium and/or silver ions, *Nanomaterials*, 2020, **10**, 120, DOI: [10.3390/nano10010120](https://doi.org/10.3390/nano10010120).
- 63 N. Ranga, E. Poonia, S. Jakhar, A. Sharma, A. Kumar, S. Devi, *et al.*, Enhanced antimicrobial properties of bioactive glass using strontium and silver oxide nanocomposites, *J. Asian Ceram. Soc.*, 2019, **7**, 75–81, DOI: [10.1080/21870764.2018.1564477](https://doi.org/10.1080/21870764.2018.1564477).
- 64 Y. Huang, X. Zhang, H. Zhang, H. Qiao, X. Zhang, T. Jia, *et al.*, Fabrication of silver- and strontium-doped hydroxyapatite/TiO<sub>2</sub> nanotube bilayer coatings for enhancing bactericidal effect and osteoinductivity, *Ceram. Int.*, 2017, **43**, 992–1007, DOI: [10.1016/j.ceramint.2016.10.031](https://doi.org/10.1016/j.ceramint.2016.10.031).
- 65 A. Anand, S. Sengupta, H. Kaňková, A. Švančárková, A. Beltrán, D. Galusek, *et al.*, Influence of copper-strontium co-doping on bioactivity, cytotoxicity and antibacterial activity of mesoporous bioactive glass, *Gels*, 2022, **8**, 743, DOI: [10.3390/gels8110743](https://doi.org/10.3390/gels8110743).
- 66 Y. Wu, X. Shi, J. Wang, Y. Li, J. Wu, D. Jia, *et al.*, A surface metal ion-modified 3D-printed Ti-6Al-4V implant with direct and immunoregulatory antibacterial and osteogenic activity, *Front. Bioeng. Biotechnol.*, 2023, **11**, DOI: [10.3389/fbioe.2023.1142264](https://doi.org/10.3389/fbioe.2023.1142264).
- 67 J. Rau, A. De Bonis, M. Curcio, K. Barbaro, M. Fosca, I. Fadeeva, *et al.*, Coated biodegradable zinc lithium alloys: Development and characterization of co-doped strontium copper tricalcium phosphate coating for antimicrobial applications, *Coatings*, 2024, **14**, 1073, DOI: [10.3390/coatings14081073](https://doi.org/10.3390/coatings14081073).
- 68 M. Yarahmadi, H. Maleki-Ghaleh, M. Mehr, Z. Dargahi, F. Rasouli and M. Siadati, Synthesis and characterization of Sr-doped ZnO nanoparticles for photocatalytic applications, *J. Alloys Compd.*, 2021, **853**, 157000, DOI: [10.1016/j.jallcom.2020.157000](https://doi.org/10.1016/j.jallcom.2020.157000).
- 69 T. Bouarroudj, Y. Messai, L. Aoudjit, B. Zaidi, D. Zioui, A. Bendjama, *et al.*, Hydrothermal-assisted synthesis of Sr-doped SnS nanoflower catalysts for photodegradation of metronidazole antibiotic pollutant in wastewater promoted by natural sunlight irradiation, *Water Sci. Technol.*, 2024, **89**(5), 1107–1123, DOI: [10.2166/wst.2024.054](https://doi.org/10.2166/wst.2024.054).
- 70 Y. Chen, Q. Wu, N. Bu, J. Wang and Y. Song, Magnetic recyclable lanthanum-nitrogen co-doped titania/strontium ferrite/diatomite heterojunction composite for enhanced visible-light-driven photocatalytic activity and recyclability, *Chem. Eng. J.*, 2019, **373**, 192–202, DOI: [10.1016/j.cej.2019.05.047](https://doi.org/10.1016/j.cej.2019.05.047).
- 71 R. Li, T. Chen and X. Pan, Metal-Organic-Framework-Based Materials for Antimicrobial Applications, *ACS Nano*, 2021, **15**, 3808–3848, DOI: [10.1021/acsnano.0c09617](https://doi.org/10.1021/acsnano.0c09617).
- 72 N. Neto, K. Matsui, C. Paskocimas, M. Bomio and F. Motta, Study of the photocatalysis and increase of antimicrobial properties of Fe<sup>3+</sup> and Pb<sup>2+</sup> co-doped ZnO nanoparticles obtained by microwave-assisted hydrothermal method, *Mater. Sci. Semicond. Process.*, 2019, **93**, 123–133, DOI: [10.1016/j.mssp.2018.12.034](https://doi.org/10.1016/j.mssp.2018.12.034).
- 73 B. Wang, Y. Li, S. Wang, F. Jia, A. Bian, K. Wang, *et al.*, Electrodeposited dopamine/strontium-doped hydroxyapatite composite coating on pure zinc for anti-corrosion, antimicrobial and osteogenesis, *Mater. Sci. Eng., C*, 2021, **129**, 112387, DOI: [10.1016/j.msec.2021.112387](https://doi.org/10.1016/j.msec.2021.112387).
- 74 H. Alshammari, F. Bakitian, J. Neilands, O. Andersen and A. Stavropoulos, Antimicrobial Properties of Strontium Functionalized Titanium Surfaces for Oral Applications, A Systematic Review, *Coatings*, 2021, **11**, 810, DOI: [10.3390/COATINGS11070810](https://doi.org/10.3390/COATINGS11070810).
- 75 A. Adawy and R. Díaz, Probing the Structure, Cytocompatibility, and Antimicrobial Efficacy of Silver-, Strontium-, and Zinc-Doped Monetite, *ACS Appl. Bio Mater.*, 2022, **5**, 1648–1657, DOI: [10.1021/acsbam.2c00047](https://doi.org/10.1021/acsbam.2c00047).
- 76 K. Zuo, L. Wang, Z. Wang, Y. Yin, C. Du, B. Liu, *et al.*, Zinc-Doping Induces Evolution of Biocompatible Strontium-Calcium-Phosphate Conversion Coating on Titanium to Improve Antibacterial Property, *ACS Appl. Mater. Interfaces*, 2022, **14**, 7690–7705, DOI: [10.1021/acsbam.1c23631](https://doi.org/10.1021/acsbam.1c23631).
- 77 Y. Chen, C. Zhou, Y. Xie, A. Xu, Y. Guan, W. Lu, *et al.*, Zinc- and strontium- co-incorporated nanorods on titanium surfaces with favorable material property, osteogenesis, and enhanced antibacterial activity, *J. Biomed. Mater. Res., Part B*, 2021, **109**, 1754–1767, DOI: [10.1002/jbm.b.34834](https://doi.org/10.1002/jbm.b.34834).
- 78 Z. Geng, Z. Cui, Z. Li, S. Zhu, Y. Liang, Y. Liu, *et al.*, Strontium incorporation to optimize the antibacterial and biological characteristics of silver-substituted hydroxyapatite coating, *Mater. Sci. Eng., C*, 2016, **58**, 467–477, DOI: [10.1016/j.msec.2015.08.061](https://doi.org/10.1016/j.msec.2015.08.061).
- 79 Z. Saeed and B. Azhdar, A novel method for synthesizing narrow particle size distribution of holmium-doped strontium hexaferrite by sol-gel auto-combustion, *Mater. Res. Express*, 2020, **7**, 045006, DOI: [10.1088/2053-1591/ab7f5e](https://doi.org/10.1088/2053-1591/ab7f5e).
- 80 J. Nicolas, S. Mura, D. Brambilla, N. Mackiewicz and P. Couvreur, Design, functionalization strategies and biomedical applications of targeted biodegradable/biocompatible polymer-based nanocarriers for drug delivery, *Chem. Soc. Rev.*, 2013, **42**(3), 1147–1235, DOI: [10.1039/c2cs35265f](https://doi.org/10.1039/c2cs35265f).
- 81 S. Oliveira, G. Bisker, N. Bakh, S. Gibbs, M. Landry and M. Strano, Protein functionalized carbon nanomaterials for biomedical applications, *Carbon*, 2015, **95**, 767–779, DOI: [10.1016/J.CARBON.2015.08.076](https://doi.org/10.1016/J.CARBON.2015.08.076).
- 82 I. Gessner and I. Neundorff, Nanoparticles Modified with Cell-Penetrating Peptides: Conjugation Mechanisms,



- Physicochemical Properties, and Application in Cancer Diagnosis and Therapy, *Int. J. Mol. Sci.*, 2020, **21**, 2536, DOI: [10.3390/ijms21072536](https://doi.org/10.3390/ijms21072536).
- 83 Y. Kumar, A. Sinha, K. Nigam, D. Dwivedi and J. Sangwai, Functionalized nanoparticles: Tailoring properties through surface energetics and coordination chemistry for advanced biomedical applications, *Nanoscale*, 2023, **15**, 6075–6104, DOI: [10.1039/d2nr07163k](https://doi.org/10.1039/d2nr07163k).
- 84 K. Ishihara, W. Chen, Y. Liu, Y. Tsukamoto and Y. Inoue, Cytocompatible and multifunctional polymeric nanoparticles for transportation of bioactive molecules into and within cells, *Sci. Technol. Adv. Mater.*, 2016, **17**, 300–312, DOI: [10.1080/14686996.2016.1190257](https://doi.org/10.1080/14686996.2016.1190257).
- 85 M. Maliki, I. H. Ifijen, E. U. Ikhuoria, *et al.*, Copper nanoparticles and their oxides: Optical, anticancer, and antibacterial properties, *Int. Nano Lett.*, 2022, **12**(4), 379–398, DOI: [10.1007/s40089-022-00380-2](https://doi.org/10.1007/s40089-022-00380-2).
- 86 I. H. Ifijen and M. Maliki, A comprehensive review on the synthesis and photothermal cancer therapy of titanium nitride nanostructures, *Inorg. Nano-Met. Chem.*, 2022, **53**(4), 366–387, DOI: [10.1080/24701556.2022.2068596](https://doi.org/10.1080/24701556.2022.2068596).
- 87 I. H. Ifijen, N. U. Udokpoh, M. Maliki, E. U. Ikhuoria and E. O. Obazee, A review of nanovanadium compounds for cancer cell therapy, in *TMS 2023 152nd Annual Meeting & Exhibition Supplemental Proceedings*, Springer, Cham, 2023, DOI: [10.1007/978-3-031-22524-6\\_59](https://doi.org/10.1007/978-3-031-22524-6_59).
- 88 L. I. Egwonor, R. F. Awoyemi, B. Owolabi, O. R. Aworinde, R. O. Kajola, A. Hazeem, *et al.*, Cutting-edge developments in zinc oxide nanoparticles: Synthesis and applications for enhanced antimicrobial and UV protection in healthcare solutions, *RSC Adv.*, 2024, **14**, 20992–21034, DOI: [10.1039/D4RA02452D](https://doi.org/10.1039/D4RA02452D).
- 89 P. Huang, C. Wang, H. Deng, Y. Zhou and X. Chen, Surface Engineering of Nanoparticles toward Cancer Theranostics, *Acc. Chem. Res.*, 2023, **56**, 1766–1779, DOI: [10.1021/acs.accounts.3c00122](https://doi.org/10.1021/acs.accounts.3c00122).
- 90 Z. Li, L. Yu, T. Yang and Y. Chen, Theranostic nanomedicine by surface nanopore engineering, *Sci. China: Chem.*, 2018, **61**, 1243–1260, DOI: [10.1007/s11426-018-9297-5](https://doi.org/10.1007/s11426-018-9297-5).
- 91 R. Prasad and K. Selvaraj, Choice of Nanoparticles for Theranostics Engineering: Surface Coating to Nanovalves Approach, *Nanotheranostics*, 2024, **8**, 12–32, DOI: [10.7150/ntno.89768](https://doi.org/10.7150/ntno.89768).
- 92 T. Seidu, P. Kutoka, D. Asante, M. Farooq, R. Alolga and W. Bo, Functionalization of Nanoparticulate Drug Delivery Systems and Its Influence in Cancer Therapy, *Pharmaceutics*, 2022, **14**, 1113, DOI: [10.3390/pharmaceutics14051113](https://doi.org/10.3390/pharmaceutics14051113).
- 93 S. Morarasu, B. Morărașu, R. Ghiarasim, A. Coroabă, C. Tiron, R. Iliescu, *et al.*, Targeted Cancer Therapy via pH-Functionalized Nanoparticles: A Scoping Review of Methods and Outcomes, *Gels*, 2022, **8**, 232, DOI: [10.3390/gels8040232](https://doi.org/10.3390/gels8040232).
- 94 J. Jhaveri, Z. Raichura, T. Khan, M. Momin and A. Omri, Chitosan Nanoparticles-Insight into Properties, Functionalization and Applications in Drug Delivery and Theranostics, *Molecules*, 2021, **26**, 272, DOI: [10.3390/molecules26020272](https://doi.org/10.3390/molecules26020272).
- 95 N. Thorat, S. Otari, R. Patil, V. Khot, A. Prasad, R. Ningthoujam, *et al.*, Enhanced colloidal stability of polymer coated La<sub>0.7</sub>Sr<sub>0.3</sub>MnO<sub>3</sub> nanoparticles in physiological media for hyperthermia application, *Colloids Surf., B*, 2013, **111**, 264–269, DOI: [10.1016/j.colsurfb.2013.06.014](https://doi.org/10.1016/j.colsurfb.2013.06.014).
- 96 S. Kumar and K. Chatterjee, Strontium eluting graphene hybrid nanoparticles augment osteogenesis in a 3D tissue scaffold, *Nanoscale*, 2015, **7**(5), 2023–2033, DOI: [10.1039/c4nr05060f](https://doi.org/10.1039/c4nr05060f).
- 97 E. Bonnelye, A. Chabadel, F. Saltel and P. Jurdic, Dual effect of strontium ranelate: stimulation of osteoblast differentiation and inhibition of osteoclast formation and resorption in vitro, *Bone*, 2008, **42**(1), 129–138, DOI: [10.1016/j.bone.2007.08.043](https://doi.org/10.1016/j.bone.2007.08.043).
- 98 H. Xie, Z. Gu, Y. He, J. Xu, C. Xu, L. Li, *et al.*, Microenvironment construction of strontium-calcium-based biomaterials for bone tissue regeneration: the equilibrium effect of calcium to strontium, *J. Mater. Chem. B*, 2018, **6**(15), 2332–2339, DOI: [10.1039/C8TB00306H](https://doi.org/10.1039/C8TB00306H).
- 99 L. Weng, S. Boda, M. Teusink, F. Shuler, X. Li and J. Xie, Binary Doping of Strontium and Copper Enhancing Osteogenesis and Angiogenesis of Bioactive Glass Nanofibers while Suppressing Osteoclast Activity, *ACS Appl. Mater. Interfaces*, 2017, **9**(29), 24484–24496, DOI: [10.1021/acsami.7b06521](https://doi.org/10.1021/acsami.7b06521).
- 100 X. Jia, Q. Long, R. Miron, C. Yin, Y. Wei, Y. Zhang, *et al.*, Setd2 is associated with strontium-induced bone regeneration, *Acta Biomater.*, 2017, **53**, 495–505, DOI: [10.1016/j.actbio.2017.02.025](https://doi.org/10.1016/j.actbio.2017.02.025).
- 101 X. Cui, Y. Zhang, J. Wang, C. Huang, Y. Wang, H. Yang, *et al.*, Strontium modulates osteogenic activity of bone cement composed of bioactive borosilicate glass particles by activating Wnt/ $\beta$ -catenin signaling pathway, *Bioact. Mater.*, 2020, **5**, 334–347, DOI: [10.1016/j.bioactmat.2020.02.016](https://doi.org/10.1016/j.bioactmat.2020.02.016).
- 102 J. Côrtes, J. Dornelas, F. Duarte, M. Messori, C. Mourão and G. Alves, The Effects of the Addition of Strontium on the Biological Response to Calcium Phosphate Biomaterials: A Systematic Review, *Appl. Sci.*, 2024, DOI: [10.3390/app14177566](https://doi.org/10.3390/app14177566).
- 103 C. Jagannathan, R. Waddington and W. Ayre, Nanoparticle and nanotopography-induced activation of the Wnt pathway in bone regeneration, *Tissue Eng., Part B*, 2023, DOI: [10.1089/ten.TEB.2023.0108](https://doi.org/10.1089/ten.TEB.2023.0108).
- 104 R. Zhang, B. Oyajobi, S. Harris, D. Chen, C. Tsao, H. Deng, *et al.*, Wnt/ $\beta$ -catenin signaling activates bone morphogenetic protein 2 expression in osteoblasts, *Bone*, 2013, **52**(1), 145–156, DOI: [10.1016/j.bone.2012.09.029](https://doi.org/10.1016/j.bone.2012.09.029).
- 105 G. Bain, T. Müller, X. Wang and J. Papkoff, Activated  $\beta$ -catenin induces osteoblast differentiation of C3H10T1/2 cells and participates in BMP2 mediated signal transduction, *Biochem. Biophys. Res. Commun.*, 2003, **301**, 84–91, DOI: [10.1016/S0006-291X\(02\)02951-0](https://doi.org/10.1016/S0006-291X(02)02951-0).



- 106 V. Salazar, G. Mbalaviele and R. Civitelli, The pro-osteogenic action of  $\beta$ -catenin requires interaction with BMP signaling, but not Tcf/Lef transcriptional activity, *J. Cell. Biochem.*, 2008, **104**, 942–952, DOI: [10.1002/jcb.21679](https://doi.org/10.1002/jcb.21679).
- 107 L. Wolff, A. Houben, C. Fabritius, M. Angus-Hill, K. Basler and C. Hartmann, Only the Co-Transcriptional Activity of  $\beta$ -Catenin Is Required for the Local Regulatory Effects in Hypertrophic Chondrocytes on Developmental Bone Modeling, *J. Bone Miner. Res.*, 2021, **36**, 2039–2052, DOI: [10.1002/jbmr.4396](https://doi.org/10.1002/jbmr.4396).
- 108 P. Duan and L. Bonewald, The role of the Wnt/ $\beta$ -catenin signaling pathway in formation and maintenance of bone and teeth, *Int. J. Biochem. Cell Biol.*, 2016, 77(Pt A), 23–29, DOI: [10.1016/j.biocel.2016.05.015](https://doi.org/10.1016/j.biocel.2016.05.015).
- 109 A. Ahmadzadeh, F. Norozi, S. Shahrabi, M. Shahjahani and N. Saki, Wnt/ $\beta$ -catenin signaling in bone marrow niche, *Cell Tissue Res.*, 2015, **363**, 321–335, DOI: [10.1007/s00441-015-2300-y](https://doi.org/10.1007/s00441-015-2300-y).
- 110 T. Li, H. Wang, Y. Jiang, Y. Guan, S. Chen, Z. Wu, *et al.*, Canonical Wnt/ $\beta$ -catenin signaling has positive effects on osteogenesis, but can have negative effects on cementogenesis, *J. Periodontol.*, 2022, **93**, 1725–1737, DOI: [10.1002/JPER.21-0599](https://doi.org/10.1002/JPER.21-0599).
- 111 M. Arioka, F. Takahashi-Yanaga, M. Sasaki, T. Yoshihara, S. Morimoto, A. Takashima, *et al.*, Acceleration of bone development and regeneration through the Wnt/ $\beta$ -catenin signaling pathway in mice heterozygously deficient for GSK-3 $\beta$ , *Biochem. Biophys. Res. Commun.*, 2013, **440**(4), 677–682, DOI: [10.1016/j.bbrc.2013.09.126](https://doi.org/10.1016/j.bbrc.2013.09.126).
- 112 H. Yu, Y. Liu, X. Yang, J. He, F. Zhang, Q. Zhong, *et al.*, Strontium ranelate promotes chondrogenesis through inhibition of the Wnt/ $\beta$ -catenin pathway, *Stem Cell Res. Ther.*, 2021, **12**, 296, DOI: [10.1186/s13287-021-02372-z](https://doi.org/10.1186/s13287-021-02372-z).
- 113 M. Rybchyn, M. Slater, A. Conigrave and R. Mason, An Akt-dependent increase in canonical Wnt signaling and a decrease in sclerostin protein levels are involved in strontium ranelate-induced osteogenic effects in human osteoblasts, *J. Biol. Chem.*, 2011, **286**, 23771–23779, DOI: [10.1074/jbc.M111.251116](https://doi.org/10.1074/jbc.M111.251116).
- 114 F. Yang, D. Yang, J. Tu, Q. Zheng, L. Cai and L. Wang, Strontium enhances osteogenic differentiation of mesenchymal stem cells and in vivo bone formation by activating Wnt/ $\beta$ -catenin signaling, *Stem Cells*, 2011, **29**, 981–991, DOI: [10.1002/stem.646](https://doi.org/10.1002/stem.646).
- 115 X. Cui, Y. Zhang, J. Wang, C. Huang, Y. Wang, H. Yang, *et al.*, Strontium modulates osteogenic activity of bone cement composed of bioactive borosilicate glass particles by activating Wnt/ $\beta$ -catenin and BMP signalling pathway, *Biotechnol eJournal*, 2019, DOI: [10.2139/ssrn.3455085](https://doi.org/10.2139/ssrn.3455085).
- 116 Z. Saidak and P. Marie, Strontium signaling: molecular mechanisms and therapeutic implications in osteoporosis, *Pharmacol. Ther.*, 2012, **136**(2), 216–226, DOI: [10.1016/j.pharmthera.2012.07.009](https://doi.org/10.1016/j.pharmthera.2012.07.009).
- 117 M. Stuss, P. Rieseke, A. Cegłowska, W. Stępień-Kłos, P. Liberski, E. Brzezińska, *et al.*, Assessment of OPG/RANK/RANKL gene expression levels in peripheral blood mononuclear cells (PBMC) after treatment with strontium ranelate and ibandronate in patients with postmenopausal osteoporosis, *J. Clin. Endocrinol. Metab.*, 2013, **98**(5), E1007–E1011, DOI: [10.1210/jc.2012-3885](https://doi.org/10.1210/jc.2012-3885).
- 118 J. Fonseca, Rebalancing bone turnover in favour of formation with strontium ranelate: implications for bone strength, *Rheumatology*, 2008, **47**, iv17–9, DOI: [10.1093/rheumatology/ken165](https://doi.org/10.1093/rheumatology/ken165).
- 119 S. Zhu, X. Hu, Y. Tao, Z. Ping, L. Wang, J. Shi, *et al.*, Strontium inhibits titanium particle-induced osteoclast activation and chronic inflammation via suppression of NF- $\kappa$ B pathway, *Sci. Rep.*, 2016, **6**, 36251, DOI: [10.1038/srep36251](https://doi.org/10.1038/srep36251).
- 120 D. Huang, F. Zhao, W. Gao, X. Chen, Z. Guo and W. Zhang, Strontium-substituted sub-micron bioactive glasses inhibit osteoclastogenesis through suppression of RANKL-induced signaling pathway, *Regener. Biomater.*, 2020, **7**, 303–311, DOI: [10.1093/rb/rbaa004](https://doi.org/10.1093/rb/rbaa004).
- 121 F. Chen, L. Tian, X. Pu, Q. Zeng, Y. Xiao, X. Chen, *et al.*, Enhanced ectopic bone formation by strontium-substituted calcium phosphate ceramics through regulation of osteoclastogenesis and osteoblastogenesis, *Biomater. Sci.*, 2022, **10**, 5925–5937, DOI: [10.1039/d2bm00348a](https://doi.org/10.1039/d2bm00348a).
- 122 T. Sun, Z. Li, X. Zhong, Z. Cai, Z. Ning, T. Hou, *et al.*, Strontium inhibits osteoclastogenesis by enhancing LRP6 and  $\beta$ -catenin-mediated OPG targeted by miR-181d-5p, *J. Cell Commun. Signaling*, 2018, **13**, 85–97, DOI: [10.1007/s12079-018-0478-y](https://doi.org/10.1007/s12079-018-0478-y).
- 123 G. Atkins, K. Welldon, P. Halbout and D. Findlay, Strontium ranelate treatment of human primary osteoblasts promotes an osteocyte-like phenotype while eliciting an osteoprotegerin response, *Osteoporosis Int.*, 2009, **20**, 653–664, DOI: [10.1007/s00198-008-0728-6](https://doi.org/10.1007/s00198-008-0728-6).
- 124 S. Peng, S. Peng, S. Peng, X. Liu, S. Huang, Z. Li, *et al.*, The cross-talk between osteoclasts and osteoblasts in response to strontium treatment: involvement of osteoprotegerin, *Bone*, 2011, **49**(6), 1290–1298, DOI: [10.1016/j.bone.2011.08.031](https://doi.org/10.1016/j.bone.2011.08.031).
- 125 S. Tat, J. Pelletier, F. Mineau, J. Caron and J. Martel-Pelletier, Strontium ranelate inhibits key factors affecting bone remodeling in human osteoarthritic subchondral bone osteoblasts, *Bone*, 2011, **49**(3), 559–567, DOI: [10.1016/j.bone.2011.06.005](https://doi.org/10.1016/j.bone.2011.06.005).
- 126 I. Ullah, Z. Hussain, S. Ullah, Q. Zahra, Y. Zhang, S. Mehmood, *et al.*, An osteogenic, antibacterial, and anti-inflammatory nanocomposite hydrogel platform to accelerate bone reconstruction, *J. Mater. Chem. B*, 2023, **11**, 5830–5845, DOI: [10.1039/d3tb00641g](https://doi.org/10.1039/d3tb00641g).
- 127 K. Yang, D. Lee, K. Lee, W. Jang, H. Lim, E. Lee, *et al.*, 3D-bioprinted bone scaffolds incorporating SR1 nanoparticles enhance blood vessel regeneration in rat calvarial defects, *Int. J. Bioprint.*, 2024, 1931, DOI: [10.36922/ijb.1931](https://doi.org/10.36922/ijb.1931).
- 128 X. Wang, J. Shao, M. Raouf, H. Xie, H. Huang, H. Wang, *et al.*, Near-infrared light-triggered drug delivery system based on black phosphorus for in vivo bone regeneration, *Biomaterials*, 2018, **179**, 164–174, DOI: [10.1016/j.biomaterials.2018.06.039](https://doi.org/10.1016/j.biomaterials.2018.06.039).



- 129 H. Liu, R. Gu, W. Li, L. Zeng, Y. Zhu, B. Heng, *et al.*, Engineering 3D-Printed Strontium-Titanium Scaffold-Integrated Highly Bioactive Serum Exosomes for Critical Bone Defects by Osteogenesis and Angiogenesis, *ACS Appl. Mater. Interfaces*, 2023, **15**, 27486–27501, DOI: [10.1021/acsami.3c00898](https://doi.org/10.1021/acsami.3c00898).
- 130 Q. Wu, X. Wang, F. Jiang, Z. Zhu, J. Wen and X. Jiang, Study of Sr–Ca–Si-based scaffolds for bone regeneration in osteoporotic models, *Int. J. Oral Sci.*, 2020, **12**, 25, DOI: [10.1038/s41368-020-00094-1](https://doi.org/10.1038/s41368-020-00094-1).
- 131 A. Herbanu, I. Ana, R. Ardhani and W. Siswomihardjo, Fibrous PVA Matrix Containing Strontium-Substituted Hydroxyapatite Nanoparticles from Golden Apple Snail (*Pomacea canaliculata* L.) Shells for Bone Tissue Engineering, *Bioengineering*, 2023, **10**, 844, DOI: [10.3390/bioengineering10070844](https://doi.org/10.3390/bioengineering10070844).
- 132 Y. Lei, Z. Xu, Q. Ke, W. Yin, Y. Chen, C. Zhang, *et al.*, Strontium hydroxyapatite/chitosan nanohybrid scaffolds with enhanced osteoinductivity for bone tissue engineering, *Mater. Sci. Eng., C*, 2017, **72**, 134–142, DOI: [10.1016/j.msec.2016.11.063](https://doi.org/10.1016/j.msec.2016.11.063).
- 133 X. Ding, X. Li, C. Li, M. Qi, Z. Zhang, X. Sun, *et al.*, Chitosan/Dextran Hydrogel Constructs Containing Strontium-Doped Hydroxyapatite with Enhanced Osteogenic Potential in Rat Cranium, *ACS Biomater. Sci. Eng.*, 2019, **5**(9), 4574–4586, DOI: [10.1021/ACSBIOMATERIALS.9B00584](https://doi.org/10.1021/ACSBIOMATERIALS.9B00584).
- 134 C. Capuccini, P. Torricelli, F. Sima, E. Boanini, C. Ristoscu, B. Bracci, *et al.*, Strontium-substituted hydroxyapatite coatings synthesized by pulsed-laser deposition: in vitro osteoblast and osteoclast response, *Acta Biomater.*, 2008, **4**(6), 1885–1893, DOI: [10.1016/j.actbio.2008.05.005](https://doi.org/10.1016/j.actbio.2008.05.005).
- 135 F. Scalera, B. Palazzo, A. Barca and F. Gervaso, Sintering of Magnesium-Strontium doped Hydroxyapatite nanocrystals: towards the production of 3D biomimetic bone scaffolds, *J. Biomed. Mater. Res., Part A*, 2019, **108**, 633–644, DOI: [10.1002/jbm.a.36843](https://doi.org/10.1002/jbm.a.36843).
- 136 J. Li, X. Liu, S. Park, A. Miller, A. Terzic and L. Lu, Strontium-substituted hydroxyapatite stimulates osteogenesis on poly(propylene fumarate) nanocomposite scaffolds, *J. Biomed. Mater. Res., Part A*, 2018, **107**(3), 631–642, DOI: [10.1002/jbm.a.36579](https://doi.org/10.1002/jbm.a.36579).
- 137 C. Codrea, D. Lincu, V. Ene, A. Nicoară, M. Stan, D. Fica, *et al.*, Three-Dimensional-Printed Composite Scaffolds Containing Poly-ε-Caprolactone and Strontium-Doped Hydroxyapatite for Osteoporotic Bone Restoration, *Polymers*, 2024, **16**, 1511, DOI: [10.3390/polym16111511](https://doi.org/10.3390/polym16111511).
- 138 R. Surmenev, S. Shkarina, D. Syromotina, E. Melnik, R. Shkarin, I. Selezneva, *et al.*, Characterization of biomimetic silicate- and strontium-containing hydroxyapatite microparticles embedded in biodegradable electrospun polycaprolactone scaffolds for bone regeneration, *Eur. Polym. J.*, 2019, **113**, 67–77, DOI: [10.1016/J.EURPOLYMJ.2019.01.042](https://doi.org/10.1016/J.EURPOLYMJ.2019.01.042).
- 139 S. Li, Y. He, J. Li, J. Sheng, S. Long, Z. Li, *et al.*, Titanium scaffold loaded with strontium and copper double-doped hydroxyapatite can inhibit bacterial growth and enhance osteogenesis, *J. Biomater. Appl.*, 2022, **37**, 195–203, DOI: [10.1177/08853282221080525](https://doi.org/10.1177/08853282221080525).
- 140 Z. Ye, Y. Qi, A. Zhang, B. Karels and C. Aparicio, Biomimetic Mineralization of Fibrillar Collagen with Strontium-doped Hydroxyapatite, *ACS Macro Lett.*, 2023, 408–414, DOI: [10.1021/acsmacrolett.3c00039](https://doi.org/10.1021/acsmacrolett.3c00039).
- 141 B. Hu, Z. Meng, Y. Zhang, L. Ye, C. Wang and W. Guo, Sr-HA scaffolds fabricated by SPS technology promote the repair of segmental bone defects, *Tissue Cell*, 2020, **66**, 101386, DOI: [10.1016/j.tice.2020.101386](https://doi.org/10.1016/j.tice.2020.101386).
- 142 Y. Tang, Q. Wang, Q. Ke, C. Zhang, J. Guan and Y. Guo, Mineralization of ytterbium-doped hydroxyapatite nanorod arrays in magnetic chitosan scaffolds improves osteogenic and angiogenic abilities for bone defect healing, *Chem. Eng. J.*, 2020, **387**, 124166, DOI: [10.1016/j.cej.2020.124166](https://doi.org/10.1016/j.cej.2020.124166).
- 143 J. Li, X. Liu, S. Park, A. Miller, A. Terzic and L. Lu, Strontium-substituted hydroxyapatite stimulates osteogenesis on poly(propylene fumarate) nanocomposite scaffolds, *J. Biomed. Mater. Res., Part A*, 2019, **107**(3), 631–642, DOI: [10.1002/jbm.a.36579](https://doi.org/10.1002/jbm.a.36579).
- 144 Q. Wang, P. Tang, X. Ge, P. Li, C. Lv, M. Wang, *et al.*, Experimental and simulation studies of strontium/zinc-codoped hydroxyapatite porous scaffolds with excellent osteoinductivity and antibacterial activity, *Appl. Surf. Sci.*, 2018, **462**, 118–126, DOI: [10.1016/J.APSUSC.2018.08.068](https://doi.org/10.1016/J.APSUSC.2018.08.068).
- 145 S. Panzavolta, P. Torricelli, S. Casolari, A. Parrilli, M. Fini and A. Bigi, Strontium-substituted hydroxyapatite-gelatin biomimetic scaffolds modulate bone cell response, *Macromol. Biosci.*, 2018, **18**(7), e1800096, DOI: [10.1002/mabi.201800096](https://doi.org/10.1002/mabi.201800096).
- 146 T. Wu, B. Li, W. Wang, L. Chen, Z. Li, M. Wang, *et al.*, Strontium-substituted hydroxyapatite grown on graphene oxide nanosheet-reinforced chitosan scaffold to promote bone regeneration, *Biomater. Sci.*, 2020, **8**, 4603–4615, DOI: [10.1039/d0bm00523a](https://doi.org/10.1039/d0bm00523a).
- 147 F. Scalera, B. Palazzo, A. Barca and F. Gervaso, Sintering of magnesium-strontium doped hydroxyapatite nanocrystals: towards the production of 3D biomimetic bone scaffolds, *J. Biomed. Mater. Res., Part A*, 2019, **108**, 633–644, DOI: [10.1002/jbm.a.36843](https://doi.org/10.1002/jbm.a.36843).
- 148 X. Zhang, Y. Chen, J. Han, J. Mo, P. Dong, Y. Zhuo, *et al.*, Biocompatible silk fibroin/carboxymethyl chitosan/strontium-substituted hydroxyapatite/cellulose nanocrystal composite scaffolds for bone tissue engineering, *Int. J. Biol. Macromol.*, 2019, **136**, 1247–1257, DOI: [10.1016/j.ijbiomac.2019.06.172](https://doi.org/10.1016/j.ijbiomac.2019.06.172).
- 149 G. Borciani, G. Montalbano, F. Perut, G. Ciapetti, N. Baldini and C. Vitale-Brovarone, Osteoblast and osteoclast activity on collagen-based 3D printed scaffolds enriched with strontium-doped bioactive glasses and hydroxyapatite nanorods for bone tissue engineering, *Biomed. Mater.*, 2024, **19**, 065007, DOI: [10.1088/1748-605X/ad72c3](https://doi.org/10.1088/1748-605X/ad72c3).
- 150 G. Li, Y. Li, X. Zhang, P. Gao, X. Xia, S. Xiao, *et al.*, Strontium and simvastatin dual loaded hydroxyapatite microsphere reinforced poly(ε-caprolactone) scaffolds



- promote vascularized bone regeneration, *J. Mater. Chem. B*, 2023, **11**, 1115–1130, DOI: [10.1039/d2tb02309a](https://doi.org/10.1039/d2tb02309a).
- 151 K. Wang, M. Gao, J. Fan, J. Huo, P. Liu, R. Ding, *et al.*, SrTiO<sub>3</sub> nanotube-based "pneumatic nanocannon" for on-demand delivery of antibacterial and sustained osseointegration enhancement, *ACS Nano*, 2024, **18**, 16011–16026, DOI: [10.1021/acsnano.4c04478](https://doi.org/10.1021/acsnano.4c04478).
- 152 W. Lu, C. Y. Zhou, J. Li, J. Jiang, Y. Chen, L. Dong, *et al.*, Improved osseointegration of strontium-modified titanium implants by regulating angiogenesis and macrophage polarization, *Biomater. Sci.*, 2022, **10**, 2198–2214, DOI: [10.1039/d1bm01488a](https://doi.org/10.1039/d1bm01488a).
- 153 Q. Pan, Y. Zheng, Y. Zhou, X. Zhang, M. Yuan, J. Guo, *et al.*, Doping engineering of piezo-sonocatalytic nanocoating confer dental implants with enhanced antibacterial performances and osteogenic activity, *Adv. Funct. Mater.*, 2024, **34**, DOI: [10.1002/adfm.202313553](https://doi.org/10.1002/adfm.202313553).
- 154 Y. Wu, S. Huo, S. Liu, Q. Hong, Y. Wang and Z. Lyu, Cu–Sr bilayer bioactive glass nanoparticles/polydopamine functionalized polyetheretherketone enhances osteogenic activity and prevents implant-associated infections through spatiotemporal immunomodulation, *Adv. Healthcare Mater.*, 2023, **12**, DOI: [10.1002/adhm.202301772](https://doi.org/10.1002/adhm.202301772).
- 155 S. Kargozar, N. Lotfibakhshaiesh, J. Ai, M. Mozafari, P. Milan, S. Hamzehlou, *et al.*, Strontium- and cobalt-substituted bioactive glasses seeded with human umbilical cord perivascular cells to promote bone regeneration via enhanced osteogenic and angiogenic activities, *Acta Biomater.*, 2017, **58**, 502–514, DOI: [10.1016/j.actbio.2017.06.021](https://doi.org/10.1016/j.actbio.2017.06.021).
- 156 R. Anushikaa, S. Ganesh, V. Victoria, A. Shanmugavadivu, K. Lavanya, S. Lekhavadhani, *et al.*, 3D-printed titanium scaffolds loaded with gelatin hydrogel containing strontium-doped silver nanoparticles promote osteoblast differentiation and antibacterial activity for bone tissue engineering, *Biotechnol. J.*, 2024, **19**(8), e2400288, DOI: [10.1002/biot.202400288](https://doi.org/10.1002/biot.202400288).
- 157 T. Xue, S. Attarilar, S. Liu, J. Liu, X. Song, L. Li, *et al.*, Surface modification techniques of titanium and its alloys to functionally optimize their biomedical properties: Thematic review, *Front. Bioeng. Biotechnol.*, 2020, **8**, 603072, DOI: [10.3389/fbioe.2020.603072](https://doi.org/10.3389/fbioe.2020.603072).
- 158 L. Pauksch, S. Hartmann, M. Rohnke, G. Szalay, V. Alt, R. Schnettler, *et al.*, Biocompatibility of silver nanoparticles and silver ions in primary human mesenchymal stem cells and osteoblasts, *Acta Biomater.*, 2014, **10**, 439–449, DOI: [10.1016/j.actbio.2013.09.037](https://doi.org/10.1016/j.actbio.2013.09.037).
- 159 J. Liu, Y. Zhou, J. Lu, R. Cai, T. Zhao, Y. Chen, *et al.*, Injectable, tough, and adhesive zwitterionic hydrogels for 3D-printed wearable strain sensors, *Chem. Eng. J.*, 2023, **475**, 146340, DOI: [10.1016/j.cej.2023.146340](https://doi.org/10.1016/j.cej.2023.146340).
- 160 B. Wang, Z. Wu, J. Lan, Y. Li, L. Xie, X. Huang, *et al.*, Surface modification of titanium implants by silk fibroin/Ag co-functionalized strontium titanate nanotubes for inhibition of bacterial-associated infection and enhancement of in vivo osseointegration, *Surf. Coat. Technol.*, 2021, **405**, 126700, DOI: [10.1016/j.surfcoat.2020.126700](https://doi.org/10.1016/j.surfcoat.2020.126700).
- 161 N. Tripathi and M. K. Goshisht, Recent advances and mechanistic insights into antibacterial activity, antibiofilm activity, and cytotoxicity of silver nanoparticles, *ACS Appl. Bio Mater.*, 2022, **5**(4), 1391–1463, DOI: [10.1021/acsnano.4c04478](https://doi.org/10.1021/acsnano.4c04478).
- 162 M. K. Parizi, K. Doll, M. I. Rahim, C. Mikolai, A. Winkel and M. Stiesch, Antibacterial and cytocompatible: combining silver nitrate with strontium acetate increases the therapeutic window, *Int. J. Mol. Sci.*, 2022, **23**(15), 8058, DOI: [10.3390/ijms23158058](https://doi.org/10.3390/ijms23158058).
- 163 W. Wang and K. W. K. Yeung, Bone grafts and biomaterial substitutes for bone defect repair: A review, *Bioact. Mater.*, 2017, **2**(4), 224–247, DOI: [10.1016/j.bioactmat.2017.05.007](https://doi.org/10.1016/j.bioactmat.2017.05.007).
- 164 D. Marx, A. R. Yazdi, M. Papini and M. Towler, A review of the latest insights into the mechanism of action of strontium in bone, *Bone Rep.*, 2020, **12**, 100273, DOI: [10.1016/j.bonr.2020.100273](https://doi.org/10.1016/j.bonr.2020.100273).
- 165 C. J. Pan, T. T. Liu, Y. Yang, T. Liu, Z. H. Gong, Y. C. Wei, *et al.*, Incorporation of Sr<sup>2+</sup> and Ag nanoparticles into TiO<sub>2</sub> nanotubes to synergistically enhance osteogenic and antibacterial activities for bone repair, *Mater. Des.*, 2020, **196**, 109086, DOI: [10.1016/j.matdes.2020.109086](https://doi.org/10.1016/j.matdes.2020.109086).
- 166 Y. Huang, Y. X. Zhang, M. Y. Li, H. Yang, J. Y. Liang, Y. Chen, *et al.*, Physicochemical, osteogenic, and antimicrobial properties of graphene oxide reinforced silver/strontium-doped hydroxyapatite on titanium for potential orthopedic applications, *Surf. Coat. Technol.*, 2022, **446**, 128788, DOI: [10.1016/j.surfcoat.2022.128788](https://doi.org/10.1016/j.surfcoat.2022.128788).
- 167 D. Li, Y. Li, A. Shrestha, S. Wang, Q. Wu, L. Li, *et al.*, Effects of programmed local delivery from a micro/nano-hierarchical surface on titanium implant on infection clearance and osteogenic induction in an infected bone defect, *Adv. Healthcare Mater.*, 2019, **8**, DOI: [10.1002/adhm.201900002](https://doi.org/10.1002/adhm.201900002).
- 168 X. He, X. Zhang, L. Bai, R. Hang, X. Huang, L. Qin, *et al.*, Antibacterial ability and osteogenic activity of porous Sr/Ag-containing TiO<sub>2</sub> coatings, *Biomed. Mater.*, 2016, **11**, 045008, DOI: [10.1088/1748-6041/11/4/045008](https://doi.org/10.1088/1748-6041/11/4/045008).
- 169 H. C. Flemming, J. Wingender, U. Szewzyk, P. Steinberg, S. A. Rice and S. Kjelleberg, Biofilms: An emergent form of bacterial life, *Nat. Rev. Microbiol.*, 2016, **14**(9), 563–575, DOI: [10.1038/nrmicro.2016.94](https://doi.org/10.1038/nrmicro.2016.94).
- 170 M. Croes, S. Bakhshandeh, I. Hengel, K. Lietaert, K. Kessel, B. Pouran, *et al.*, Antibacterial and immunogenic behavior of silver coatings on additively manufactured porous titanium, *Acta Biomater.*, 2018, **81**, 315–327, DOI: [10.1016/j.actbio.2018.09.051](https://doi.org/10.1016/j.actbio.2018.09.051).
- 171 Y. Kuo, C. Chen, P. Dash, Y. Lin, C. Hsu, S. Shih, *et al.*, Angiogenesis, osseointegration, and antibacterial applications of polyelectrolyte multilayer coatings incorporated with silver/strontium containing mesoporous bioactive glass on 316L stainless steel, *Front. Bioeng. Biotechnol.*, 2022, **10**, 818137, DOI: [10.3389/fbioe.2022.818137](https://doi.org/10.3389/fbioe.2022.818137).



- 172 Z. Mao, Y. Li, Y. Yang, Z. Fang, X. Chen, Y. Wang, *et al.*, Osteoinductivity and antibacterial properties of strontium ranelate-loaded poly(lactic-co-glycolic acid) microspheres with assembled silver and hydroxyapatite nanoparticles, *Front. Pharmacol.*, 2018, **9**, 368, DOI: [10.3389/fphar.2018.00368](https://doi.org/10.3389/fphar.2018.00368).
- 173 T. Geng, Y. Wang, K. Lin, C. Zhang, J. Wang, Y. Liu, *et al.*, Strontium-doping promotes bone bonding of titanium implants in osteoporotic microenvironment, *Front. Bioeng. Biotechnol.*, 2022, **10**, 1011482, DOI: [10.3389/fbioe.2022.1011482](https://doi.org/10.3389/fbioe.2022.1011482).
- 174 X. Shen, K. Fang, K. Yie, Z. Zhou, Y. Shen, S. Wu, *et al.*, High proportion strontium-doped micro-arc oxidation coatings enhance early osseointegration of titanium in osteoporosis by anti-oxidative stress pathway, *Bioact. Mater.*, 2021, **10**, 405–419, DOI: [10.1016/j.bioactmat.2021.08.031](https://doi.org/10.1016/j.bioactmat.2021.08.031).
- 175 H. Qiao, C. Zhang, X. Dang, H. Yang, Y. Wang, Y. Chen, *et al.*, Gallium loading into a polydopamine-functionalised SrTiO<sub>3</sub> nanotube with combined osteoinductive and antimicrobial activities, *Ceram. Int.*, 2019, **45**, 22183–22195, DOI: [10.1016/j.ceramint.2019.07.240](https://doi.org/10.1016/j.ceramint.2019.07.240).
- 176 Y. Wu, S. Huo, S. Liu, Q. Hong, Y. Wang and Z. Lyu, Cu–Sr bilayer bioactive glass nanoparticles/polydopamine functionalized polyetheretherketone enhances osteogenic activity and prevents implant-associated infections through spatiotemporal immunomodulation, *Adv. Healthcare Mater.*, 2023, **12**, 2301772, DOI: [10.1002/adhm.202301772](https://doi.org/10.1002/adhm.202301772).
- 177 K. Wang, M. Gao, J. Fan, J. Huo, P. Liu, R. Ding, *et al.*, SrTiO<sub>3</sub> nanotube-based "pneumatic nanocannon" for on-demand delivery of antibacterial and sustained osseointegration enhancement, *ACS Nano*, 2024, **18**, 16011–16026, DOI: [10.1021/acsnano.4c04478](https://doi.org/10.1021/acsnano.4c04478).
- 178 Y. Chen, C. Zhou, Y. Xie, A. Xu, Y. Guan, W. Lu, *et al.*, Zinc and strontium- co-incorporated nanorods on titanium surfaces with favorable material property, osteogenesis, and enhanced antibacterial activity, *J. Biomed. Mater. Res., Part B*, 2021, **109**, 1754–1767, DOI: [10.1002/jbm.b.34834](https://doi.org/10.1002/jbm.b.34834).
- 179 V. Offermanns, O. Z. Andersen, G. Riede, M. Sillassen, C. S. Jeppesen, K. P. Almtoft, *et al.*, Effect of strontium surface-functionalized implants on early and late osseointegration: A histological, spectrometric and tomographic evaluation, *Acta Biomater.*, 2018, **69**, 385–394, DOI: [10.1016/j.actbio.2018.01.049](https://doi.org/10.1016/j.actbio.2018.01.049).
- 180 J. Liu, S. Rawlinson, R. Hill and F. Fortune, Strontium-substituted bioactive glasses in vitro osteogenic and antibacterial effects, *Dent. Mater.*, 2016, **32**(3), 412–422, DOI: [10.1016/j.dental.2015.12.013](https://doi.org/10.1016/j.dental.2015.12.013).
- 181 W. Lu, C. Zhou, J. Li, J. Jiang, Y. Chen, L. Dong and F. He, Improved osseointegration of strontium-modified titanium implants by regulating angiogenesis and macrophage polarization, *Biomater. Sci.*, 2022, **10**, 2198–2214, DOI: [10.1039/d1bm01488a](https://doi.org/10.1039/d1bm01488a).
- 182 D. Cheng, R. Ding, X. Jin, Y. Lu, W. Bao, Y. Zhao, S. Chen, C. Shen, Q. Yang and Y. Wang, Strontium ion-functionalized nano-hydroxyapatite/chitosan composite microspheres promote osteogenesis and angiogenesis for bone regeneration, *ACS Appl. Mater. Interfaces*, 2023, **15**, 19951–19965, DOI: [10.1021/acsami.3c00655](https://doi.org/10.1021/acsami.3c00655).
- 183 Z. Geng, L. Ji, Z. Li, J. Wang, H. He, Z. Cui, X. Yang and C. Liu, Nano-needle strontium-substituted apatite coating enhances osteoporotic osseointegration through promoting osteogenesis and inhibiting osteoclastogenesis, *Bioact. Mater.*, 2020, **6**, 905–915, DOI: [10.1016/j.bioactmat.2020.09.024](https://doi.org/10.1016/j.bioactmat.2020.09.024).
- 184 L. Hayann, V. Da Rocha, M. Candido, R. Vicente, L. Andrioli, S. Fukada, M. Brassesco, P. Ciancaglini, E. Engel and A. Ramos, A nontoxic strontium nanoparticle that holds the potential to act upon osteocompetent cells: an in vitro and in vivo characterization, *J. Biomed. Mater. Res., Part A*, 2024, **112**, 1518–1531, DOI: [10.1002/jbm.a.37708](https://doi.org/10.1002/jbm.a.37708).
- 185 W. Zhang, H. Cao, X. Zhang, G. Li, Q. Chang, J. Zhao, Y. Qiao, X. Ding, G. Yang, X. Liu and X. Jiang, A strontium-incorporated nanoporous titanium implant surface for rapid osseointegration, *Nanoscale*, 2016, **8**(9), 5291–5301, DOI: [10.1039/c5nr08580b](https://doi.org/10.1039/c5nr08580b).
- 186 D. Gopi, S. Ramya, D. Rajeswari, P. Karthikeyan and L. Kavitha, Strontium, cerium co-substituted hydroxyapatite nanoparticles: synthesis, characterization, antibacterial activity towards prokaryotic strains and in vitro studies, *Colloids Surf., A*, 2014, **451**, 172–180, DOI: [10.1016/j.colsurfa.2014.03.035](https://doi.org/10.1016/j.colsurfa.2014.03.035).
- 187 A. Kasthuri and P. Pandian, Eco-friendly synthesis of strontium oxide nanoparticles using Solanum nigrum leaf extract: characterization and antibacterial potential, *Orient. J. Chem.*, 2023, **39**, 1344–1350, DOI: [10.13005/ojc/390531](https://doi.org/10.13005/ojc/390531).
- 188 R. Hamarawf, D. Tofiq and K. Omer, Correction: Green synthesis of M-type manganese-substituted strontium hexaferrite SrMnxFe<sub>12</sub>–xO<sub>19</sub> nanoparticles with intrinsic antibacterial activity against human pathogenic bacteria, *New J. Chem.*, 2023, DOI: [10.1039/d3nj90122j](https://doi.org/10.1039/d3nj90122j).
- 189 K. Ilavenil, A. Kasthuri and P. Pandian, Biosynthesis and anti-microbial investigation of strontium oxide (SrO) nanoparticles by Lantana camara leaf extract, *Rasayan J. Chem.*, 2023, **16**, 596–603, DOI: [10.31788/rjc.2023.1628221](https://doi.org/10.31788/rjc.2023.1628221).
- 190 S. Swain and T. Rautray, Assessment of polarized piezoelectric SrBi<sub>4</sub>Ti<sub>4</sub>O<sub>15</sub> nanoparticles as an alternative antibacterial agent, *bioRxiv*, 2021, preprint, DOI: [10.1101/2021.01.02.425094](https://doi.org/10.1101/2021.01.02.425094).
- 191 W. Lu, C. Zhou, J. Li, J. Jiang, Y. Chen, L. Dong and F. He, Improved osseointegration of strontium-modified titanium implants by regulating angiogenesis and macrophage polarization, *Biomater. Sci.*, 2022, **10**, 2198–2214, DOI: [10.1039/d1bm01488a](https://doi.org/10.1039/d1bm01488a).
- 192 D. Cheng, R. Ding, X. Jin, Y. Lu, W. Bao, Y. Zhao, S. Chen, C. Shen, Q. Yang and Y. Wang, Strontium ion-functionalized nano-hydroxyapatite/chitosan composite microspheres promote osteogenesis and angiogenesis for bone regeneration, *ACS Appl. Mater. Interfaces*, 2023, **15**, 19951–19965, DOI: [10.1021/acsami.3c00655](https://doi.org/10.1021/acsami.3c00655).



- 193 X. Gao, M. Li, F. Zhou, X. Wang, S. Chen and J. Yu, Flexible zirconium-doped strontium titanate nanofibrous membranes with enhanced visible-light photocatalytic performance and antibacterial activities, *J. Colloid Interface Sci.*, 2021, **600**, 127–137, DOI: [10.1016/j.jcis.2021.05.005](https://doi.org/10.1016/j.jcis.2021.05.005).
- 194 A. Aloufi, Green synthesis of strontium-doped tin dioxide (SrSnO<sub>2</sub>) nanoparticles using the *Mahonia bealei* leaf extract and evaluation of their anticancer and antimicrobial activities, *Green Process. Synth.*, 2023, **12**, DOI: [10.1515/gps-2022-8116](https://doi.org/10.1515/gps-2022-8116).
- 195 M. Dapporto, M. Tavoni, E. Restivo, F. Carella, G. Bruni, L. Mercatali, L. Visai, A. Tampieri, M. Iafisco and S. Sprio, Strontium-doped apatitic bone cements with tunable antibacterial and antibiofilm ability, *Front. Bioeng. Biotechnol.*, 2022, **10**, DOI: [10.3389/fbioe.2022.969641](https://doi.org/10.3389/fbioe.2022.969641).
- 196 H. Alshammari, J. Neilands, C. Jeppesen, K. Almqvist, O. Andersen and A. Stavropoulos, Antimicrobial potential of strontium-functionalized titanium against bacteria associated with peri-implantitis, *Clin. Exp. Dent. Res.*, 2024, **10**, DOI: [10.1002/cre2.903](https://doi.org/10.1002/cre2.903).
- 197 R. Hamarawf, D. Tofiq and K. Omer, Correction: Green synthesis of M-type manganese-substituted strontium hexaferrite SrMnxFe<sub>12</sub>-xO<sub>19</sub> nanoparticles with intrinsic antibacterial activity against human pathogenic bacteria, *New J. Chem.*, 2023, DOI: [10.1039/d3nj90122j](https://doi.org/10.1039/d3nj90122j).
- 198 K. Ilavenil, A. Kasthuri and P. Pandian, Biosynthesis and anti-microbial investigation of strontium oxide (SrO) nanoparticles by Lantana camara leaf extract, *Rasayan J. Chem.*, 2023, **16**, 596–603, DOI: [10.31788/rjc.2023.1628221](https://doi.org/10.31788/rjc.2023.1628221).
- 199 S. Swain and T. Rautray, Assessment of polarized piezoelectric SrBi<sub>4</sub>Ti<sub>4</sub>O<sub>15</sub> nanoparticles as an alternative antibacterial agent, *bioRxiv*, 2021, preprint, DOI: [10.1101/2021.01.02.425094](https://doi.org/10.1101/2021.01.02.425094).
- 200 I. Pal, D. Bhattacharyya, R. Kar, D. Zarena, A. Bhunia and H. Atreya, A Peptide-Nanoparticle System with Improved Efficacy against Multidrug Resistant Bacteria, *Sci. Rep.*, 2019, **9**, 4485, DOI: [10.1038/s41598-019-41005-7](https://doi.org/10.1038/s41598-019-41005-7).
- 201 S. Siemer, D. Westmeier, M. Barz, J. Eckrich, D. Wünsch, C. Seckert, *et al.*, Biomolecule-corona formation confers resistance of bacteria to nanoparticle-induced killing: Implications for the design of improved nanoantibiotics, *Biomaterials*, 2019, **192**, 551–559, DOI: [10.1016/j.biomaterials.2018.11.028](https://doi.org/10.1016/j.biomaterials.2018.11.028).
- 202 M. Alkhraisat, C. Rueda, J. Cabrejos-Azama, J. Lucas-Aparicio, F. Mariño, J. García-Denche, *et al.*, Loading and release of doxycycline hyclate from strontium-substituted calcium phosphate cement, *Acta Biomater.*, 2010, **6**(4), 1522–1528, DOI: [10.1016/j.actbio.2009.10.043](https://doi.org/10.1016/j.actbio.2009.10.043).
- 203 R. Jayasree, T. Kumar, G. Perumal and M. Doble, Drug and ion releasing tetracalcium phosphate based dual action cement for regenerative treatment of infected bone defects, *Ceram. Int.*, 2018, **44**, 9227–9235, DOI: [10.1016/j.ceramint.2018.02.133](https://doi.org/10.1016/j.ceramint.2018.02.133).
- 204 X. Wei, X. Zhang, Z. Yang, L. Li and H. Sui, Osteoinductive potential and antibacterial characteristics of collagen coated iron oxide nanosphere containing strontium and hydroxyapatite in long term bone fractures, *Arabian J. Chem.*, 2021, **14**, 102984, DOI: [10.1016/j.arabj.2020.102984](https://doi.org/10.1016/j.arabj.2020.102984).
- 205 D. Khajuria, R. Vasireddi, M. Trebbin, D. Karasik and R. Razdan, Novel therapeutic intervention for osteoporosis prepared with strontium hydroxyapatite and zoledronic acid: In vitro and pharmacodynamic evaluation, *Mater. Sci. Eng., C*, 2017, **71**, 698–708, DOI: [10.1016/j.msec.2016.10.066](https://doi.org/10.1016/j.msec.2016.10.066).
- 206 D. Li, K. Chen, L. Duan, T. Fu, J. Li, Z. Mu, *et al.*, Strontium Ranelate Incorporated Enzyme-Cross-Linked Gelatin Nanoparticle/Silk Fibroin Aerogel for Osteogenesis in OVX-Induced Osteoporosis, *ACS Biomater. Sci. Eng.*, 2019, **5**(3), 1440–1451, DOI: [10.1021/ACSBIOMATERIALS.8B01298](https://doi.org/10.1021/ACSBIOMATERIALS.8B01298).
- 207 N. Lee, M. Kang, T. Kim, D. Yoon, N. Mandakhbayar, S. Jo, *et al.*, Dual actions of osteoclastic-inhibition and osteogenic-stimulation through strontium-releasing bioactive nanoscale cement imply biomaterial-enabled osteoporosis therapy, *Biomaterials*, 2021, **276**, 121025, DOI: [10.1016/j.biomaterials.2021.121025](https://doi.org/10.1016/j.biomaterials.2021.121025).
- 208 B. Kołodziejaska, N. Stępień and J. Kolmas, The Influence of Strontium on Bone Tissue Metabolism and Its Application in Osteoporosis Treatment, *Int. J. Mol. Sci.*, 2021, **22**, 6564, DOI: [10.3390/ijms22126564](https://doi.org/10.3390/ijms22126564).
- 209 P. Marie, Strontium as therapy for osteoporosis, *Curr. Opin. Pharmacol.*, 2005, **5**(6), 633–636, DOI: [10.1016/J.COPH.2005.05.005](https://doi.org/10.1016/J.COPH.2005.05.005).
- 210 I. Pal, D. Bhattacharyya, R. Kar, D. Zarena, A. Bhunia and H. Atreya, A peptide-nanoparticle system with improved efficacy against multidrug resistant bacteria, *Sci. Rep.*, 2019, **9**, 1–13, DOI: [10.1038/s41598-019-41005-7](https://doi.org/10.1038/s41598-019-41005-7).
- 211 S. Siemer, D. Westmeier, M. Barz, J. Eckrich, D. Wünsch, C. Seckert, *et al.*, Biomolecule-corona formation confers resistance of bacteria to nanoparticle-induced killing: Implications for the design of improved nanoantibiotics, *Biomaterials*, 2019, **192**, 551–559, DOI: [10.1016/j.biomaterials.2018.11.028](https://doi.org/10.1016/j.biomaterials.2018.11.028).
- 212 M. Alkhraisat, C. Rueda, J. Cabrejos-Azama, J. Lucas-Aparicio, F. Mariño, J. García-Denche, *et al.*, Loading and release of doxycycline hyclate from strontium-substituted calcium phosphate cement, *Acta Biomater.*, 2010, **6**(4), 1522–1528, DOI: [10.1016/j.actbio.2009.10.043](https://doi.org/10.1016/j.actbio.2009.10.043).
- 213 R. Jayasree, T. Kumar, G. Perumal and M. Doble, Drug and ion releasing tetracalcium phosphate-based dual action cement for regenerative treatment of infected bone defects, *Ceram. Int.*, 2018, **44**(8), 9203–9212, DOI: [10.1016/j.ceramint.2018.02.133](https://doi.org/10.1016/j.ceramint.2018.02.133).
- 214 X. Wei, X. Zhang, Z. Yang, L. Li and H. Sui, Osteoinductive potential and antibacterial characteristics of collagen coated iron oxide nanosphere containing strontium and hydroxyapatite in long term bone fractures, *Arabian J. Chem.*, 2021, **14**, 102984, DOI: [10.1016/j.arabj.2020.102984](https://doi.org/10.1016/j.arabj.2020.102984).
- 215 D. Khajuria, R. Vasireddi, M. Trebbin, D. Karasik and R. Razdan, Novel therapeutic intervention for osteoporosis prepared with strontium hydroxyapatite and



- zoledronic acid: In vitro and pharmacodynamic evaluation, *Mater. Sci. Eng., C*, 2017, **71**, 698–708, DOI: [10.1016/j.msec.2016.10.066](https://doi.org/10.1016/j.msec.2016.10.066).
- 216 D. Li, K. Chen, L. Duan, T. Fu, J. Li, Z. Mu, *et al.*, Strontium ranelate incorporated enzyme-cross-linked gelatin nanoparticle/silk fibroin aerogel for osteogenesis in OVX-induced osteoporosis, *ACS Biomater. Sci. Eng.*, 2019, **5**(3), 1440–1451, DOI: [10.1021/acsbomaterials.8b01298](https://doi.org/10.1021/acsbomaterials.8b01298).
- 217 N. Lee, M. Kang, T. Kim, D. Yoon, N. Mandakhbayar, S. Jo, *et al.*, Dual actions of osteoclastic-inhibition and osteogenic-stimulation through strontium-releasing bioactive nanoscale cement imply biomaterial-enabled osteoporosis therapy, *Biomaterials*, 2021, **276**, 121025, DOI: [10.1016/j.biomaterials.2021.121025](https://doi.org/10.1016/j.biomaterials.2021.121025).
- 218 B. Kołodziejaska, N. Stępień and J. Kolmas, The influence of strontium on bone tissue metabolism and its application in osteoporosis treatment, *Int. J. Mol. Sci.*, 2021, **22**, 6564, DOI: [10.3390/ijms22126564](https://doi.org/10.3390/ijms22126564).
- 219 P. Marie, Strontium as therapy for osteoporosis, *Curr. Opin. Pharmacol.*, 2005, **5**(6), 633–636, DOI: [10.1016/j.coph.2005.05.005](https://doi.org/10.1016/j.coph.2005.05.005).
- 220 R. Sasikala, M. Kandasamy, S. Suresh, V. Ragavendran, V. Sasirekha, J. Pearce, *et al.*, Enhanced dye-sensitized solar cell performance using strontium titanate perovskite integrated photoanodes modified with plasmonic silver nanoparticles, *J. Alloys Compd.*, 2022, **889**, 161693, DOI: [10.1016/j.jallcom.2021.161693](https://doi.org/10.1016/j.jallcom.2021.161693).
- 221 R. Khalifehzadeh and H. Arami, DNA-templated strontium-doped calcium phosphate nanoparticles for gene delivery in bone cells, *ACS Biomater. Sci. Eng.*, 2019, **5**(7), 3201–3211, DOI: [10.1021/ACSBOMATERIALS.8B01587](https://doi.org/10.1021/ACSBOMATERIALS.8B01587).
- 222 A. Ahmad, H. Akbar, I. Zada, F. Anjum, A. Afzal, S. Javed, *et al.*, Improvement of the self-controlled hyperthermia applications by varying gadolinium doping in lanthanum strontium manganite nanoparticles, *Molecules*, 2023, **28**, 7860, DOI: [10.3390/molecules28237860](https://doi.org/10.3390/molecules28237860).
- 223 S. Kasap, E. Aslan and İ. Öztürk, Investigation of MnO<sub>2</sub> nanoparticles-anchored 3D-graphene foam composites (3DGF-MnO<sub>2</sub>) as an adsorbent for strontium using the central composite design (CCD) method, *New J. Chem.*, 2019, **43**, 2981–2989, DOI: [10.1039/C8NJ05283B](https://doi.org/10.1039/C8NJ05283B).
- 224 V. Höllriegl and H. München, Strontium in the environment and possible human health effects, *Encyclopedia of Environmental Health*, 2011, pp. 268–275, DOI: [10.1016/B978-0-444-52272-6.00638-3](https://doi.org/10.1016/B978-0-444-52272-6.00638-3).
- 225 A. Burger and I. Lichtscheidl, Strontium in the environment: Review about reactions of plants towards stable and radioactive strontium isotopes, *Sci. Total Environ.*, 2019, **653**, 1458–1512, DOI: [10.1016/j.scitotenv.2018.10.312](https://doi.org/10.1016/j.scitotenv.2018.10.312).
- 226 C. Roh, T. Nguyen, J. Shim and C. Kang, Physico-chemical characterization of caesium and strontium using fluorescent intensity of bacteria in a microfluidic platform, *R. Soc. Open Sci.*, 2019, **6**, 182069, DOI: [10.1098/rsos.182069](https://doi.org/10.1098/rsos.182069).
- 227 M. Zaoui, B. Sellami, F. Boufahja, F. Faloda, S. Nahdi, A. Alrezaki, *et al.*, Effects of ferroelectric oxides of barium strontium titanate (Ba<sub>0.85</sub>Sr<sub>0.15</sub>TiO<sub>3</sub>) nanoparticles on *Ruditapes decussatus* assessed through chemical, physiological, and biochemical methods, *Chemosphere*, 2020, 129078, DOI: [10.1016/j.chemosphere.2020.129078](https://doi.org/10.1016/j.chemosphere.2020.129078).
- 228 P. Ramakrishnan, S. Nagarajan, V. Thiruvengatam, T. Palanisami, R. Naidu, M. Mallavarapu, *et al.*, Cation doped hydroxyapatite nanoparticles enhance strontium adsorption from aqueous system: a comparative study with and without calcination, *Appl. Clay Sci.*, 2016, **134**, 136–144, DOI: [10.1016/j.clay.2016.09.022](https://doi.org/10.1016/j.clay.2016.09.022).
- 229 V. Forest, Combined effects of nanoparticles and other environmental contaminants on human health - an issue often overlooked, *NanoImpact*, 2021, **23**, 100344, DOI: [10.1016/j.impact.2021.100344](https://doi.org/10.1016/j.impact.2021.100344).
- 230 M. Tsang, G. Philippot, C. Aymonier and G. Sonnemann, Anticipatory life-cycle assessment of supercritical fluid synthesis of barium strontium titanate nanoparticles, *Green Chem.*, 2016, **18**, 4924–4933, DOI: [10.1039/C6GC00646A](https://doi.org/10.1039/C6GC00646A).
- 231 K. Khalil, S. Riyadh, N. Alkayal, A. Bashal, K. Alharbi and W. Alharbi, Chitosan-strontium oxide nanocomposite: Preparation, characterization, and catalytic potency in thiadiazoles synthesis, *Polymers*, 2022, **14**, 2827, DOI: [10.3390/polym14142827](https://doi.org/10.3390/polym14142827).
- 232 M. Kim, S. Hong, N. Shin, Y. Lee and Y. Shin, Synthesis of strontium titanate nanoparticles using supercritical water, *Ceram. Int.*, 2016, **42**, 17853–17857, DOI: [10.1016/J.CERAMINT.2016.08.120](https://doi.org/10.1016/J.CERAMINT.2016.08.120).
- 233 J. Ahmad, R. Wahab, M. Siddiqui, Q. Saquib, N. Ahmad and A. Al-Khedhairi, Strontium-doped nickel oxide nanoparticles: Synthesis, characterization, and cytotoxicity study in human lung cancer A549 cells, *Biol. Trace Elem. Res.*, 2021, **200**, 1598–1607, DOI: [10.1007/s12011-021-02780-5](https://doi.org/10.1007/s12011-021-02780-5).
- 234 A. Vaio and L. Varriale, Management innovation for environmental sustainability in seaports: Managerial accounting instruments and training for competitive green ports beyond the regulations, *Sustainability*, 2018, **10**, 783, DOI: [10.3390/SU10030783](https://doi.org/10.3390/SU10030783).
- 235 J. Wright and P. Kurian, Ecological modernization versus sustainable development: The case of genetic modification regulation in New Zealand, *Sustainable Dev.*, 2010, **18**, 398–412, DOI: [10.1002/SD.430](https://doi.org/10.1002/SD.430).
- 236 M. Howes, L. Wortley, R. Potts, A. Dedekorkut-Howes, S. Serrao-Neumann, J. Davidson, *et al.*, Environmental sustainability: A case of policy implementation failure?, *Sustainability*, 2017, **9**, 165, DOI: [10.3390/SU9020165](https://doi.org/10.3390/SU9020165).
- 237 A. Traxler, D. Schrack and D. Greiling, Sustainability reporting and management control - A systematic exploratory literature review, *J. Cleaner Prod.*, 2020, **276**, 122725, DOI: [10.1016/j.jclepro.2020.122725](https://doi.org/10.1016/j.jclepro.2020.122725).

